



TECHNISCHE  
UNIVERSITÄT  
WIEN

Diplomarbeit

# Influence of growth rate ( $\mu$ ) on the specific penicillin production rate ( $q_{\text{Pen}}$ ) during fermentations with the filamentous fungus *Penicillium* *chrysogenum*

---

Ausgeführt am Institut für

Verfahrenstechnik, Umwelttechnik und Technische Biowissenschaften

der Technischen Universität Wien

unter der Anleitung von Univ. Prof. Dr. Christoph Herwig

und Dipl.-Ing. Mag. Daniela Ehgartner

durch Thomas Hartmann, BSc

Im Werd 15/5, 1020 Wien, Österreich



## Abstract

Nowadays, antibiotics are a crucial part of modern medicine. As generally known, the first one which was discovered by Alexander Fleming by accident, is penicillin. Penicillin is a bactericide substance which is produced by the filamentous fungus *Penicillium chrysogenum*, next to other fungi species, under carbon source limited conditions. Though nowadays fermentation conditions are highly optimized for maximal production rates, there is still room for further process optimization which is topic of several research groups worldwide targeting different aspects which may lead to the desired results. The scientific approaches are various. One of them is the the impact of the growth rate ( $\mu$ ).

The growth rate is in the main focus of this Thesis. As described for different strains, the viable growth rate is linked to the specific penicillin production rate,  $q_{pen}$ . The aim of my master thesis was to examine if the stated correlation does exist for the here applied penicillin V producing strain by comparing the  $q_{pen}$  as well as the absolute penicillin concentrations of fed-batch cultivations with different constant, viable growth rates and to identify optimal conditions. Finally, the resulting relation was explored under oxygen limited conditions.

In order to compare different  $\mu$  set points, it was necessary to establish an adequate control strategy which enabled to reach and keep the aimed specific growth rate. Therefore, a soft sensor for the specific growth rate was used which was based on the measurement of the viable biomass via capacitance measurements. The method was optimized throughout the Thesis and controlled with adequate atline as well as offline methods.

After establishing an adequate control strategy, several cultivations were performed with different  $\mu$  set points and the outcomes evaluated. Therefore, different criteria for data evaluation were used and thus the dependency of the specific penicillin production rate on the specific growth rate determined.

Finally, one cultivation with a certain  $\mu$  set point was reproduced but with a decreased dissolved oxygen level of 4% in order to explore the correlation between viable growth rate the specific growth rate and viable specific penicillin production rate under oxygen limited conditions.

The resulting relation between  $\mu$  and  $q_{pen}$  was similar as previously published by Douma et al., 2010, revealing a specific growth rate dependence of the specific penicillin production rate. The low oxygen level of 4% of the last cultivation negatively affected the specific penicillin production rate, leading to decreased specific penicillin production rates throughout the process. Nevertheless, several cultivations with different  $\mu$  set points have to be performed in order to specify the results.



## Kurzfassung

Antibiotika sind heutzutage ein essentieller Bestandteil der modernen Medizin. Wie allgemein bekannt, war Penicillin eines der Ersten und wurde zufällig von Alexander Fleming entdeckt. Penicillin ist ein Bakterizid, welches unter anderem vom filamentösen Pilz *Penicillium chrysogenum*, neben anderen *Penicillium* Spezies, unter bestimmten Bedingungen produziert wird. Obwohl heutige Fermentationsbedingungen bereits mit dem Ziel einer maximalen Produktion optimiert sind, wird nach weiteren Möglichkeiten gesucht um die produzierten Mengen zu erhöhen. Ein Ansatz ist den Einfluss der Wachstumsrate,  $\mu$ , auf spezifische Penicillin Produktionsrate,  $q_{pen}$ , nutzbar zu machen.

Hauptaugenmerk dieser Diplomarbeit liegt auf eben jenem Einfluss der Wachstumsrate. Der Einfluss der Wachstumsrate auf die spezifische Penicillin Produktionsrate wurde bereits für verschiedene Stämme beschrieben. Ziel meiner Diplomarbeit war es, eine derartige Korrelation für den hier verwendeten Penicillin V produzierenden Stamm zu erforschen. Dafür wurden mehrere Fermentationen mit unterschiedlichen, konstant gehaltenen Wachstumsraten durchgeführt und anschließend die erhaltenen  $q_{pen}$  sowie absoluten Penicillin Konzentrationen verglichen und in Korrelation gesetzt um Optima zu identifizieren. Schließlich wurde eine Fermentation mit stark verringertem Niveau an Gelöstsauerstoff durchgeführt und die Effekte ausgewertet.

Um verschiedene  $\mu$  Sollwerte vergleichen zu können, war es zunächst nötig eine adäquate Kontrollstrategie zu entwickeln, welche es ermöglichte angestrebte  $\mu$  Sollwerte zu erreichen und zu halten. Hierfür wurde ein „Softsensor“ für die spezifische Wachstumsrate verwendet, welcher auf der Ermittlung der viablen Biomasse mittels Kapazitätsmessung basierte. Die Methode wurde im Laufe der Diplomarbeit optimiert und mit adäquaten „atline“ und „offline“ Methoden kontrolliert.

Nach dem Etablieren einer adäquaten Kontrollstrategie, wurden mehrere Kultivierungen mit unterschiedlichen  $\mu$  Sollwerten durchgeführt und die Resultate ausgewertet sowie miteinander verglichen. Die Datenauswertung folgte verschiedenen Kriterien und die Abhängigkeit von  $q_{pen}$  von  $\mu$  wurde bestimmt.

Zuletzt wurde eine Kultivierung mit einem bestimmten  $\mu$  Sollwert repliziert, allerdings mit einem stark verringerten Niveau an Gelöstsauerstoff von 4%. Anschließend wurden die erhaltenen Daten mit denen der Kultivierung mit einem Niveau an Gelöstsauerstoff laut „SOP“ verglichen.

Die resultierende Beziehung zwischen  $\mu$  und  $q_{pen}$  für den hier verwendeten Stamm entspricht weitestgehend der von Douma et al., 2010, Publizierten. Außerdem konnte gezeigt werden, dass das verringerte Niveau an Gelöstsauerstoff von 4% einen negativen Effekt auf die spezifische Penicillin Produktionsrate bei gegebener viabler Wachstumsrate hat. Allerdings müssen in Zukunft weitere Kultivierungen mit anderen  $\mu$  Sollwerten durchgeführt werden um die Ergebnisse zu spezifizieren.



## Acknowledgements

I want to express my sincere appreciation to Prof. Christoph Herwig for giving me the opportunity to work on this project in his research group and for his constant guidance and constructive inputs.

My gratefulness is addressed to my supervisor Daniela Ehgartner for the wonderful collaboration, her dedication and ongoing support.

Furthermore, I want to thank Jens Fricke for his cooperation, especially for his professional advices in experimental planning.

I want to thank Sandoz GmbH (Kundl, Austria) for providing the strain used in this work and for their support as well as Christian Doppler Forschungsgesellschaft, Vienna, Austria.

My deepest gratitude is expressed to my family, especially to my parents, my sister and my grandparents. Without their unconditional support throughout my whole life I would never have reached my goals.

Last but not least, I want to thank my friends, Laura Siedler, Julia Mildner, Johanna Hausjell and Maximilian Krippel, who I found during the practical work. They supported me throughout the hard working days as well as the time outside of work, and they still do.





## Table of Content

Abstract .....	3
Kurzfassung .....	5
Acknowledgements .....	7
Table of Content.....	9
1. Introduction.....	12
1.1. History of antibiotics with main focus on penicillin .....	12
1.2. Characterization of <i>P. chrysogenum</i> .....	13
1.3. Penicillin and its biosynthetic pathway .....	15
1.4. Fungal morphology as an interlink between process parameters and productivity .....	18
1.5. Growth rate $\mu$ as factor influencing the specific penicillin production rate $q_{\text{Pen}}$ .....	20
1.6. Motivation and goal .....	22
2. Material & Methods .....	24
2.1. Material .....	24
2.1.1. Strain .....	24
2.1.2. Setup/Equipment .....	24
2.1.3. Media and Feeds .....	25
<b>Feed</b> .....	25
<b>Chemical</b> .....	25
<b>Concentration [g/L] / [ml/L]</b> .....	25
2.2. Methods .....	26
2.2.1. Cultivation strategy .....	26
2.2.2. Batch.....	27
2.2.3. Transfer .....	27
2.2.4. Fed-batch phase .....	27
2.2.5. Down regulation of dissolved oxygen during $\mu$ controlled fed-batch phase .....	28
2.2.6. Control strategy of $\mu_{\text{viable}}$ .....	29
2.2.6.1. Atline .....	29
2.2.6.2. Online .....	30
2.2.7. Analytical methods.....	30
2.2.7.1. Offline methods.....	30
2.2.7.1.1. CFU determination of spore solution .....	30
2.2.7.1.2. Ergosterol extraction and preparation for HPLC measurement .....	31
2.2.7.1.3. Measurements of several sugars via ion-exchange chromatography .....	31
2.2.7.1.4. Cell dry weight – CDW determination.....	32

2.2.7.2. Atline methods .....	32
2.2.7.2.1. Measurement of Phenoxyacetate and Penicillin V .....	32
2.2.7.2.2. Viability assay – propidium iodide staining .....	33
2.2.7.2.3. Confocal microscopy .....	34
2.2.7.2.4. Enzymatic assays .....	35
2.2.7.2.5. Atline biomass determination .....	35
2.2.7.3. Data evaluation .....	36
3. Results .....	37
3.1. Overview of cultivations .....	37
3.2. Batch phase .....	38
3.2.1. Trend of pH and CO <sub>2</sub> .....	38
3.2.2. Trend of dissolved oxygen and agitator speed .....	38
3.2.3. Sugars & metabolites .....	39
3.2.4. Ergosterol concentration and calculated biomass concentration as well as $\mu_{\max}$ of the batch phase .....	40
3.4. Fed-Batch cultivation .....	41
3.4.1. C <sub>x</sub> over time .....	41
3.4.2. C <sub>Pen</sub> over time .....	42
3.4.3. Sugar concentrations during fed-batch .....	42
3.4.4. Y <sub>X/S</sub> over time .....	43
3.4.5. Growth rate “ $\mu$ ” & specific penicillin production rate “q <sub>Pen</sub> ” .....	44
3.5. Atline methods for biomass concentration determination .....	45
3.6. Correlation between dCap signal and viable biomass .....	46
3.7. Comparison of $\mu$ -control strategies .....	46
3.8. $\mu$ -q <sub>Pen</sub> evaluation .....	48
3.8.1. Single data points .....	48
3.8.2. Mean values .....	49
3.8.3. Maximal specific penicillin production rate .....	50
3.8.4. After ~44 hours since fed-batch start .....	51
3.8.5. After ~45g consumed glucose/initial biomass of FB [g/(g/L)] .....	52
3.9. Influence of a pO <sub>2</sub> =4% on q <sub>Pen, viable</sub> .....	53
3.9.1. Comparison of CDW .....	53
3.9.2. Comparison of $\mu_{\text{viable}}$ .....	53
3.9.3. Comparison of c <sub>Pen</sub> [g/L] .....	54
3.9.4. Comparison of q <sub>pen, viable</sub> [mmol/c-mol*h] .....	54

3.9.5. $\mu_{\text{viable}} - q_{\text{pen}}$ relation .....	55
3.9.5.1. Single data points .....	55
3.9.5.2. Mean values .....	56
3.9.5.3. Maximal $q_{\text{pen, viable}}$ .....	56
3.9.5.4. After ~44 hours since fed-batch start .....	57
3.9.5.5. After ~45 g/(g/l) consumed Glucose/initial BM of FB .....	58
4. Discussion .....	60
4.1. Batch .....	60
4.2. Fed-Batch .....	61
4.2.1. General process evaluation .....	61
4.2.2. Control .....	62
4.2.3. Growth rate and specific penicillin production rate .....	63
4.2.4. $\mu$ - $q_{\text{pen}}$ evaluation .....	63
4.2.5. Comparison of differing $pO_2$ levels .....	65
5. Conclusion .....	66
5.1. Batch .....	66
5.2. Fed-Batch .....	66
6. Outlook .....	67
6.1. Batch .....	67
6.2. Fed-Batch .....	67
7. Literature .....	69
8. List of Figures .....	75
9. List of Tables .....	77

# 1. Introduction

## 1.1. History of antibiotics with main focus on penicillin

Nowadays, antibiotics are a crucial part in modern medicine as treatment for diseases caused by bacteria, and thereby, helping to cure and drive back some of the most common infection diseases in earlier times, like syphilis. Nevertheless, the targeted elimination of a pathogen by a secondary metabolite of another microbe has a relatively short history and started 90 years ago when Alexander Fleming, a Scottish biologist, accidentally discovered penicillin.

However, evidence for the usage of mould as treatment for infected, superficial wounds dates back to the ancient Egypt where the healer Imhokep applied mouldy bread on superficial wounds (Wainwright et al., 1989). This usage of moulds continued throughout the centuries, for example suggested the English apothecary John Parkington to use moulds on infections due to their positive effects (Wainwright et al., 1989). Nevertheless, an actual knowledge of the mode of action did not exist.

Furthermore, the fluorescent microscopically examination of bone material from ancient populations from Sudanese Nubia (Bassett et al., 1980; Nelson et al., 2010), as well as from the Dakhleh Oasis dating back to the late Roman period (Cook et al., 1989) revealed the presence of the antibiotic tetracycline. Thus, indicating that even in ancient time some cultures had a continuous uptake, possible via *Streptomyces* contaminated grain in their food. Nevertheless, all these examples for the intended usage of antibiotic containing mould or the possible unaware consumption of contaminated food have in common that there was no knowledge about the actual component responsible for the positive effects (Bassett et al., 1980; Nelson et al., 2010; Cook et al., 1989).

The actual rise of the “antibiotic era” started with the earlier mentioned accidental discovery of penicillin by Alexander Fleming. Returning to his laboratory from a vacation, he made an interesting discovery on the Petri dishes on which he had initially cultivated *Staphylococci*. Though it was colonized by bacteria, it was contaminated with a mould in which environment no bacteria were detectable (Bendinger, 1989). Fleming concluded that the mould was inhibiting the growth of *Staphylococci*. Ongoing experiments confirmed the ability of the fungus to produce and secrete a substance with bacteriostatic as well as bacteriocidal properties depending on its concentration and the targeted bacteria. Moreover, he discovered that only certain bacteria are affected while others are unharmed (Ligon, 2004).

Finally, Fleming presented his serendipitous discoveries on the 13<sup>rd</sup> February 1929 at the Medical Research Club (Fleming, 1929). Unfortunately, his accomplishments weren’t credited by the scientific community remaining unheard and resulting in no further interest by other research groups. Nevertheless, having the importance of his findings in mind, he contacted several chemists with the goal to purify the crude extract but with no success. Finally, Harold Raistrick, a chemist and expert for fungal metabolites, took interest into Fleming’s discovery (Ligon, 2004).

Raistrick struggled with the purification of the still unknown substance as a result of its instability. Therefore, he decided to concentrate his efforts on a yellow pigment of the fungus, called chrysoygenin (Ligon, 2004) as he thought that it would be easier to track. Finally, Raistrick succeeded

in isolating chrysogenin with the help of his colleagues R. Lovell, a bacteriologist, and P.W. Clutterbuck, a chemist. Nevertheless, the derived solution did not show a sign of the desired characteristics of penicillin (Clutterbuck et al., 1932). Failing in the attempt to successfully purify penicillin on his own as well as with the help of others, Fleming stopped looking for other experts but still provided samples of the fungi to those who showed interest (Ligon, 2004).

For the next few years, the scientific interest in penicillin was nearly completely missing. Eventually in 1938, the Australian pharmacologist and pathologist Howard Florey, at the time professor at the Lincoln College in Oxford, continued with his colleagues Ernst Chain and Norman Heatley the research on penicillin. Among other things, Florey tested penicillin on humans, being the first one who performed clinical tests and thus providing an important contribution on the way to the medical usage of penicillin. In 1940 and 1941 they published their results proving the application of penicillin as well as describing a possible effort for synthesis and purification of penicillin (Chain et al., 1940; Abraham et al., 1941). Despite the scientific success of the team, they finally split up due to personal differences. While Chain went to Rome, Florey and Heatley left for the states where a funding by Rockefeller Foundation enabled ongoing research on penicillin (Ligon, 2004).

Between 1941 and 1943 Heatley pursued in Peoria, Illinois, with his colleagues R. D. Coghill and A. J. Moyer the approach to develop a large-scale cultivation of the *Penicillium* strain they had brought from England. In order to increase the amount of produced penicillin per cultivation, he and his colleagues started to look for other, more productive strains (Ligon, 2004). Moreover, during this time they discovered that the addition of corn steep liquor resulted in an increased productivity (Liggett et al., 1948) and tested more than 1000 different mould samples in order to find a better producer. Next to the original strain provided from Fleming, only two other strain being capable of producing penicillin were discovered, underlining the rareness of penicillin producers and the fortunate circumstances leading to its discovery (Henderson et al., 1997). The description of the different strains follows in chapter 1.2 which gives an overview and more detailed information.

Simultaneously, Florey was looking for pharmaceutical companies with capacities for a large scale production of penicillin. Finally, he managed to organise funding by the government and was able to interest some firms in his idea of a large scale production of penicillin (Richards, 1964; Bennett et al., 2001). Through this initiative, several concerns started with the production of penicillin and by the entrance of the United States into the Second World War on the 7<sup>th</sup> December, 1941, the rise of penicillin production started.

## **1.2. Characterization of *P. chrysogenum***

Since this time, penicillin and its derivatives are one of most commonly used therapeutics for certain diseases caused by bacterial infections worldwide (Ryu et al., 1980; Keefer et al., 1943). Nevertheless, its production and the development of new derivatives are topic of ongoing research as its production is quite complex and industry has to face the increasing problem of resistance against antibiotics (Swartz, 1979; Aminov, 2010).

Since high scale production of penicillin has started, the chosen organism for mass production is the filamentous fungus *Penicillium chrysogenum*. *P. chrysogenum*, or previously known as *P. notatum*, belongs to the phylum Ascomycota, next to the phyla Zygomycetes and Basidiomycetes, of the kingdom Fungi which corresponds to a division into subgroups according to their sexual spore

forming characteristics (Nielsen, 1997). As generally known, *Penicillium* represents a diverse, own genus within the division of Ascomycota and its species are ubiquitous soil fungi found worldwide. Furthermore, their importance for mankind ranges from a high economic importance to potential pathogens (Ustianowski et al., 2008; Ozcengiz et al., 2013). The taxonomic classification of *P. chrysogenum* is given in Table 1.

**Table 1: Scientific classification of the filamentous fungus *Penicillium chrysogenum***

<b>Kingdom</b>	Fungi
<b>Division</b>	Ascomycota
<b>Class</b>	Eurotiomycetes
<b>Order</b>	Eurotiales
<b>Family</b>	Trichocomaceae
<b>Genus</b>	Penicillium
<b>Species</b>	<i>P. chrysogenum</i>

In general, *Penicillium* species are part of the degradation process of organic material, for men most importantly food. Thus, their relevance for the food industry is given especially by the ability of several *Penicillium* species, for example *P. expansum* or *P. digitatum*, to produce mycotoxins as patulin (El-Bama et al, 1987). Nevertheless, while some *Penicillium* species are responsible for some challenges in food production and storage, others are indispensable for the ripening of several cheeses, for example *P. roqueforti* or *P. camemberti* (Lund et al.; 1995), or for the taste and conservation of sausages and ham like *P. nalgiovense* (Marianski et al., 2009).

Next to the importance of some *Penicillium* species in food industry, a potential therapeutic usage of other metabolites next to penicillin has been proven by several studies. For example, Griseofulvin produced by *P. griseofulvum* respectively *P. patulum* as antifungal drug (Blank et al., 1959) or several fungal compounds as potential anti-cancer drug (Bladt et al., 2013).

As most filamentous fungi, *P. chrysogenum* is a saprobiontic organism and is able to grow on sparse medium due to its broad biosynthetic ability (Nielsen, 1997). In order to gain the necessary nutrients for maintenance metabolism as well as growth, *P. chrysogenum* can utilize several different sources (Moss, 1987). According to Stone and Farrell (1946) and Jarvis and Johnson (1950) the requirements of *P. chrysogenum* for essential inorganic elements, like S, P, K, Mg, Fe and Cu are similar to those of other filamentous fungi. Nevertheless, the need for certain elements, namely S, P and Fe, are increased during penicillin synthesis (Jarvis and Johnson, 1950).

Though the penicillin producing fungus which has been studied by Alexander Fleming was later identified as *P. rubens* (Houbraken et al., 2011), the now common strains are certain mutants of *P. chrysogenum*. Reason for the change of used species was the low yield of produced penicillin, 1.2 µg/ml, resulting in high costs and low amounts of product. Soon after the organism change, an even more productive strain, NRRL 1249.B21, was developed, but the search for an even more productive one continued. Therefore, soil samples all over the world were tested. Finally, a *P. chrysogenum* strain fitting the criteria was discovered in Peoria, 1943. This strain, which was isolated from the

stem of a cantaloupe with the name NRRL 1951, is the progenitor to all now common industrial strains (Jami et al., 2010). A graphical illustration of the genealogy of the nowadays used strains is given in Figure 1.

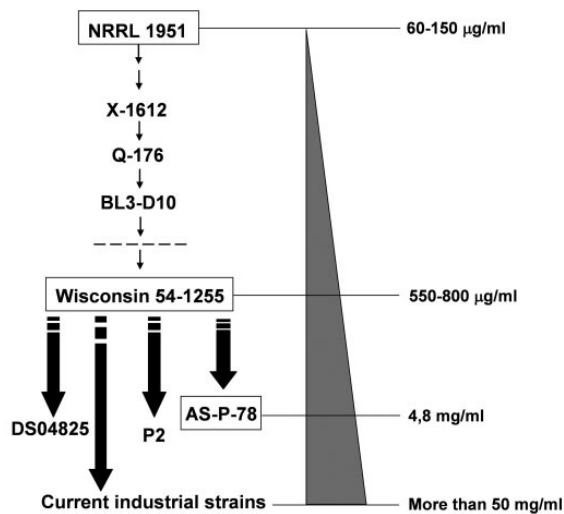


**Figure 1: Illustration of the strain development process of the nowadays used strains of *P. chrysogenum* in industry. On the left side the genealogical sequence of developed strains is visible while the right side shows the amount of produced Penicillin. Taken from Jami et al., 2010.**

During the process of strain improvement, most commonly based on classical mutagenesis, the organism acquired certain changes on genetic level as well as in its proteome (Jami et al., 2010). These modifications include the duplication of gene loci coding for the biosynthetic pathway which are necessary for the penicillin production (Francisco et al., 1995) and the down as well as up regulation of certain pathways (Jami et al., 2010). A proteomic comparison of the wild-type (NRRL 1951), an early industrial strain (Wisconsin 54-1255) and high producer strain (AS-P-78) revealed that a progressing mutagenesis with the aim to obtain high producer strains concerns the organism on several level. On the one hand, proteins important for virulence and degradation of plant material are expressed in a lower content. On the other hand, enzymes necessary for the biosynthesis of certain amino acids, namely cysteine and valine, as well as enzymes which are involved in the pentose phosphate pathway are over expressed (Jami et al., 2010).

Keeping the unnatural conditions and new challenges for the fungi during fermentations in mind, the results seem to be conclusive. For example, the change to fermentation conditions made enzymes for virulence and degradation of plant material less necessary (Jami et al., 2010) while cysteine is crucial for ACV formation (Nasution et al., 2008). Moreover, several proteins which are part of the response to oxidative stress are over expressed in the AS-P-78 strain (Jami et al., 2010).

Thus, nowadays strains are high yield producers originating from programs with the aim to find and generate them. They are highly mutated and adapted to the unnatural conditions of a fermentation process on genetic as well as metabolic levels (Jami et al., 2010).

### 1.3. Penicillin and its biosynthetic pathway

As generally known, Penicillin and its different derivatives belong next to others to the group of  $\beta$ -lactam antibiotics which share a four-membered  $\beta$ -lactam ring in their core structure which is visible

in Figure 2 and act as an antibiotic substance by inhibiting the cell wall biosynthesis of certain bacteria.

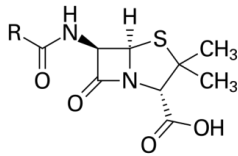


Figure 2: Chemical ground structure of penicillin. “R” represents different residues, characterizing specific penicillin derivatives.

As mentioned above, penicillin acts by inhibiting the cell wall biosynthesis of certain bacteria, or more precise by inhibiting the cross-linking of the peptidoglycan of the bacterial cell wall. Therefore the four-membered  $\beta$ -lactam ring of penicillin binds to the DD-transpeptidase, the enzyme which catalyses the cross-linking. Thereby the integrity of the cell wall is destabilized leading to lysis and consequently cell death due to the inability to compensate the osmotic pressure (Tomasz et al.; 1975).

Penicillin is synthesised by *Aspergillus* and different *Penicillium* species, such as *A. nidulans*, *P. chrysogenum*, *P. nalgioense* or *P. rubens* (Penalva et al., 1998; Houbraken et al., 2012). Though the known penicillin producing species underwent divergent evolution leading to their splitting up into different species, the gene set for penicillin biosynthesis is always clustered and reveals a high degree of homology (Liras et al., 2006). As visible in Figure 3, it is produced in three steps by three enzymes, namely  $\delta$ -(L- $\alpha$ -aminoadipyl)-L-cysteine-D-valine synthase (ACVS), isopenicillin N synthase (IPNS) and acetyl-CoA:isopenicillin N acyltransferase (AT), which are encoded within a gene cluster by the genes pcbC (IPNS), pcbAB (ACVNS) and penDE (AT) .

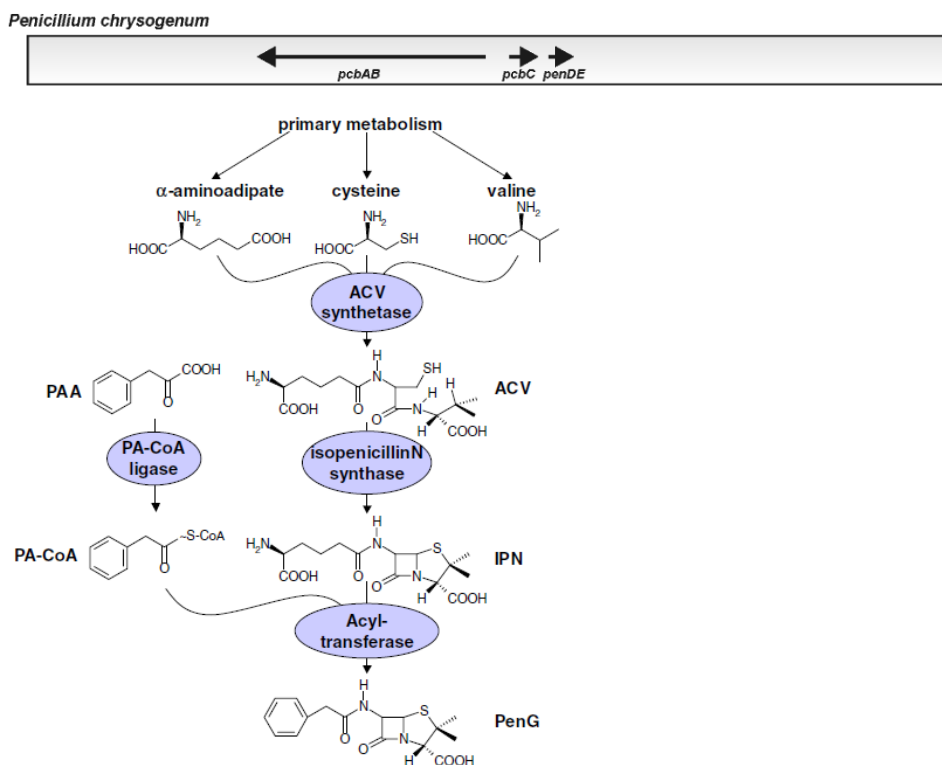


Figure 3: Gene cluster encoding for the enzymes necessary for penicillin production (Liras et al., 2006) and biosynthetic pathway of penicillin G (van der Berg et al., 2007)



In a first step the enzyme ACVS catalyzes the non-ribosomal tripeptide synthesis from the non-proteinogenic amino acid L- $\alpha$ -Aminoadipic acid, L-Cystein and L-Valine. Next, the typical four-membered  $\beta$ -lactam ring is formed by oxidative ring closure resulting in isopenicillin N, the first bioactive intermediate, and is catalyzed by IPNS. The final reaction is performed by the enzyme AT and replaces the hydrophobic acyl group by another residue. Depending on the presence of available precursor which can be used to exchange the hydrophobic acyl group, different penicillin derivatives are produced, for example Benzylpenicillin (PenG) or if phenoxyacetate is added to the cultivation media, Phenoxymethylpenicillin (PenV). Moreover, the side chain can be exchanged by other residues after the cultivation process. Reason for the substitution is the acquisition of new characteristics such as pH resistance or a wider or new activity spectre (Rolinson et al., 1973). An overview of some penicillin derivatives is given in Figure 4.

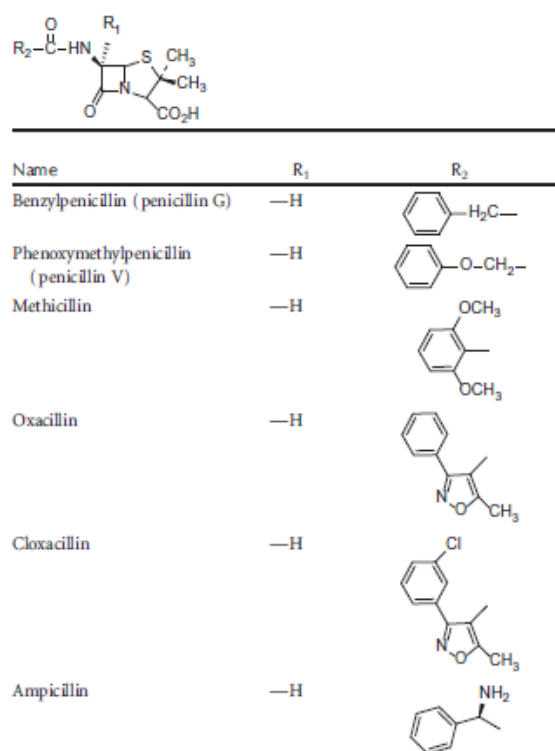


Figure 4: Illustration of some penicillin derivatives. Taken from Bush et al., 2016.

The regulation mechanism of the gene cluster encoding the penicillin biosynthetic pathway has been in focus of countless studies. In general, the results suggest that fungal biosynthetic machinery is in some kind regulated by carbon catabolite repression though it is unclear if the control is mediated via the widely spread *creA* repressor or another carbon regulatory protein (Brakhage, 1998; Cepeda-Garcia et al., 2014). As studies have shown, the highest product titres are accomplished by supplying the culture with the disaccharide lactose as C-source, while glucose or sucrose as substrate results in a drastic reduction of product titres (Brakhage et al., 1998).

It is generally known, that filamentous fungi can grow on a wide range of different pH, thus the metabolism of the microorganism has to adapt to the different conditions. One major transcription factor which is necessary for an adequate reaction to alkaline environment by repressing acid specific genes is *pacC* which has been described in filamentous fungi such as *A. niger* or *P. chrysogenum* (Brakhage, 1998). Next to its regulatory part as repressor, *pacC* reveals an activating effect of the genes *ipnA* and most likely *acvA* at alkaline pH (Tilburn et al., 1995; Bergh et al., 1998). These findings

support the result of a study which showed that cultures of *A. nidulans* with pH of 8.1 had higher penicillin titers compared to cultures with a pH of 6.5 respectively 5.0 (Shah et al., 1991). Moreover, alkaline conditions enabled the fungi to surpass the negative effect of repressing carbon sources, namely sucrose and glucose, on penicillin biosynthesis in *A. nidulans* (Espeso et al. 1993).

Nevertheless, the positive effect of an increased pH on the productivity in *A. nidulans* could not be reproduced in *P. chrysogenum*. Furthermore, the overriding effect of repressing carbon sources mediated by an alkaline pH in *A. nidulans* was not detected in *P. chrysogenum* (Suarez et al., 1996).

Next to pH and available carbon source, the availability of nitrogen, most commonly in form of ammonium, demonstrated to influence the penicillin biosynthetic pathway as well. Similar to the cephalosporin C production with *A. chrysogenum*, relatively high concentrations of ammonium interfere with the penicillin biosynthesis in *P. chrysogenum* (Shen et al., 1984; Feng et al. 1994). As studies revealed, this repressing effect is most probably mediated by the global nitrogen regulatory protein NRE (Haas et al., 1995).

Moreover, certain amino acids may play a role as regulator in penicillin biosynthesis, as it was shown for *A. chrysogenum* and *A. nidulans*. While addition of L,D-methionine to the culture broth led to an increase in cephalosporin C production, it was strongly indicated that L-lysine and L-methionine have a repressing effect on penicillin production (Brakhage et al., 1992; Velasco et al., 1994; Bergh et al., 1998), possibly regulated by a still unknown mechanism of gene regulation. As data show, the amino acid dependent effect may be mediated by a central transcriptional activator of the cross-pathway control for  $\alpha$ -amino adipate pathway which is necessary for the synthesis of L-lysine as well as  $\alpha$ -amino adipic acid. Under amino acid limitation, metabolic capacities are used for amino acid biosynthesis instead of secondary metabolites, like penicillin, as shown for *A. nidulans* (Busch et al., 2003). Nevertheless, there are no comparable studies with *P. chrysogenum*. So far, only a repressing effect of L-lysine has been reported for low-producing and industrial strains (Luengo et al., 1979).

Next to the carbon source, nitrogen source as well as concentration, amino acid concentration and availability of oxygen have been found to be agents influencing gene expression (Henriksen et al., 1997; Vardar et al., 1982).

#### **1.4. Fungal morphology as an interlink between process parameters and productivity**

Contrary to other cultivated microorganisms like bacteria, filamentous fungi have a more complex morphology, ranging from single spores to large pellets, with consequences for process parameters and cultivation conditions (Krull et al., 2010; Posch et al., 2013). Fungal growth starts with the germination of spores and thereby the building of conidia after a certain lag phase, whereby its duration depends on several factors. These structures are the starting point of the growing mycelia by further hyphal elongation and hyphal branching which may result in the formation of pellets. Furthermore, the single elements tend to agglomerate due to hyphal growth on the outer sphere of the clumps (Krull et al., 2010; Nielsen, 1997). The typical development of the fungal morphology is illustrated in Figure 5.

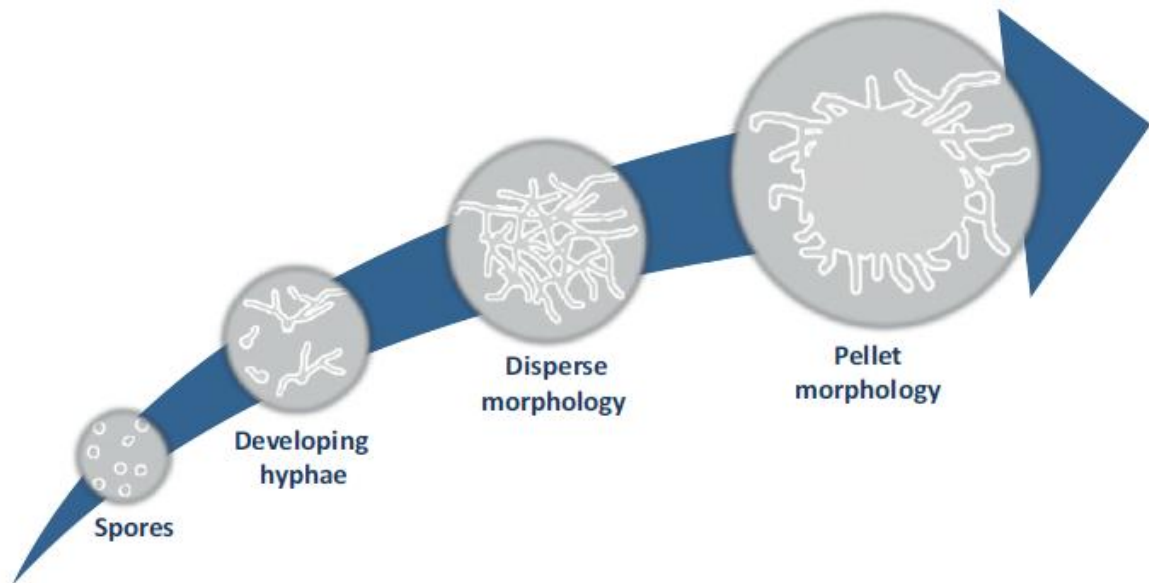


Figure 5: Morphological development of *P. chrysogenum* during cultivation conditions. Taken from Posch et al. 2013.

The development of the different fungal morphologies and the morphological composition of the culture, respectively, are influenced by several process parameters and affects itself process parameters (Cui et al., 2007; Grimm et al., 2004). Moreover, a relation between the morphology of filamentous fungi and their productivity has been described in literature (Grimm et al., 2005). Nevertheless, it seems to be a complex and not yet completely understood link.

The fungal morphology is part of a complex network which is closely interlinked and –active. Next to the morphology, it includes the fungal physiology as well as process parameters. Moreover, the morphology is influenced by initial conditions such as concentration, quality and viability of the inoculums, thus expressing the complexity of this key process parameter (Grimm et al., 2004; Ehgartner et al., 2016).

Moreover, the fungal morphology is directly influenced by the agitation, as it was shown that high agitation which is needed for an adequate mass transfer causes fragmentation of pellets due to the resulting shear stress (Cui et al., 2007).

While cultures consisting mainly of pellets generally reveal relatively low viscosity and more Newtonian rheology, processes with a high amount of hyphae and few pellets demonstrate the opposite behavior resulting in less efficient gas-liquid mass transfer and a high power input. Thus pellet cultures are generally preferred as it prolongs the production time. Nevertheless, pellet show oxygen and nutrients limitations in their core after passing a certain critical radius as a consequence of poor mass transfer and thus negatively affects fungal physiology which finally results in autolysis of the inner cells (Wang et al., 2005; Posch et al., 2013). Moreover, pellets themselves are a diverse morphological group which undergoes changes throughout an ongoing process and show inhomogeneities in their density along the radial coordinate (Krull et al., 2010).

Furthermore, a direct, potential influence of the fungal morphology on productivity has been discussed, as it was shown that in a high producing strain certain cell differentiation and morphology genes are over expressed next to others. (van der Berg et al., 2008). Nevertheless, a clear correlation between productivity and morphology hasn't been found yet.

Though the role of the morphology is controversial, high agitation revealed negative effects on penicillin production (Smith et al., 1990; Makagiansar et al., 1993). This observation may be linked to the concentration of certain gases within the culture broth, as it was shown that dissolved oxygen as well as carbon dioxide levels affect the volumetric penicillin production rate ( $r_{\text{Pen}}$ ). While low dissolved oxygen levels below 30% resulted in a decrease of  $r_{\text{Pen}}$  and levels below 10% lead to a final and irreversible loss of productivity, high dissolved carbon dioxide levels caused a decline of  $r_{\text{Pen}}$  as well (Vardar et al., 1982; Henriksen et al., 1997; Pirt et al., 1975).

## 1.5. Growth rate $\mu$ as factor influencing the specific penicillin production rate $q_{\text{Pen}}$

Since the discovery of antibiotics, it is generally assumed that they are synthesised by certain microorganisms as potential inhibitory metabolites under conditions of limited resources and thus decreased growth. Therefore, they are commonly seen as molecules which are produced in order to ensure the survival of the producing microorganism in case it is in competition with other species for nutrients. Similar conditions are used during penicillin production as concentration and type of carbon and nitrogen source effect the productivity (Brakhage et al., 1998; Haas et al., 1995).

Nevertheless, the role of antibiotics in nature is still a matter of discussion as some studies indicate a role communication molecule in microbial communities (Aminov, 2009; Linares et al., 2006).

Initial indication that the penicillin production is linked to the growth rate was published by Pirt and Righelato in 1967. They cultivated the *P. chrysogenum* strain Wis 54-1255 in glucose limited chemostat processes but with differing ranges of dilution and thus growth rates in order to investigate the kinetics of penicillin production,  $q_{\text{Pen}}$ . As their results revealed, the specific penicillin production rate is independent from the growth rate from one-eighth of the maximal growth rate to just below the maximal growth rate, but decline if the growth rate falls below one-eighth of the maximal growth rate (Pirt et al., 1967). Nevertheless, their experimental conditions differ dramatically from batch and fed-batch conditions as for example the maximal  $q_{\text{Pen}}$  is higher in batch respectively fed-batch than in continuous batch processes. Such differences can be explained by changing concentrations of enzymes involved in the penicillin biosynthesis. Therefore, a  $\mu$ - $q_{\text{Pen}}$  relation obtained from chemostat conditions does not reflect the situation in fed-batch cultivations appropriately due to a changing growth rate over time (Douma et al., 2010).

Since then, several studies aiming the investigation of a potential dependency of  $q_{\text{Pen}}$  from the growth rate were performed and some of them focused on computer based models for the prediction of the growth rate and the product formation using different approaches.

One of the first presented models was a mechanistic one based on simple substrate-inhibition kinetics for the regulation of product formation in combination with Contois kinetics for fungal growth (Bajpai & Reuss, 1980). Meanwhile, Heijnen and his colleagues used an unstructured model based on elementary balancing in combination with simple kinetics for the prediction of the penicillin production during fed-batches (Heijnen et al., 1979). A more recent model was generated by Birol and his colleagues who presented a modular, unstructured model for penicillin production (Birol et al., 2002). However, since Pirt and Righelato made first efforts exploring the linkage between the growth rate and the specific penicillin production rate, it has been the motivation of some modelling

approaches. Having in common that the data supports a growth rate dependency of the specific penicillin production rate.

Latest contribution to the data situation was a study performed by Douma and his colleagues in 2010 with the purpose to investigate a possible growth rate dependent specific penicillin production rate in *P. chrysogenum*. As described in their publication, they presented a “dynamic gene regulation” model which assumes that  $q_{pen}$  is a linear function of a single, rate-limiting enzyme of the penicillin biosynthesis pathway. Including the influence of gene expression into a stoichiometric model, they developed a model which is able to describe a  $\mu$ - $q_{pen}$  relation for steady state conditions as well as for dynamic systems as fed-batch cultivations (Douma et al., 2010).

Necessarily, enzyme activity assays were performed revealing IPNs as enzymatic bottleneck in the hierarchical regulation of the penicillin production pathway. Based on the identification of IPNS as rate-limiting enzyme combined with the knowledge that glucose represses penicillin synthesis (Gutiérrez et al, 1999), the expression of the IPNS gene is assumed to be a function of the glucose concentration and thereby,  $q_{pen}$  is proportional to its concentration. Furthermore, terms concerning the mRNA decay and the decay of IPNS itself are included (Douma et al., 2010).

As the main focus of the study presented by Douma et al. (2010) was the relation between the growth rate and the specific penicillin production rate, an adequate connection between the two of them had to be accomplished. Therefore, the Herbert-Pirt relation and the Monod kinetic for the specific substrate uptake rate were used. In general, the created model is structurally seen a stoichiometric model. Thus, the concentrations of extracellular components are calculated with an adequate mass balance (Douma et al., 2010).

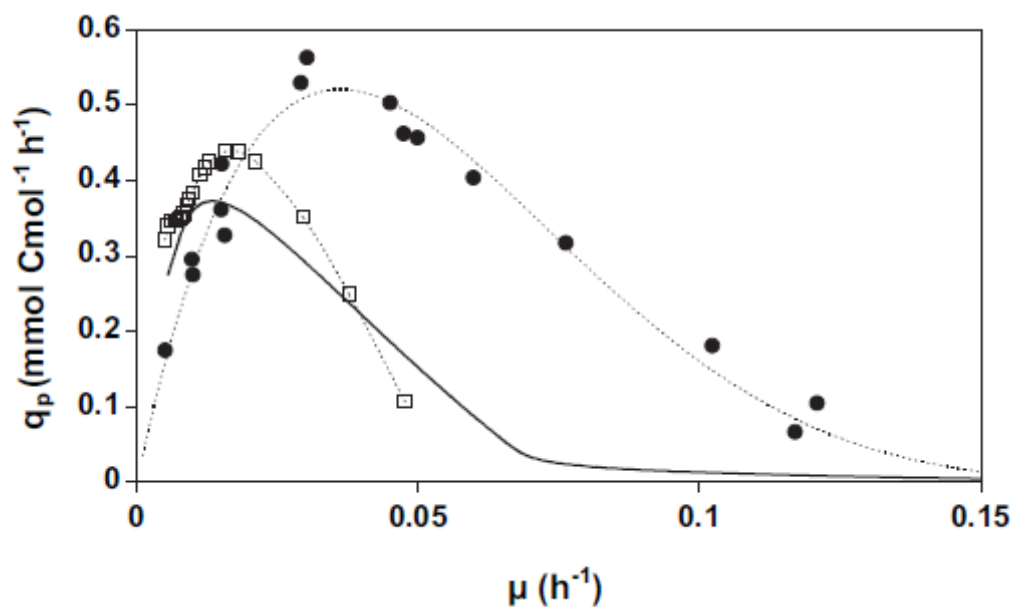


Figure 6: Illustration of  $\mu$ - $q_{pen}$  Model established by Douma et al., 2010. “-“shows  $\mu$ - $q_{pen}$  during fed-batch condition simulated by the model, “□” as simulated by the model and “•” during chemostat cultivations.

As visible in Figure 6, the resulting “dynamic gene regulation” model sufficiently describes the dependency of the specific penicillin production rate from the specific growth rate during continuous

batch as well as fed-batch experiments. Thus, it is more suitable to describe the developments during fed-batch cultivations than models based on steady state data.

## 1.6. Motivation and goal

As mentioned before, antibiotics are a fundamental cornerstone of modern medicine. Moreover, penicillin and its derivatives are still a major part of the industrially produced, therapeutically used antibiotics with a market volume of 5 billion dollar in 2003 (Ozcengiz et al., 2013). Thus, the ongoing development and investigation, optimization as well as improved control of the production procedure are necessary in order to meet the needs of the market as well as to be able to compete on it.

Concerning especially the penicillin production and thus the cultivation of *P. chrysogenum*, varieties from batch to batch are still an occurring phenomenon resulting in financial insecurities due to differing production efficiencies. Thus, models enabling an accurate prediction as well as an adequate control of the process are in the focus of ongoing interest.

In general, the basic conditions of the performed experiments are comparable to those of the experimental set-up in the study presented by Douma et al. (2010), for example the used organism and a batch followed by a fed-batch. Nevertheless, our experimental design differs in some major points to the one Douma used to create his model:

- A different *P. chrysogenum* strain is used.
- During our study PenV was produced, contrary to PenG by Douma et al. (2010)
- Data for the  $\mu$ - $q_{\text{Pen}}$  curve are obtained from several runs with different  $\mu$  set points, while Douma used a single fermentation during which the growth rate changed.
- The viability of the culture changes throughout an ongoing process. One reason is the continuous growth of pellets which tend to have dead cores as a consequence of decreased mass transfer. Thus, the viability is measured in order to obtain more precise data and a more robust control strategy. Contrary, Douma neglected the influence of the viability, using total, respectively raw data.

These differences have to be kept in mind, in order to explain possible differences between our results and the one presented by Douma et al. (2010).

Based on the motivation and keeping our experimental set-up in mind following goals are defined:

1. Control of  $\mu_{\text{viable}}$  on different levels under dynamic fed-batch conditions
2. Investigate if the viable growth rate,  $\mu_{\text{viable}}$ , has an influence on the viable specific penicillin production rate  $q_{\text{Pen, viable}}$
3. Explore a potential correlation between viable growth rate  $\mu_{\text{viable}}$  and viable specific penicillin production rate  $q_{\text{Pen, viable}}$  under oxygen limited conditions

In order to pursue the set goals, a sufficient method for the control of the growth rate has to be established. Therefore, a capacitance probe, which measures the amount of viable biomass, is used as soft sensor for the growth rate and explained in more detail in section 2.2.6. In parallel, a photometric viability assay based on PI staining is used in combination with an atline determination

of the biomass concentration during the sampling events as control for capacitance data and improvement the  $\mu$  control strategy.

The sufficient completion of the first goal is necessary to fulfill the second one. With the establishment of an adequate control strategy of the growth rate, we are able to conduct several processes with different  $\mu_{\text{viable}}$  set points and compare the corresponding specific penicillin production rates. Therefore, different criteria for the selection of data pairs are tested in order to determine the most suitable one.

Finally, if a correlation between the specific growth rate and the specific penicillin production rate has been found, the influence of oxygen limited conditions on the established correlation can be tested. Therefore, several fermentations with identical  $\mu_{\text{viable}}$  set-points to the previous cultivations are conducted. The resulting  $\mu_{\text{viable}}-q_{\text{Pen, viable}}$  data is compared according to the same criteria before, in order to reveal differences to the  $\mu_{\text{viable}}-q_{\text{Pen, viable}}$  established not oxygen limited conditions.

## 2. Material & Methods

### 2.1. Material

#### 2.1.1. Strain

As model organism, a *P. chrysogenum* strain which was derived from an ancestral strain, BCB1, with the code “BCB1\_V2” was used and kindly donated from Sandoz GmbH (Kundl, Austria)

#### 2.1.2. Setup/Equipment

In Table 2, an overview of the used bioreactor setup is given:

Table 2: Overview of the used instruments which were directly as well as indirectly attached to the fermenter

Device/instrument	Company
Techfors-S bioreactor	Infors, Bottmingen, Switzerland
Overpressure valve	Infors, Bottmingen, Switzerland
Mass flow controller	Vögtlin Instruments, Aesch, Switzerland
Pressure sensor	Keller, Winterthur, Switzerland
Temperature probe	Infors, Bottmingen, Switzerland
pH probe	Hamilton, Bonaduz, Switzerland
pO <sub>2</sub> probe	Hamilton, Bonaduz, Switzerland
Off-gas analyzer	M. Müller AG, Esslingen, Switzerland
Permittivity probe	Aber Instruments, Wales, UK
Biomass Monitor 220	Aber Instruments, Wales, UK
iBiomass Biomass sensor	FOGALE nanotech, Nimes, France
Preciflow pumps	Lambda Laboratory Instruments, Baar, Switzerland
Scales	Sartorius, Göttingen, Germany

The cultivations were performed in two Techfors-S bioreactors with a maximal working volume of 10 L and 20 L, respectively. Nevertheless, cultivations were carried out with a start volume of 6.5 L and 13 L, respectively. Excess cultivation broth was removed regularly during sampling. Optimal mass transfer as well as distribution within the broth was ensured with three six bladed Rushton turbine impellers per fermenter. While two of them were installed in a submerged position, one was positioned above the media closely to the top of the fermenter in order to reduce excess foam. Dissolved oxygen and pH of the culture broth were measured with above mentioned probes which were located at side-inlets of the bioreactor. Further, raw data for offgas analytics were derived from an offgas analyzer.

pH, temperature, pressure, air flow, agitator speed and dissolved oxygen were regulated either via control panels which were connected directly to the bioreactors or via the process control system Lucullus (Lucullus PIMS, Securecell AG, Schlieren, Switzerland). While dissolved oxygen regulation was performed with the agitator speed, pH control was executed by adding base or acid, respectively, using peristaltic pumps attached to the tower of the fermenter. The flux of the feeds, namely carbon, nitrogen and product precursor, were ensured using the preciflow pumps, which are



listed in Table 2. Amount of the influx of all feeds, including acid as well as base, were recorded via connected scales. A graphical representation of the fermenter set up including online measurements, except delta capacitance, as well as all mentioned feeds is given in Figure 7. The measurement and control strategy is explained in chapter 2.6.6.

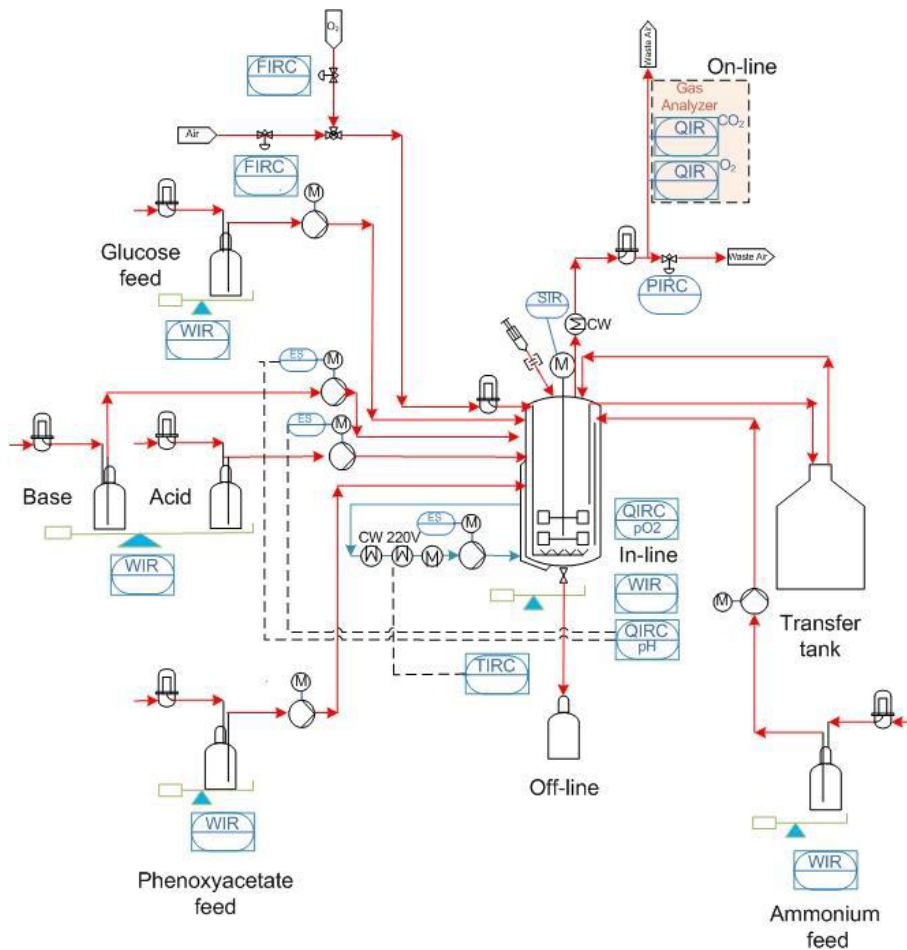


Figure 7: Illustration of the fermenter setup (Seyer, 2015)

The viable biomass concentration was measured using the probes measuring the delta capacitance via radio frequency impedance spectroscopy within the broth. Therefore, the delta capacitance was measured in dual frequency mode with frequencies of 100kHz respectively 15650kHz per minute.

### 2.1.3. Media and Feeds

The composition of the media which was used for the experiments is similar as described in the publication of Posch & Herwig (2014).

Following feeds, as described in Table 3, were used:

Table 3: List of the used feeds and their composition

Feed	Chemical	Concentration [g/L] / [ml/L]
Carbon source	C <sub>6</sub> H <sub>12</sub> O <sub>6</sub>	550
Nitrogen source	(NH <sub>4</sub> ) <sub>2</sub> SO <sub>4</sub>	100

Precursor	POX	160
Base	KOH	200
Acid	H <sub>2</sub> SO <sub>4</sub>	150

## 2.2. Methods

### 2.2.1. Cultivation strategy

In general, the performed experiments could be split up into a batch and a fed-batch phase. The batch phase could be seen as preculture and was characterized by spore germination and exponential growth, but lacking penicillin production. Contrary, fed-batch phase was the actual production phase where growth was limited, also known as idiophase.

In order to ensure that all experiments were conducted with the same amount of living spores, the living spore cell concentration of the available inoculi was determined prior to the cultivations using colony forming unit determination. Based on the concentration, the batch media was inoculated with a defined amount of spore suspension. pH was not controlled in this phase of the cultivation. At the end of the batch, which was indicated by a pH increase of 0.5 units after its minimum, a “transfer” event initiated the transition to two, simultaneously performed fed-batches. The fed-batch phase itself was divided into an uncontrolled fed-batch with constant feed followed by a  $\mu$ -controlled phase. An overview with the focus on  $\mu$  and the carbon source feed flow of the cultivation was given in Figure 8.

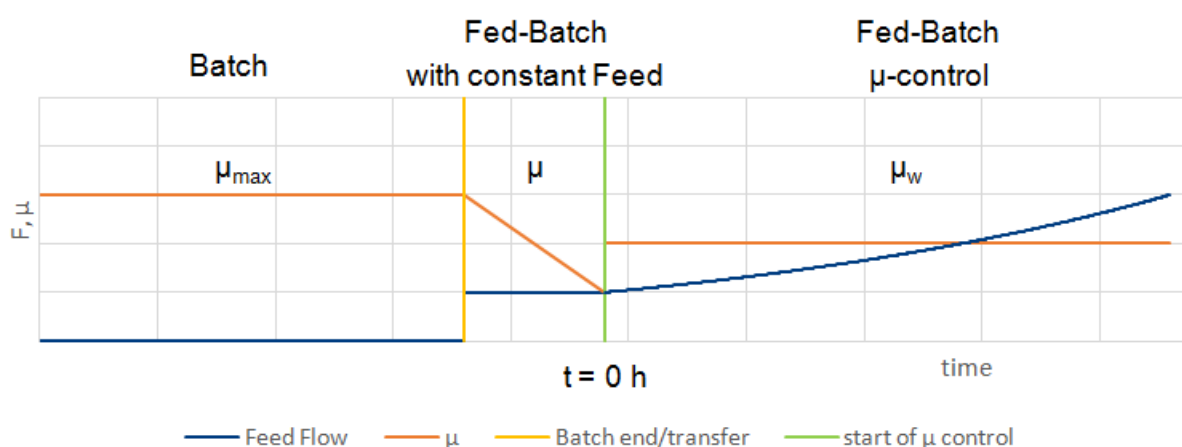


Figure 8: Illustration of the cultivation strategy

Within the first 24 h of the fed-batch, the growth rate was not controlled, as other carbon sources next to glucose were available, but a constant feed of 1.01 mL/(g\*h) was set. Therefore, a depletion of mentioned carbon sources was reached, while the growth rate decreased due to decreasing amount of available carbon source for the increasing biomass. Afterwards, during the  $\mu$ -controlled phase, the fungal growth was controlled via the feed flow as described later in chapter 2.6.6.

During the whole process, samples were taken in a 12 h rhythm. Nevertheless, sample processing differs between batch and fed-batch phase due to different requirements as the processes as well as goals differ.

The processing of the samples of the batch:

- Ergosterol determination
- Sugar analytics

The processing of the samples taken during the fed-batch was more complex:

- Cell Dry Weight, CDW
- Sugar analytics
- PEN/POX analytics
- Viability determination
- Atline determination of CDW via different methods
- Atline determination of ammonium and glucose concentration
- Light as well as confocal microscopy

### 2.2.2. Batch

The batch phases were conducted within the smaller Techfors-S bioreactor with a maximal volume of 10 L. Therefore, 6.5 L of the complex batch media were prepared as described in Posch & Herwig (2014). The pH probe was calibrated according to the manual during the setting up of the fermenter, while pO<sub>2</sub> probe and off gas analyzer were calibrated after the autoclaving.

With the inoculation of spores the actual batch phase starts. While certain process parameters were kept constant, see Table 4, the pH was not controlled. An exemplarily course of the pH among others can be seen in 3.2.1.

Table 4: Initial batch process parameters

Initial batch conditions		
Reactor volume	6.5	L
Temperature	25	°C
Pressure	1	bar
Aeration rate	1	vvm
pO <sub>2</sub>	≥ 40	%
Agitator speed	325	rpm

At the begin of the batch phase, the pH had a value of 5.5 - 6.5 due to the complex media components which differed from batch to batch, and was not corrected any further. The dissolved oxygen was kept above 40% via an increase of the agitator speed which is illustrated later in 3.2.2.

### 2.2.3. Transfer

The transfer marked a major step during the cultivation, as it represented the transition from batch to fed-batch phase. During the transfer event, the biomass was reduced to 10% and the undefined batch media was replaced by defined fed-batch media. Moreover, the broth was split up into two bioreactors and the biomass diluted 1:10 with defined fed-batch media.

### 2.2.4. Fed-batch phase

Directly after the transfer, the fed-batch phase began. In Table 5, the process parameters during the fed-batch are listed up:

Table 5: Initial fed-batch conditions

Initial fed-batch process conditions		
Reactor volume	6.5/ 13	L
pH	6.5 ± 0.05	-
Temperature	25	°C
Pressure	1	bar
Aeration rate	1	vvm
pO <sub>2</sub>	≥ 40	%
Agitator speed	500	rpm

As mentioned in Chapter 2.1.1,  $\mu$  control started after 24h of fed-batch cultivation. Moreover, 12 h after fed-batch start, above mentioned nitrogen and product precursor (POX) feeds were started and adapted according to certain criteria throughout the process. The regulation criteria for the two last-mentioned feeds are shown in Table 6.

Table 6: Initial rates of POX and nitrogen feed as well as manual regulation criteria during fed-batch.  $C_{\text{POX, broth}}$  and  $C_{\text{NH}_3, \text{broth}}$  are the concentrations of POX and ammonium, respectively, within the broth

Feed	Rate [mL/(L*h)]	Adaption
POX	0.3	$C_{\text{POX, broth}} \text{ [g/L]} < 1.5 \text{ [g/L]} \rightarrow$ increase of 20%
Nitrogen	1.0	$0.5 \text{ [g/L]} \leq C_{\text{NH}_3, \text{broth}} \leq 1.5 \text{ [g/L]}$ $\rightarrow \pm 20\%$ of feed rate

The cultivation process was terminated if one of following criteria was met:

- Drop of penicillin production or complete decline , respectively
- Increased broth viscosity, making an adequate mixing of the broth and mass transfer impossible

### 2.2.5. Down regulation of dissolved oxygen during $\mu$ controlled fed-batch phase

During the final run, FB9, the dissolved oxygen levels were decreased to 5% during the  $\mu$ -controlled phase of the fed-batch. The strategy is illustrated in Figure 9. Therefore a mixture of nitrogen and air was used instead of pure air. Moreover, the remaining process parameters were completely identical and the cultivation was conducted as the others.

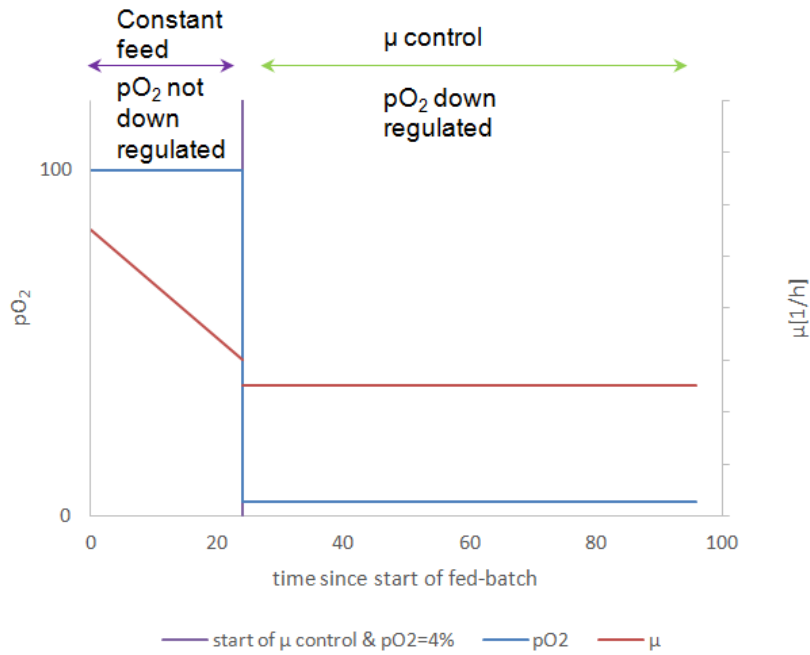


Figure 9: pO<sub>2</sub> control strategy during the final fed-batch

In order to increase the reproducibility, especially compared to FB7 as they had the same  $\mu$  set-point, an alternative strategy mimicking the possible effect of the agitator speed had to be chosen. Therefore, an atline CDW determination, of 25 g/L was chosen as criteria for a linear increase of the agitator speed.

## 2.2.6. Control strategy of $\mu_{viable}$

### 2.2.6.1. Atline

1. Determination of the viable biomass concentration according to equation 1:

**Equation 1:**  $c_{x, viable}$  is the viable biomass concentration.  $c_{x, total}$  is the biomass concentration including viable as well as already dead biomass. Viability is the percentage of viable biomass of the culture.

$$c_{x,viable} [g/L] = viability [\%] * c_{x,total} [g/L]$$

The values for viability and  $c_{x, total}$  were obtained according to the methods described in Chapter 2.2.7.2.2. and 2.2.7.5.5., respectively.

2. Calculation of a linear regression between  $c_{x, viable}$  and the corresponding delta capacitance signal of the last 3-4 sampling points:

**Equation 2:**  $c_{x, viable online}$  is the calculated viable biomass concentration based on the delta capacitance signal.  $p_{offset}$  as well as  $p_{slope}$  are the intercept respectively slope of the linear regression.  $dCap_{smoothed}$  is the smoothed delta capacitance signal with Savitzky-Golay-filter.

$$c_{x,viable online} [g/L] = p_{offset} + dCap_{smoothed} * p_{slope}$$

3. Calculation of  $r_x$  based on equation 3:

**Equation 3:**  $r_x$  is the volumetric building rate of the biomass.  $c_{x, viable online}$  is the calculated viable biomass concentration based on the delta capacitance signal.  $RV$  is the reactor volume.  $\mu_{aimed}$  the  $\mu$  set point.

$$r_x [g/h] = c_{x,viable online} [g/L] * RV [L] * \mu_{aimed} [1/h]$$

4. Calculation of  $r_s$  based on equation 4:

**Equation 4:**  $r_s$  is the volumetric substrate uptake rate.  $r_x$  is the volumetric building rate of the biomass.  $Y_{x/s}$  is the biomass per substrate yield

$$r_s[\text{g/L}] = r_x[\text{g/L}] / Y_{x/s}[\text{g/g}]$$

Finally, the calculated volumetric substrate uptake rate,  $r_s$  was used to adapt the feed flow via the density and concentration of the glucose feed.

Nevertheless, this method was dismissed during the practical work of my Thesis, as it showed several disadvantages:

- Not automated as the yield  $Y_{x/s}$  had to be constantly adapted and a regular recalibration was necessary
- Inaccuracy due to error of at line determination of  $c_{c, \text{total}}$  [g/L]

### 2.2.6.2. Online

Based on CDW and delta capacitance data points of previous experiments, a single linear regression was calculated including all available data points. Thereby, the  $\mu$ -control strategy needed less human interaction and drastically was simplified.

The viable biomass was calculated as followed:

**Equation 5:**  $c_{x, \text{viable online}}$  is the calculated viable biomass concentration based on the delta capacitance signal.  $p_{\text{offset}}$  as well as  $p_{\text{slope}}$  are the intercept respectively slope of the linear regression.  $d\text{Cap}_{\text{smoothed}}$  is the smoothed delta capacitance signal with Savitzky-Golay-filter.

$$c_{x, \text{viable online}} [\text{g/L}] = p_{\text{offset}} + (d\text{cap}_{\text{smoothed}} + p_{\text{offset corrected}}) * p_{\text{slope}}$$

In the next step, a PID controller was used to calculate the viable growth rate based on  $c_{x, \text{viable online}}$  of the last 300 data points, which corresponds to 5 minutes, and compared it to the set point of the growth rate. If necessary the feed flow was adapted. Thus, only one atline determination of the viable biomass was necessary in order to calculate the offset of the permittivity probe.

## 2.2.7. Analytical methods

### 2.2.7.1. Offline methods

#### 2.2.7.1.1. CFU determination of spore solution

In order to ensure that all batches were inoculated with the same amount of living spores, the CFU of the available spore solution was determined directly before the cultivation start. Therefore, several dilutions of the spore inoculum were plated on agar and incubated for at least 7 days at 25°C. The medium for the agar plates was similar to the complex batch medium with the addition 25g/L agar.

After counting the colony forming units, the living spore concentration was calculated and used to determine the needed volume of the spore solution for the batch inoculation.

### **2.2.7.1.2. Ergosterol extraction and preparation for HPLC measurement**

The measurement of the ergosterol concentration was performed during the batch in order to calculate the biomass concentration due to error prone results of the CDW method. Reason for the inaccuracy of the CDW during the batch phase was the composition of the media, as it contained calcium oxide and complex components. These components are not appropriately removed during the washing step which prepared the samples for CDW measurement.

Previous in-house investigations revealed a linear correlation between ergosterol- and biomass concentration during a time point of approximately 30 h cultivation time. Thus, the ergosterol extraction and measurement could be used to replace CDW for the determination of the biomass concentration during a constraint time period.

For the ergosterol determination, broth was taken at 36 h of the batch and at the batch end, frozen at -20°C and stored for the actual sample preparation.

In order to extract the ergosterol, 2-4 mL of the sample were centrifuged at 4800 rpm and 4°C in glass vials. Next, the supernatant was discarded and the pellet resuspended in 5 mL deionized water and again centrifuged at the same conditions. Afterwards, 3ml of 10% KOH in methanol was added, vortexed for approximately 5 seconds, transferred to a new glass vial with screw cap and again vortexed for about one minute. Finally, the closed glass vials were saponified in a water bath at 80°C for 60 minutes. Moreover, the first 10 minutes the ultrasonic was turned on as well.

After cooling to room temperature, 1 mL of deionized water and 2 mL hexane were added and vortexed until no phase separation was detectable. Next, the hexane phase was transferred into another vial and the step repeated. Subsequently, the glass eprouvette was dried with pressured air over night.

In a final step, the dried pellet was resuspended in 800 µL methanol, centrifuged for 5 minutes at 14 000 rpm, transferred into HPLC vials and stored at -20°C until the actual measurement.

For the HPLC measurement of ergosterol, a Thermo Scientific UlitMate 300 system (Thermo Fisher Scientific, Massachusetts, US) in combination with an Eclipse Plus C18 column (Agilent, US), a reversed phase column, was used. As buffer respectively mobile phase 95% methanol which was degassed in a Sonorex Super RK 514 BH ultrasonic bath (Bandelin electronic GmbH, Berlin, Germany) was prepared. The flow rate for the elution was set to 1mL/min and the column heated to 23°C. The peaks of ergosterol were detected via an UV/VIS detector at 282nm. The resulting chromatograms were evaluated with Chromeleon 7 Chromatography Data System (Thermo Fisher Scientific, Massachusetts, US).

The samples were measured in triplicates.

### **2.2.7.1.3. Measurements of several sugars via ion-exchange chromatography**

Ion-exchange chromatography was used to quantify and qualify several sugars and metabolites during the batch as well as the fed-batch. Those sugars and metabolites were namely mannitol, fructose, galactose, glucose, sucrose, lactose and gluconic acid. Their measurement was necessary in order to calculate the C-balance and several rates, thus were needed for an adequate evaluation of the cultivations.

For sample preparation, broth was centrifuged twice for 10 minutes at 4°C and 4800 rpm, the supernatant transferred and diluted with Milli-Q water.

As chromatographic system an ion chromatography system in combination with a Dionex column and a Dionex electrochemical PAD detector (Thermo Fisher Scientific, Massachusetts, US) in quadrupole potential mode was used. The column temperature was set to 30°C and eluted with a gradient profile of Milli-Q water, 0.1N as well as 1N NaOH. For evaluation of the chromatograms, Chromeleon 7 Chromatography Data System (Thermo Fisher Scientific, Massachusetts, US) was used.

#### 2.2.7.1.4. Cell dry weight – CDW determination

The CDW measurement was performed in order to determine the development of the biomass throughout the process. Thereby, it enabled the calculation of several rates, yields and specific rates such as specific uptake or production rates, as well as the specific growth rate.

For the CDW determination, which was performed in quadruplicate, 5mL of broth were transferred into weighted glass vials and centrifuged for 10 minutes at 4°C and 4800 rpm. After removal of the supernatant, which was partly used for other analytics, the pellet was resuspended in 5mL of deionized water via vortexing and again centrifuged at the same conditions. Next, the supernatant was discarded and the glass vial containing the pellet dried for at least 72h at 105°C.

In a final step, the dried vials were weighted, after cooling down to room temperature in a desiccator, and used to calculate the CDW.

#### 2.2.7.2. Atline methods

##### 2.2.7.2.1. Measurement of Phenoxyacetate and Penicillin V

As it was the goal of my Thesis to prove a dependency of the specific penicillin production rate from the growth rate, an accurate determination of the penicillin concentration was a basic prerequisite. Moreover, the determination of the precursor phenoxyacetate was necessary in order to ensure a sufficient supplementation.

Sample preparation was as following: the broth supernatant which was removed during the CDW processing was again centrifuged for 10 minutes at 4°C and 14 000 rpm, and if necessary, diluted with a citrate buffer (3.8200 g/L citrate, pH set to 5.5 using NaOH).

The chromatographic system and program for evaluation were the same as the ones for the ergosterol measurement, which was described in Chapter 2.2.7.1.2.

For elution the buffer shown in Table 7 was used:

**Table 7: Composition of the mobile phase used for PEN/POX analytics via HPLC; before usage the buffer was degassed using an ultrasonic bath as described in the ergosterol measurement section**

Compound	Concentration	Unit
C <sub>2</sub> H <sub>3</sub> N	280	mL/L
KH <sub>2</sub> PO <sub>4</sub>	0.6805	g/L
H <sub>3</sub> PO <sub>4</sub>	0.692	mL/L



The elution was performed with a flow rate of 1.0 mL/min and a column temperature of 30°C. As detection wavelengths, 192 nm as well as 210 nm were set.

#### 2.2.7.2.2. Viability assay – propidium iodide staining

In order to determine the amount of viable biomass, a viability assay based on propidium iodide, PI, was chosen. PI is a dye which cannot pass through intact cell membranes of living cells but through the perforated one of dead cells. As described above in section 2.6.6, this method was necessary for the  $\mu$ -control strategy as well as to correlate a certain delta capacitance to a certain viable biomass concentration.

For the PI based viability assay, fresh broth was diluted 1:5 with PBS buffer. One aliquot was microwave treated for 30 seconds at 940 W (Philips, Amsterdam, Netherlands). This step was performed in order to determine the total DNA amount of the sample, as we assumed that the microwave treatment led to an overall cell membrane perforation of the population. Further, two one millilitre aliquots of each - microwaved treated and untreated sample - were transferred into 1.5 mL micro-centrifuge tubes (VWR, Pennsylvania, USA) and centrifuged for 15 minutes at 500 rpm at room temperature, RT. In order to wash the samples, 600  $\mu$ L supernatant were removed and 800  $\mu$ L PBS buffer added, resuspended and centrifuged at the same conditions. Afterwards, 800  $\mu$ L supernatant were removed and 600  $\mu$ L PBS buffer added.

Finally, three times 100  $\mu$ L from each aliquot were transferred into a well of a 96 well-plate. Furthermore, 1  $\mu$ L of a 200  $\mu$ M PI solution was added, shortly vortexed and incubated for 20 minutes at RT in the dark.

For the fluorescence determination, a TECAN Infinite® 200 Pro plate reader (Tecan Trading AG, Männedorf, Switzerland) with following settings (see Table 8) was used:

**Table 8: TECAN settings which were used for the viability determination**

<b>Excitation wavelength</b>	535
<b>Emission wavelength</b>	600
<b>Excitation bandwidth</b>	9
<b>Emission bandwidth</b>	20
<b>Gain</b>	100
<b>Number of flashes</b>	25
<b>Integration time</b>	20
<b>Lag phase</b>	0
<b>Settle time</b>	0
<b>Z-position (manual)</b>	20000

Based on the result of the fluorescence measurement, the viability percentage of the culture was determined as follows:

**Equation 6: Calculation of the viability**

$$Viability = 1 - \frac{\text{average of not microwaved sample}}{\text{average of microwaved sample}}$$

The composition of the PBS buffer is shown in Table 9.

**Table 9: PBS buffer**

Component	Concentration
CaCl <sub>2</sub> stock solution (2.65 g CaCl <sub>2</sub> *2H <sub>2</sub> O per 1000 mL dH <sub>2</sub> O)	50 mL/L
KCl	0.2 g/L
KH <sub>2</sub> PO <sub>4</sub>	0.2 g/L
MgCl*6H <sub>2</sub> O	0.1 g/L
NaCl	8.0 g/L
Na <sub>2</sub> HPO <sub>4</sub> *2H <sub>2</sub> O	0.764 g/L

### 2.2.7.2.3. Confocal microscopy

In order to underline the viability measurement via PI staining, confocal microscopy was used. As staining agents, PI was used for dead cells while fluorescein diacetate, FDA, was used to stain metabolically active and therefore viable cells.

For sample preparation, fresh broth was diluted 1:10 with PBS buffer with a final volume of 1 mL, transferred into 1.5 micro-centrifuge tubes (VWR, Pennsylvania, USA) and centrifuged for 2 minutes at 500 rpm and room temperature. Next, the sample was washed by replacing 800 µL supernatant, which was discarded, with 800 µL PBS buffer, the pellet resuspended, centrifuged it with the same conditions as before and, again, replacing 800 µL supernatant with 800 µL PBS buffer. The PBS buffer which was used for confocal microscopy was the same as the one for the PI based viability assay and described in Table 9. Afterwards, 10 µL of 200 µM PI solution were added and the samples were incubated for at least 10 minutes.

For microscoping, 20 µL of the prepared sample were pipetted onto a microscope slide (Carl Roth GmbH, Karlsruhe, Germany) and 2 µL of a 1:100 with PBS buffer diluted FDA solution added before covering with a cover slide.

As confocal microscope, an eclipse TE2000-E (Nikon, Tokyo, Japan) was used. PI and FDA were measured separately. Therefore, the corresponding lasers and settings for the transmission detector were adapted successively. The settings of the confocal microscope are given Table 10:

**Table 10: Excitation and emission wavelength for PI and FDA**

Dye	Excitation wavelength [nm]	Emission wavelength [nm]
PI	543	580
FDA	488	507

Due to an increasing fluorescence caused by FDA over time, the gain and offset were adjusted if necessary. The resulting pictures were recorded at a resolution of 1024 dpi and about 2  $\mu$ s pixel gain time.

#### **2.2.7.2.4. Enzymatic assays**

In order to fulfil the ammonium ranges according to the SOP, given in Table 6, as well as glucose limitation, their concentrations had to be determined. Therefore, a Cedex bio HT Analyzer (Roche Diagnostics, Mannheim, Switzerland) in combination with the corresponding, commercial available enzymatic assay kits was used.

For preparation, supernatant taken from CDW measurement was centrifuged for 10 minutes at 14800 rpm and 4°C and diluted with deionized water if necessary.

#### **2.2.7.2.5. Atline biomass determination**

At the beginning of my Thesis, the atline biomass determination via cell culture vials was used. Nevertheless, it appeared to be insufficient. Therefore, several other methods, which were described as well, are developed and tested in order to obtain a more reliable measurement.

##### **2.2.7.5.1. Cell culture vials**

The biomass were determined by transferring 5  $\mu$ L of fresh broth into PCV packed cell volume tubes (TPP, Trasadingen, Switzerland) which was centrifuged for 10 minutes at 7000 rpm. Then the tubes were turned by 180° in order to prevent a one-sided sedimentation as well as blockage of the canal and centrifuged for another 10 minutes but 10 000 rpm. Afterwards the volume of the biomass was read.

The CDW was finally calculated via a linear regression which was created based on previous data.

##### **2.2.7.5.2. Falcons**

For the biomass determination using falcon tubes (Centrifuge Tubes Super Clear®, VWR, Pennsylvania, USA), 5 mL of fresh cultivation broth were transferred into 15 mL falcon tubes and treated identically like sample for to the CDW measurement. After a first centrifugation step for 10 minutes and 4500 rpm, the biomass was washed by replacing the supernatant with 5 mL of deionized water, and again centrifuged with the same conditions. Finally, the volume of the biomass was read.

Again, the CDW was finally calculated based on a linear regression which has been created using previous data.

##### **2.2.7.5.3. Serological pipettes**

Therefore, 5 mL of fresh cultivation broth were pipetted into 5 mL serological pipettes and the endings closed with Parafilm (PARAFILM®M, Pennsylvania, USA). After 10 minutes for sedimentation, the volume of the biomass was read.

##### **2.2.7.5.4. 1.5 micro-centrifuge tubes**

For the biomass determination via 1.5 micro-centrifuge tubes (VWR, Pennsylvania, USA) 1.5 mL of fresh cultivation broth were filled into 1.5 micro-centrifuge tubes and centrifuged for 10 minutes at 14800 rpm. Afterwards, the volume of the biomass was read.

#### **2.2.7.5.5. Wet weight**

The “wet weight” method for determination was identical to the offline CDW method as described in Chapter 2.2.7.1.4., just omitting the drying step.

The CDW was calculated via an exponential regression.

All of the described methods were tested during the first experiment and afterwards evaluated. The most sufficient one was the one based on the “wet weight”. Thus, it was the only one used after the first experiment (FB01 and FB02).

#### **2.2.7.3. Data evaluation**

Yields, rates and specific rates like the specific growth rate were calculated as stated elsewhere (Sagmeister et al., 2012). For data evaluation, MATLAB R2013b (The Mathworks, Massachusetts, USA) was used.

## 3. Results

### 3.1. Overview of cultivations

Overall, 9 fermentations were performed. They were carried out according to the ordinary SOP and the altered SOP with decreased dissolved oxygen respectively, as described in Chapters from 2.2.1. to 2.2.6.. Major difference between the cultivations was the aimed  $\mu$  set point and the used atline method for estimating the total biomass at a certain set point. An overview of all conducted cultivations is given in Table 11.

**Table 11: Fed-batch number, atline method for estimation of the total biomass,  $\mu$  setpoint [1/h], average  $\mu$  [1/h], used SOP and fed-batch ID of all performed cultivations.**

Fed-batch number	Method for atline determination of total biomass	$\mu$ set point [1/h]	Average $\mu$ [1/h]	SOP	Fed-batch ID
1	cell culture vials	0.050	0.049	Ordinary SOP	1_0.049
2	cell culture vials	0.020	0.007	Ordinary SOP	2_0.007
3	wet weight	0.040	0.038	Ordinary SOP	3_0.038
4	wet weight	0.020	0.020	Ordinary SOP	4_0.020
5	wet weight	0.030	0.032	Ordinary SOP	5_0.032
6	wet weight	0.020	0.012	Ordinary SOP	6_0.012
7	wet weight, but just as control	0.012	0.020	Ordinary SOP	7_0.020
8	wet weight, but just as control	0.004	0.007	Ordinary SOP	8_0.007
9	wet weight, but just as control	0.012	0.016	Altered SOP with decreased $pO_2$ of 4%	9_0.016

Throughout all performed experiments, except the dissolved oxygen limits of the final run, the process parameters were identical. Therefore, not every single cultivation is described completely, but only one batch and one fed-batch are described exemplarily. As reference batch cultivation, the first batch was chosen and FB4 representing the fed-batch cultivation. Results concerning the  $\mu_{viable}$ - $q_{pen}$ , viable relation include data of all performed data.

## 3.2. Batch phase

### 3.2.1. Trend of pH and CO<sub>2</sub>

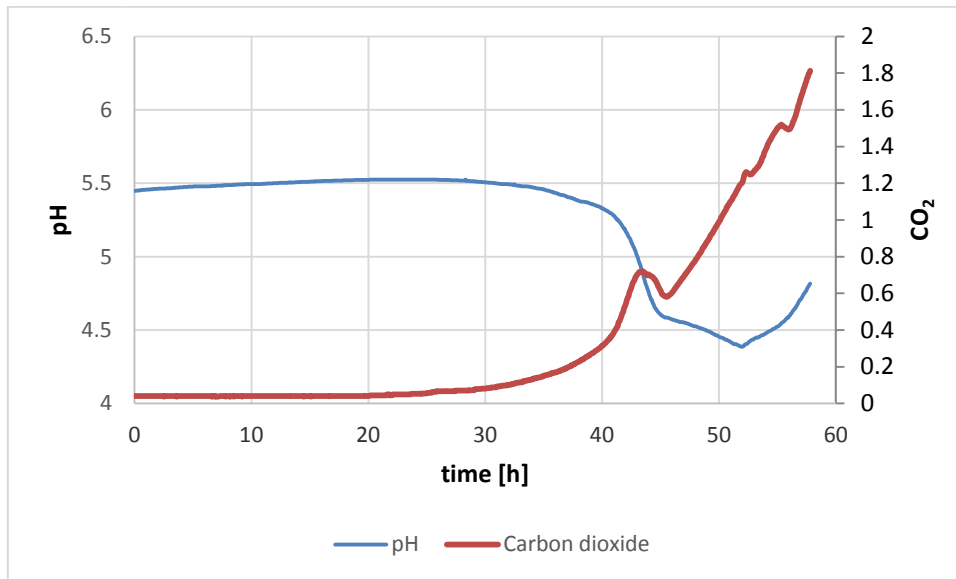


Figure 10: CO<sub>2</sub> content within the offgas and pH during the batch phase

Till the 24<sup>th</sup> hour of the batch neither changes on the CO<sub>2</sub> content in the offgas nor the pH are detectable as visible in Figure 10. The CO<sub>2</sub> is 0.04 % which is equal to the amount of CO<sub>2</sub> in the air while the pH has a value of 5.5. At 24 hours after the start of the batch, the CO<sub>2</sub> content in the offgas starts to increase, while the pH decreases. The positive trend of an increasing CO<sub>2</sub> offgas content continues throughout the remaining batch. The pH reaches a minimum of 4.4 at 51.1 hours of the batch and starts to increase until the criteria for the fed-batch start, a pH shift of 0.5 after reaching the minimum is fulfilled and the batch ended.

### 3.2.2. Trend of dissolved oxygen and agitator speed

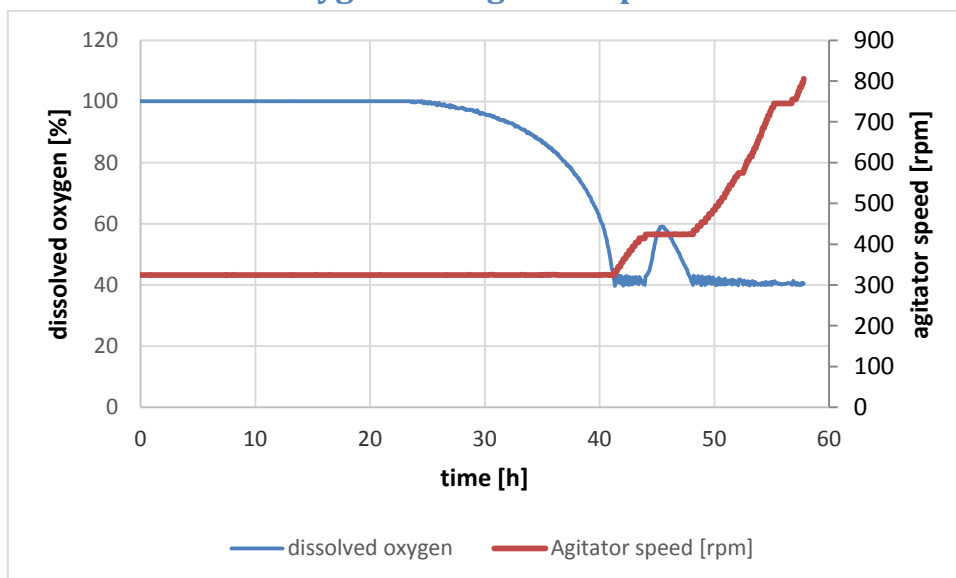


Figure 11: Dissolved oxygen [%] as well as stirrer speed [rpm] during the batch phase

As illustrated in Figure 11, during the first 24 hours of the batch no changes of the dissolved oxygen occur. Thus, the agitator speed does not change and stays constant at 325 rpm. At about 26.6 hours the amount of dissolved oxygen starts to decrease with increasing speed, but not resulting in a change of the agitator speed. Finally, at about 41.2 hours, the dissolved oxygen has fallen below the set threshold value of 40 % and therefore resulting in an increasing stirrer speed. After 43.9 hours since inoculation, dissolved oxygen level increases again reaching a maximum of 59 % at 45.5 hours and sinks within 3 hours to 40 %. During this time, agitator speed stays constant at a level of 425 rpm. The moment dissolved oxygen level falls again below the threshold value of 40 %, the agitator speed increases constantly throughout the remaining batch reaching 795 rpm at the batches end.

### 3.2.3. Sugars & metabolites

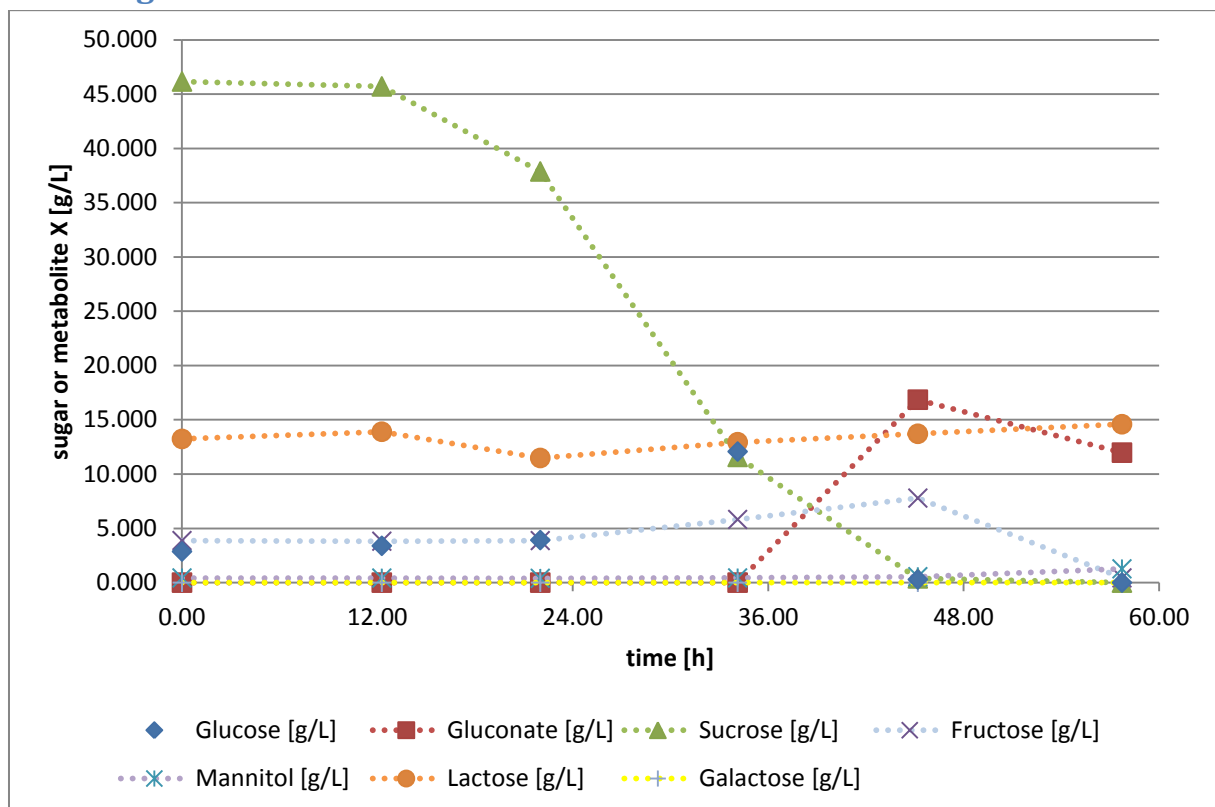


Figure 12: Concentration of the glucose, sucrose, fructose, lactose, lactose, mannitol and gluconate [g/L] within the batch media during the batch phase of the fermentation.

Figure 12 gives an overview of the trend of sugars and metabolites throughout the batch. Within the first 12 hours of the batch phase the concentrations of all carbon sources stay nearly constant. The most strongly represented component is the sugar sucrose with a concentration of approximately 45 g/L, followed by 13 g/L lactose, 4 g/L fructose, 3 g/L glucose and 0.4 g/L mannitol. Neither galactose nor gluconate are detected.

34 hours after inoculation the sucrose concentration has already declined to 38 g/L and is nearly completely consumed at 45 hours. At the end of the batch no sucrose is detectable. Contrary, the glucose concentration increases and reaches its highest measured concentration of 12 g/L at 34 hours, but has completely vanished at the batches end as well.

At the same time, fructose has slightly increased to 8 g/L compared to the start concentration of 4 g/L, but is finally no more detectable at the end of the batch.

The salt of gluconic acid, gluconate, is only detected at the end of the batch with a concentration of 12 g/L.

The mannitol concentration is constant during the batch phase while galactose is not detected at all throughout the batch.

### 3.2.4. Ergosterol concentration and calculated biomass concentration as well as $\mu_{max}$ of the batch phase

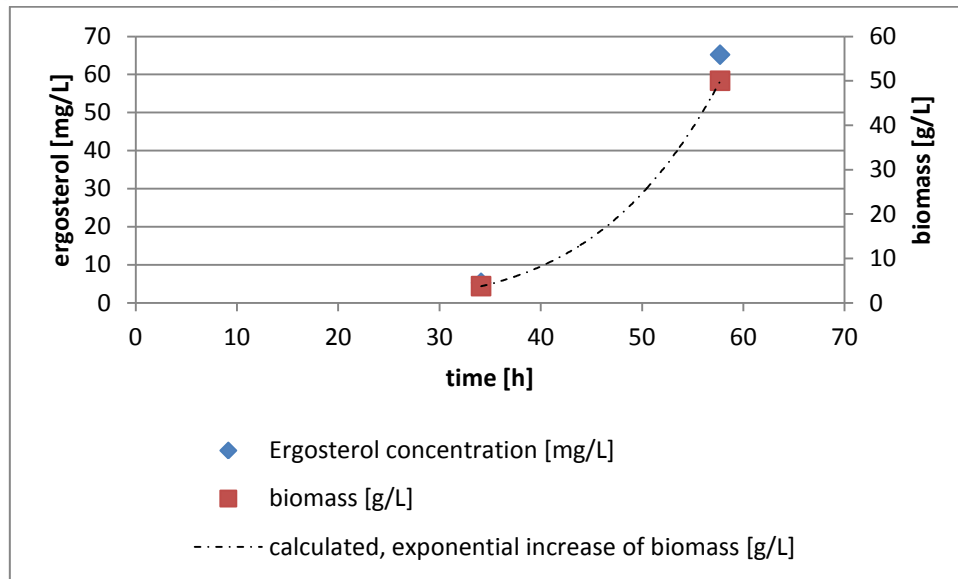


Figure 13: Ergosterol [mg/L] data as well as calculated biomass [g/L] of FB1.

In Figure 13 the results of the ergosterol measurement as well as the calculated biomass concentration are illustrated. At 34.12 hours after inoculation, a concentration of 5.26 mg/L ergosterol was measured. After 57.72 hours, the ergosterol concentration has increased to 65.18 mg/L. Based on these data, the biomass concentration was calculated using linear regression with the result of 3.76 g/L after 34.12 hours respectively 50.0 g/L after 57.72 hours. These biomass concentrations are used to calculate the maximal growth rate,  $\mu_{max}$ , of the batch phase based on following formula. The calculated maximal growth rate of the batch phase is given in Table 12.

Equation 7: Formula to calculate the grown biomass under optimal conditions.  $X$  is the absolute amount of the biomass.  $X_0$  is the initial biomass,  $e$  is the exponential function.  $\mu_{max}$  is the maximal growth rate.  $t$  is the time.

$$X = X_0 * e^{\mu_{max} * t}$$

In order to calculate the maximal growth rate,  $\mu_{max}$  the formula was rearranged:

Equation 8: Rearrangement of the formula

$$\mu_{max} = \frac{1}{t} * \ln \left( \frac{X}{X_0} \right)$$

Table 12: Result of  $\mu_{max}$

$\mu_{max}$ [1/h]	0.109
-------------------	-------



## 3.4. Fed-Batch cultivation

### 3.4.1. $C_x$ over time

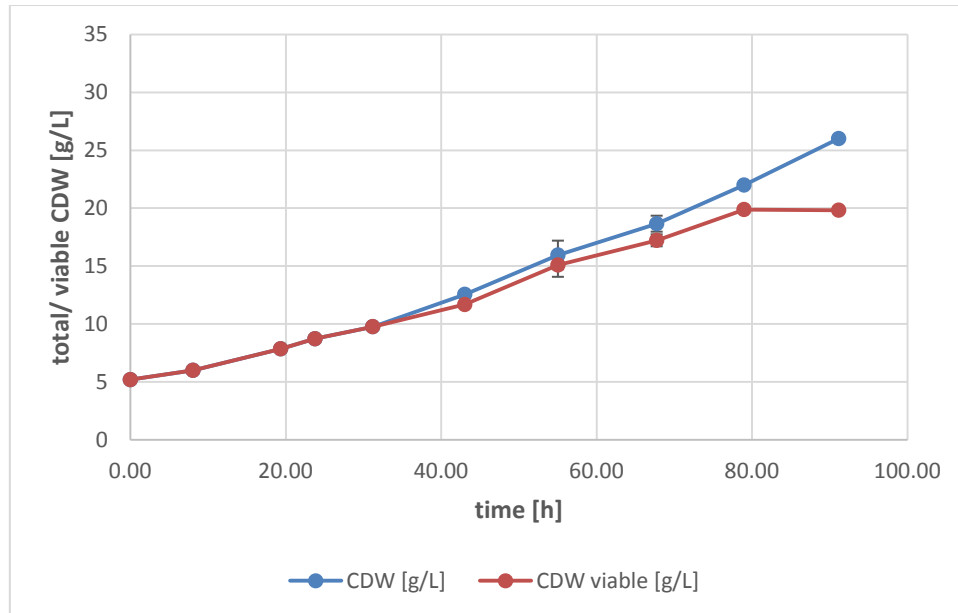


Figure 14: Development of the total cell dry weight [g/L] (blue) as well as viable cell dry weight [g/L] (red) of the fed-batch phase of the fourth cultivation with a  $\mu$  set point of  $0.02 \text{ h}^{-1}$ .

During the fed-batch phase of the cultivation a continuous as well as statistically significant increase of the total cell dry weight, including dead and viable biomass is visible in Figure 14. The same trend, a continuous and statistically significant increase, is exhibited by the viable cell dry weight, which excludes dead biomass. Comparing the two of them, the viable with the total cell dry weight, a nearly identical trend of biomass increase can be seen. Nevertheless, the viable cell dry weight exhibits a lower slope than the total cell dry weight which results in a lower value of 19.8 g/L at the end of the fed-batch compared to the total cell dry weight of 26.0 g/L, though they share an identical initial biomass of 5 g/L.

### 3.4.2. $C_{Pen}$ over time

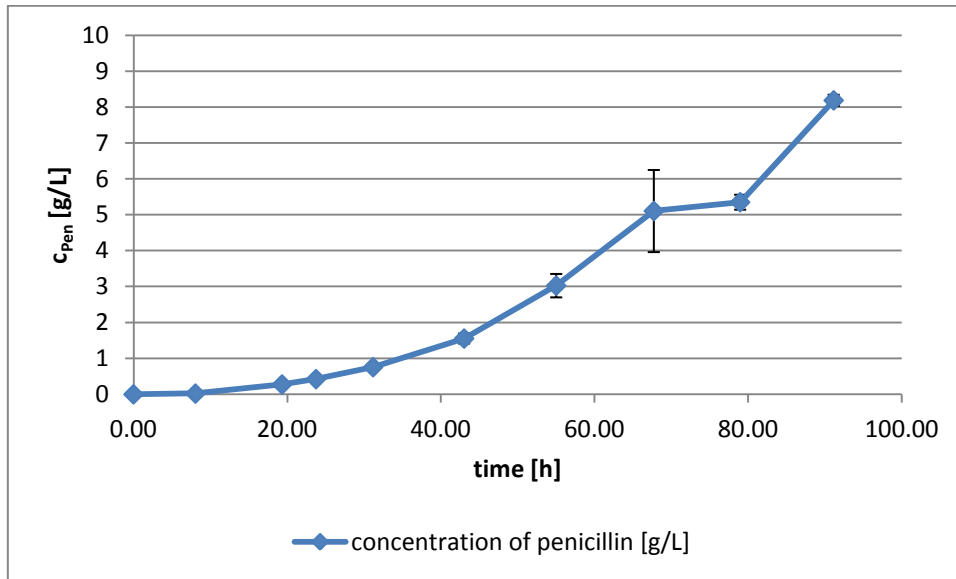


Figure 15: Penicillin concentration [g/L] in the supernatant of the fermentation broth during the ongoing cultivation FB4 with a  $\mu$  set point of  $0.02 \text{ h}^{-1}$ .

Figure 15 exhibits the development of the penicillin concentration of the FB4 during the fed-batch phase. At the beginning of the fed-batch ( $t=0$ ), there was no penicillin detectable. Nevertheless, within the first few hours penicillin production started and revealed a continuous as well as statistically significant increase during the whole cultivation resulting in 8.2 g/L penicillin at the end of the fed-batch.

### 3.4.3. Sugar concentrations during fed-batch

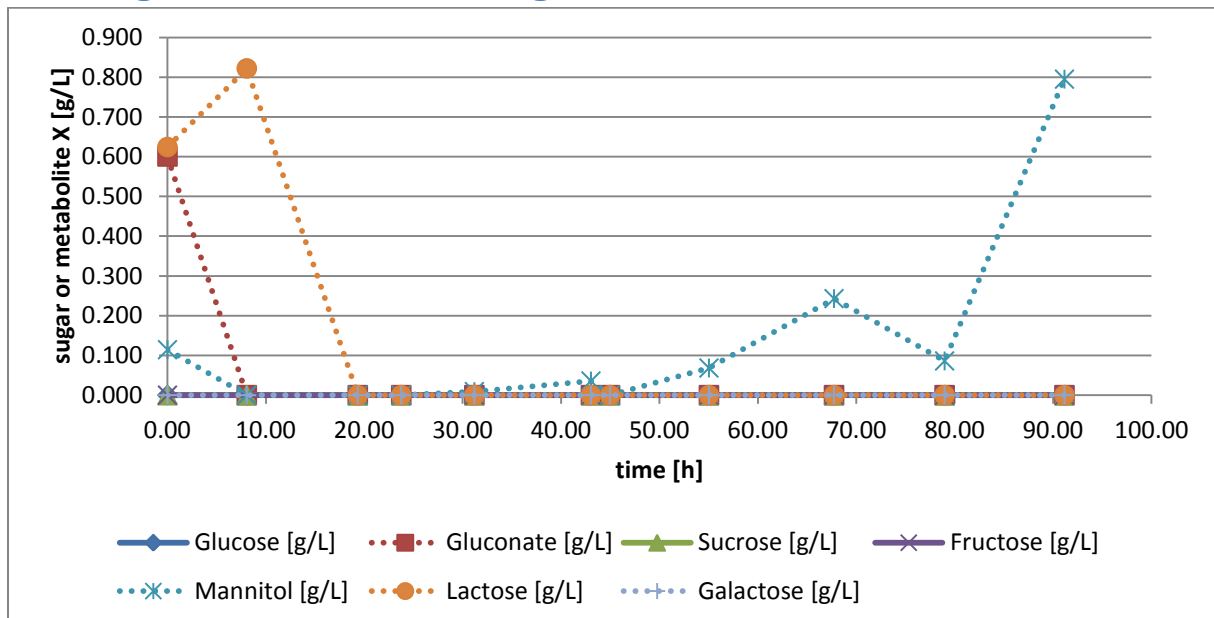


Figure 16: Progress of the concentration of different sugars (glucose, gluconate, sucrose, fructose, mannitol, lactose and galactose) within the fermentation broth during the fed-batch phase. Start of fed-batch is  $t=0$

Figure 16 gives an overview of the trend of sugars and metabolites throughout the fed-batch. Throughout the whole fermentation no glucose was detectable - the same trend is revealed for other

sugars, namely sucrose, fructose as well as galactose. No trace of one of this sugar was detectable through the whole fed-batch process.

Contrary, the sugars and metabolites gluconate, lactose and mannitol exhibit a different development. On the one hand, gluconate as well as lactose are present at the start of the fed-batch phase but decrease and finally vanish completely within the first 20 hours. On the other hand, low concentrations of mannitol are detectable in the beginning of the fed-batch cultivation, but vanish rapidly similar to lactose and gluconate. Nevertheless, in contrast to lactose and gluconate which are after depletion no more present within the fermentation broth, mannitol is slowly restored and its concentrations increased during the remaining cultivation time until abortion.

#### 3.4.4. $Y_{x/s}$ over time

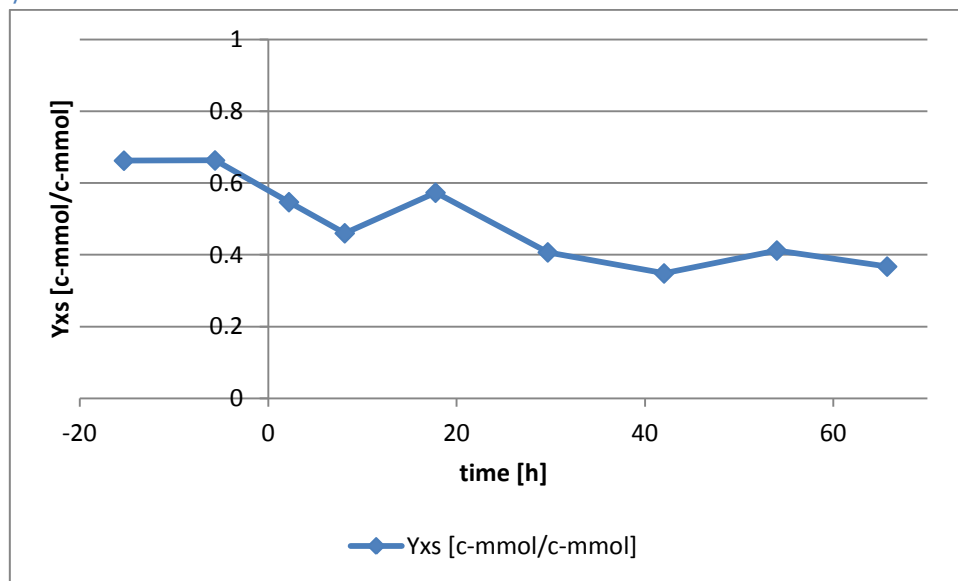


Figure 17:  $Y_{x/s}$  [c-mmol/c-mmol] during the progress of the fermentation FB4. T=0 is start of  $\mu$  control, before start of  $\mu$  control the culture was fed with a constant feed rate.

The yield of biomass per substrate " $Y_{x/s}$ " exhibits as visible in Figure 17, drastic changes during the fermentation. During the phase with a constant feed, until 0h, it is constant at 0.66 c-mmol/c-mmol and decreases rapidly the moment, the  $\mu$  control is started. Within the first 18 hours of the  $\mu$  controlled phase, " $Y_{x/s}$ " increases until reaching a second maximum of 0.57 c-mmol/c-mmol. Afterwards, it drops and exhibits a negative trend resulting in a constantly decreasing  $Y_{x/s}$  throughout the fermentation.

### 3.4.5. Growth rate “ $\mu$ ” & specific penicillin production rate “ $q_{pen}$ ”

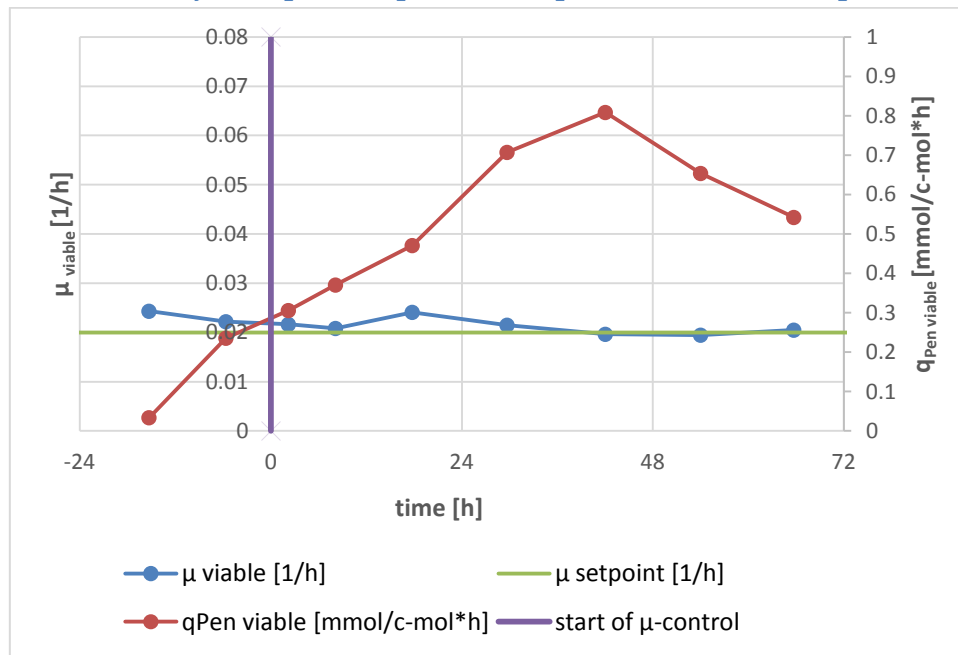


Figure 18: Growth rate of viable biomass  $\mu_{viable}$  [1/h] (blue marks) and specific penicillin production rate of viable biomass  $q_{pen, viable}$  [mmol/c-mol\*h] (red marks) of FB4. As time point zero, the start of the  $\mu$  control was chosen (violet line). The aimed growth rate of the fermentation is 0.02 [1/h] (green line). T=0 is start of  $\mu$  control, before start of  $\mu$  control the culture was fed with a constant feed rate.

Figure 18 plots the development of the viable biomass growth rate “ $\mu_{viable}$ ” [1/h] as well as its specific penicillin production rate “ $q_{pen, viable}$ ” in mmol/c-mol\*h during the fourth fed-batch “FB4”. Taking a closer look at  $\mu_{viable}$ , a slow decrease during the first 24 hours, the not  $\mu$  controlled phase, of the fed-batch is visible. After the start of the  $\mu$  control,  $\mu_{viable}$  approximates the chosen set point, 0.02 1/h, for the cultivation and stays nearly constant throughout the remaining fed-batch. Contrary, the specific penicillin production rate of the viable biomass exhibits drastic changes over the course of time. At the beginning of the cultivation,  $q_{pen, viable}$  starts near zero and increases during the first 24 h of the fed-batch. This trend, the increase of  $q_{pen, viable}$  continues in a constant way after the start of  $\mu$  control. Nevertheless, after reaching a maximum at 42 h,  $q_{pen, viable}$  starts to decrease without recovery during the remaining cultivation.

### 3.5. Atline methods for biomass concentration determination

Though 5 different atline methods for the determination of the biomass concentration were mentioned, only three of them are presented here. Reason for this, is that problems during the performance of the method occurred. The pellet at the end of the 1.5 mL-tube-method was too unstable making an accurate reading of the biomass impossible. Further, the sealing of the serological pipettes was problematic. Thus, only cell culture vials, biovolume and wet weight are presented here.

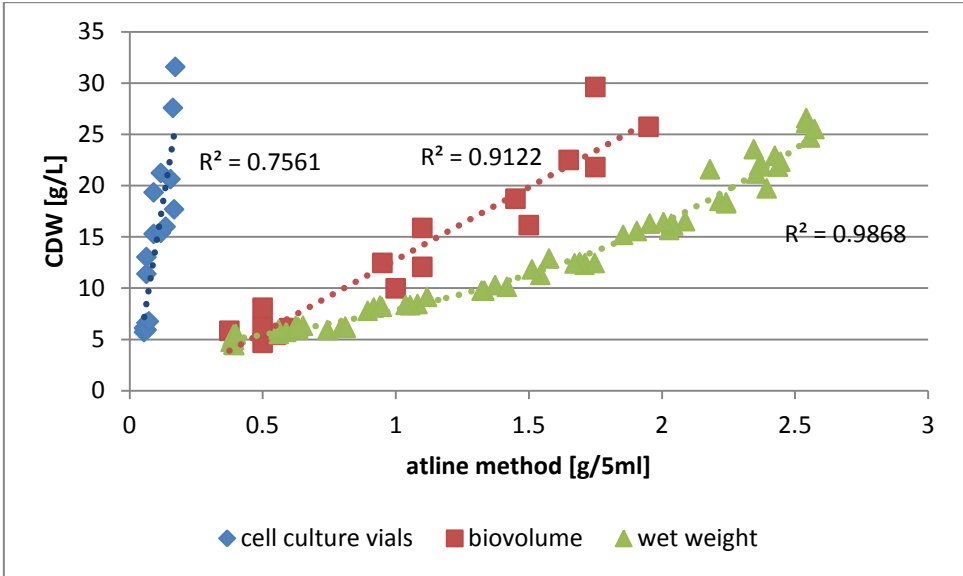


Figure 19: Comparison of the applicable methods for the atline biomass concentration. Cell culture vials and biovolume data fitted with a linear regression, wet weight data with an exponential regression.

As visible in Figure 19, the presented atline methods for the determination of  $c_x$ , differ in the  $R^2$ , the coefficient of determination. The weakest method with a  $R^2$  of 0.7561 is the one based on the cell culture vials. According to the  $R^2$  of 0.9122 respectively 0.9868 of the biovolume and wet weight method, these show a significantly better performance.

### 3.6. Correlation between dCap signal and viable biomass

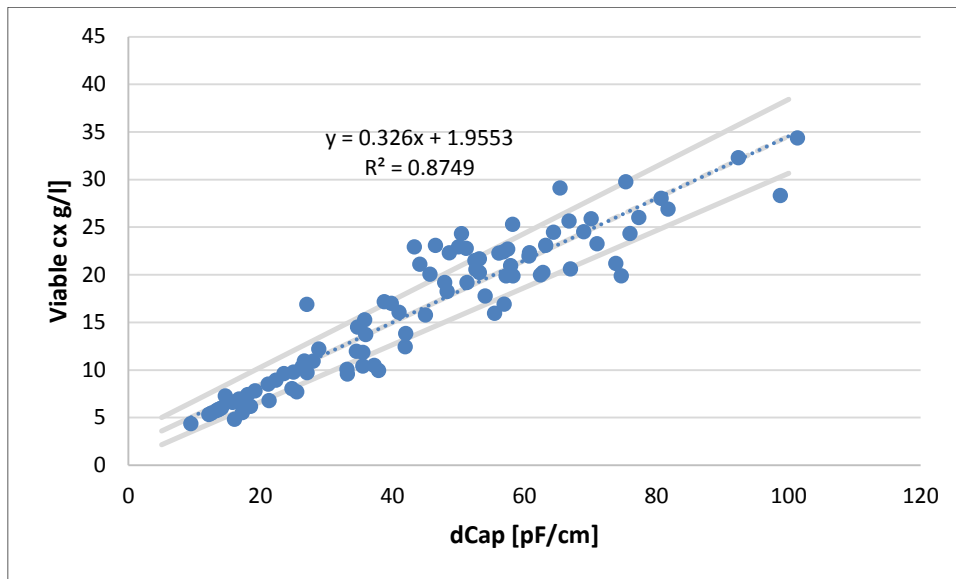


Figure 20: Correlation of the delta capacitance signal and the viable biomass concentration.

The dCap signal and the correlated biomass concentrations show a linear correlation with a regression line visible in Figure 20. Moreover, the regression line has a coefficient of regression of 0.8749.

### 3.7. Comparison of $\mu$ -control strategies

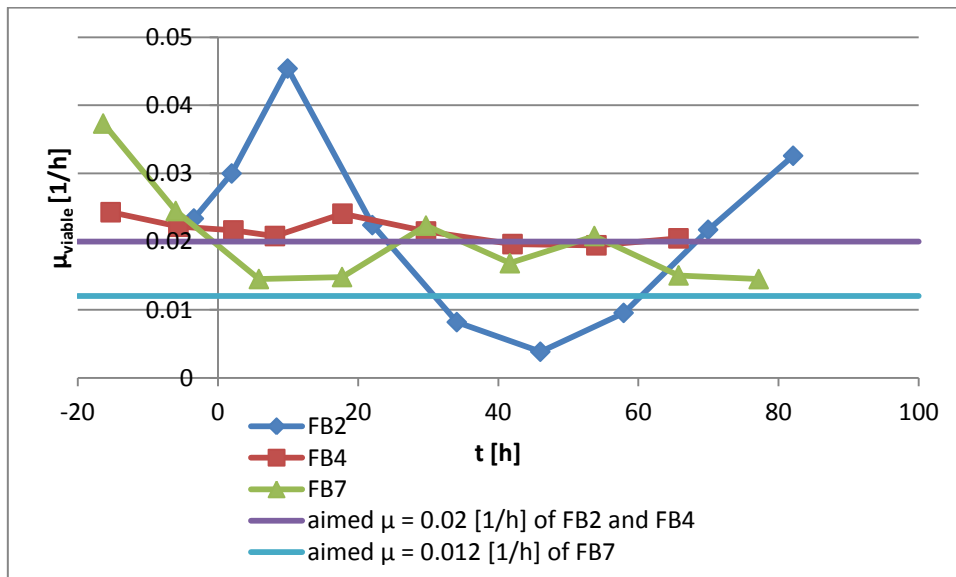


Figure 21: Comparison of different variations of the  $\mu$  control strategy via the achieved viable growth rate  $\mu_{viable}$ .  $T=0$  is start of  $\mu$  control, before start of  $\mu$  control the cultures were fed with a constant feed rate.

Figure 21 illustrates the comparison of different variations of the  $\mu$  control strategy. FB2 and FB4 were performed with a continuously recalibration of the online biomass estimation by calculating the biomass at distinct sample points. While the biomass was estimated via biomass vials during FB2, the  $c_x$  estimation during FB4 was carried out via the wet weight method. Contrary, FB7 is performed without continuously recalibration of the online biomass estimation. The complete control strategy is

based on a correlation which was created from data of previous runs and thus is carried out online without including atline measurement.

During the first 24 h of the fed-batch, which is the uncontrolled phase, the viable growth rates of the fermentation performed with different variations of the control strategy are not constant but approximate a certain value. After activating the  $\mu$  control their behavior differs. Taking a closer look at the development of the viable growth rate of FB2, you see that it increases at first, then starts to decrease which leads to constant phase of nearly 24 hours and finally increases again. Contrary, FB4 is constant throughout the whole process, not showing major changes in its viable growth rate. The viable growth rate of FB7 is nearly constant over the whole process, though not as constant as FB4. After the start of the  $\mu$  controlled phase,  $\mu_{\text{viable}}$  is constant for the first 20 hours, then slightly increases but finally decreases, reaching values close to the beginning.

### 3.8. $\mu$ - $q_{Pen}$ evaluation

#### 3.8.1. Single data points

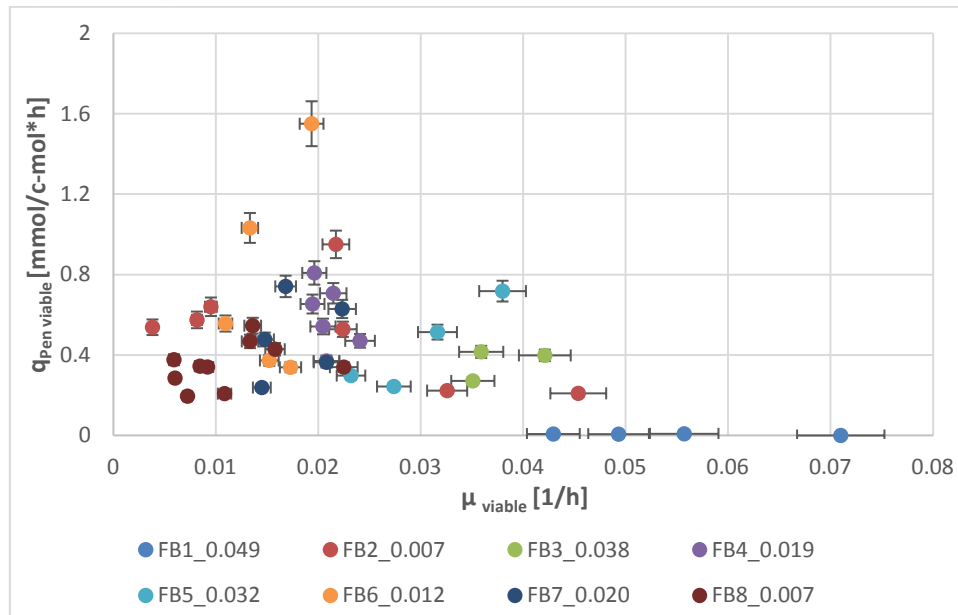


Figure 22: Plot of  $\mu_{viable}$  and corresponding  $q_{pen,viable}$  data points of all performed cultivations. Values before  $\mu$  controlled phase are not included, only data pairs recorded after start of  $\mu$  control are shown.

Figure 22 shows all calculated  $\mu_{viable}$ - $q_{pen,viable}$  data pairs derived from all performed cultivations. The range of controlled  $\mu_{viable}$  which were evaluated from all performed fermentation according to standard operation procedure varies from a minimum of 0.004 1/h to a maximal growth rate of 0.071 1/h. Corresponding  $q_{pen,viable}$  ranges from a minimum of 0 mmol/c-mol\*h to a maximum of 1.55 mmol/c-mol\*h. In general, data pairs of  $\mu_{viable}$  and  $q_{pen,viable}$  are located in a  $\mu$  range of 0.004-0.045 1/h, excluding FB1 through which carbon limitation wasn't completely/continuously accomplished, and a  $q_{pen,viable}$  are of 0.2-1mmol/c-mol\*h, excluding the maximal  $q_{pen,viable}$  of FB6 which was only reached once throughout all experiments.



### 3.8.2. Mean values

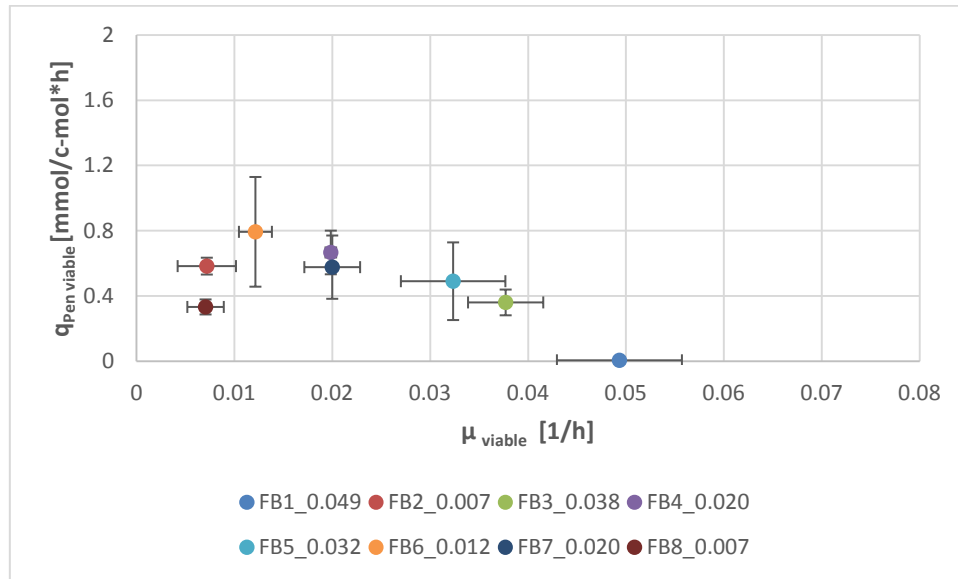


Figure 23: Illustration of  $\mu_{viable}$ -  $q_{pen, viable}$  relation. Shown data points are  $\mu_{viable}$  and  $q_{pen, viable}$  mean values of a single fermentation during the  $\mu$  controlled phase as well as over a time period of 24h through which  $\mu$  was considered as constant.

Figure 23 illustrates the mean values of  $\mu_{viable}$  and corresponding  $q_{pen, viable}$  which were calculated from six independently performed cultivations. As visible, the maximum of the specific penicillin production rate of 0.8 mmol/c-mol\*h is reached at a viable growth rate of 0.012 1/h while a decrease or an increase of the viable specific growth rate results in a decreasing  $q_{pen, viable}$ . On the left side of the maximal  $q_{pen, viable}$ , thus a lower viable growth rate, the average growth rate of the fed-batches 2 and 8 reveal the same growth rate, but a difference in corresponding  $q_{pen, viable}$ . The same is visible on the right side of the curve showing the average values of fermentation with growth rates higher than 0.012 1/h: FB4 and FB7 have an identical average  $\mu_{viable}$ , but contrary to FB2 and FB8, the  $q_{pen, viable}$  of FB4 and FB7 are within each other's standard deviation. Moreover, the data reveal that during FB1 which was performed with an average growth rate of 0.049 1/h, the average  $q_{pen, viable}$  is nearly zero with a value of 0.007 mmol/c-mol\*h.

Nevertheless, the high error bars of the  $q_{pen, viable}$  of the fed-batches 5 and 6 cover the average  $q_{pen, viable}$  of all the other fermentations, excluding FB1.

### 3.8.3. Maximal specific penicillin production rate

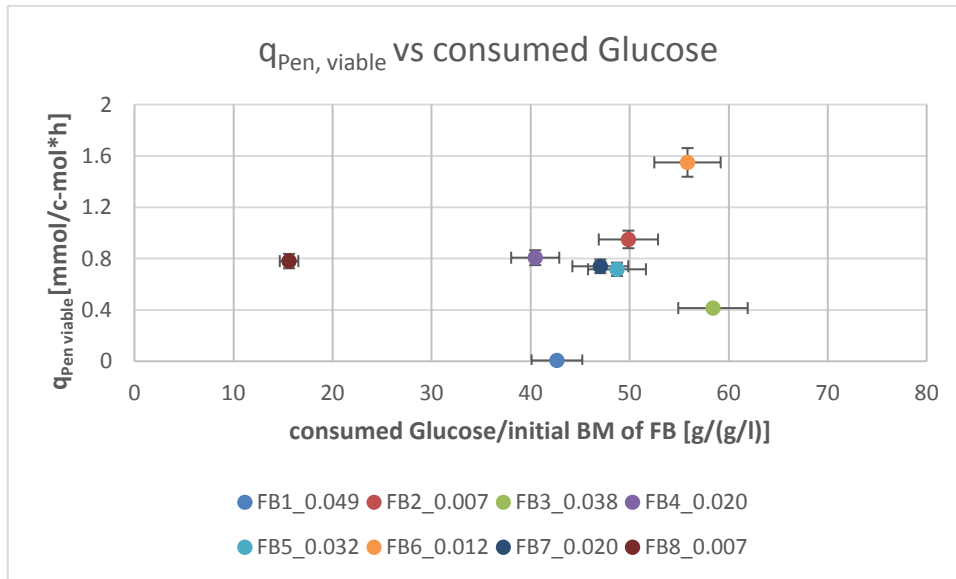


Figure 24: Plot of the maximal  $q_{pen, viable}$  [mmol/c-mol\*h] of the performed cultivations against the consumed glucose per initial biomass of the fed-batches [g/(g/L)] at the time of the maximal  $q_{pen, viable}$  [mmol/c-mol\*h].

As visible in Figure 24, all the maximal  $q_{pen, viable}$  values for all fermentations, except FB8 are reached with the consumption of at least 40-60g Glucose per initial biomass of the fed-batches g/(g/L).

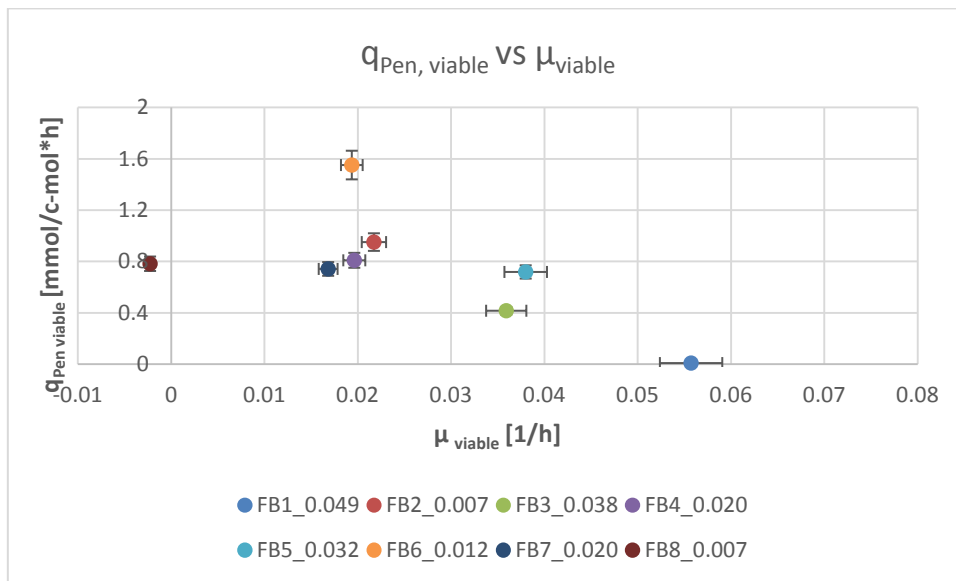


Figure 25: Plot of the maximal  $q_{pen, viable}$  [mmol/c-mol\*h] of every performed cultivation against their corresponding  $\mu_{viable}$  [1/h].

Figure 25 shows the calculated  $\mu_{viable\_q_{pen, viable}}$  data pairs according to the criteria of the maximal viable, specific penicillin production rate. The highest values for a maximal  $q_{pen, viable}$  are observed at a viable growth rate near 0.02 1/h. A higher or lower  $\mu_{viable}$  correlate with decreased maximal  $q_{pen, viable}$ . It is shown that FB4 and FB6 have the same  $\mu_{viable}$  but differ in the maximal  $q_{pen, viable}$ . Again, the exceeding of a viable growth rate of 0.055 1/h results in a sharply decreased  $q_{pen, viable}$ .

### 3.8.4. After ~44 hours since fed-batch start

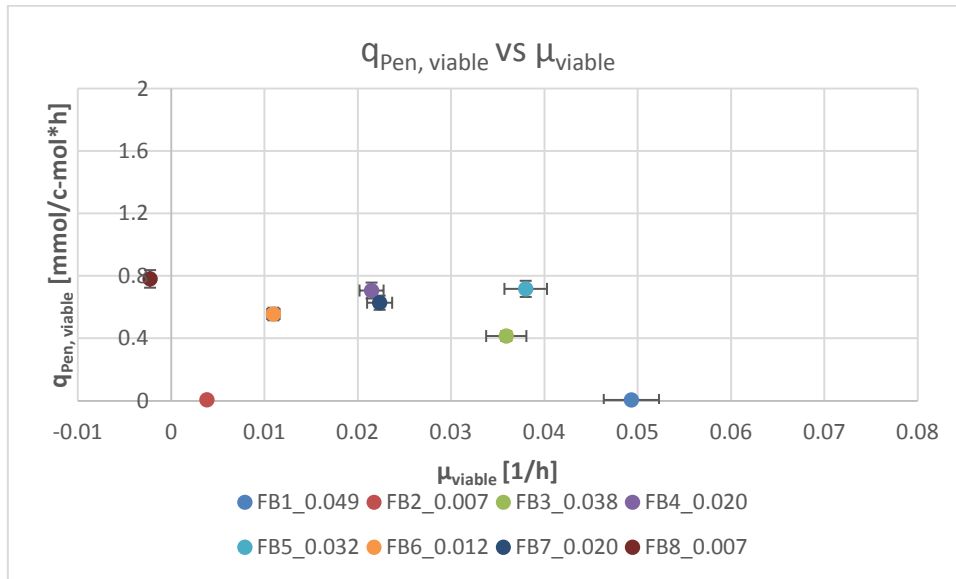


Figure 26:  $\mu_{viable}$  -  $q_{pen, viable}$  data points at ~44 hours after start of fed-batch from FB1-8.

In figure 26, 2 maxima of  $q_{pen, viable}$  with a value of 0.7 mmol/c-mol\*h are visible, one at a  $\mu_{viable}$  of 0.021 1/h and the other one at a  $\mu_{viable}$  of 0.038 1/h. All the other values for  $q_{pen, viable}$  fall below the maxima at growth rates higher or lower a  $\mu_{viable}$  of 0.021 1/h. Moreover, at a growth rate of 0.004 1/h and 0.049 1/h  $q_{pen, viable}$  is nearly 0 with values of 0.007 mmol/c-mol\*h.

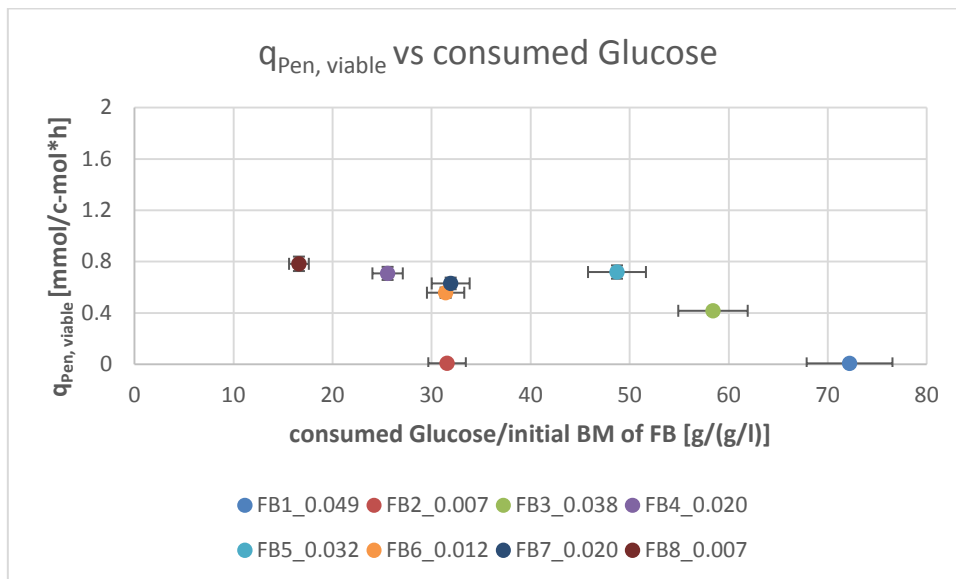


Figure 27:  $q_{pen, viable}$  [mmol/c-mol] of all performed cultivations after ca. 44h of fed-batch plotted against consumed glucose/initial biomass of FB [g/(g/L)].

Figure 27 shows the calculated  $\mu_{viable}$ \_ $q_{pen, viable}$  data pairs according to the criteria of passing ~44 since fed-batch start. The  $q_{pen, viable}$  after 44 hours since fed-batch start of the FB1 and FB2 are close to 0. Contrary, the  $q_{pen, viable}$  after 44 hours since fed-batch start of the FB3-8 vary within a range of 0.4 and 0.8 mmol/c-mol\*h.

### 3.8.5. After ~45g consumed glucose/initial biomass of FB [g/(g/L)]

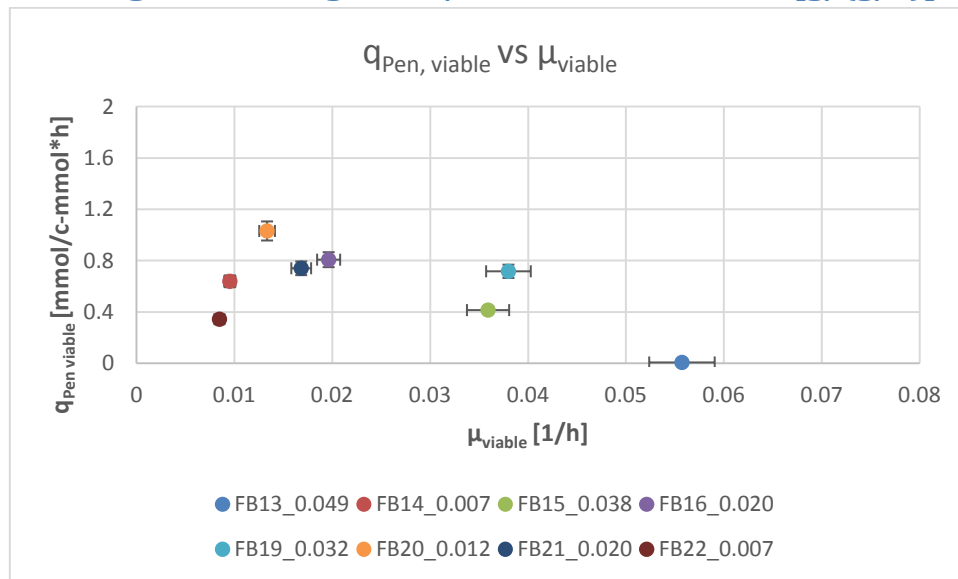


Figure 28: Illustration of the  $q_{pen, viable}$  [mmol/c-mol\*h] against  $\mu_{viable}$  [1/h] after ca. 45g consumed glucose/initial biomass of FB [g/(g/L)].

As visible in Figure 28, the values for  $\mu_{viable}$  after 45g consumed glucose/initial biomass of fed-batch are within a range of 0.008 1/h to 0.056 1/h. Corresponding  $q_{pen, viable}$  are located between a minimum of 0.01 mmol/c-mol\*h and a maximum of 1.03 mmol/c-mol\*h. The highest  $q_{pen, viable}$  of 1.03 mmol/c-mol\*h was determined at a viable growth rate of 0.12 1/h. With a decreasing or increasing growth rate the corresponding  $q_{pen, viable}$  declines. At the highest growth rate which was investigated, 0.056 1/h  $q_{pen, viable}$  has declined to the minimum.

### 3. 9. Influence of a $pO_2=4\%$ on $q_{Pen, viable}$

#### 3.9.1. Comparison of CDW

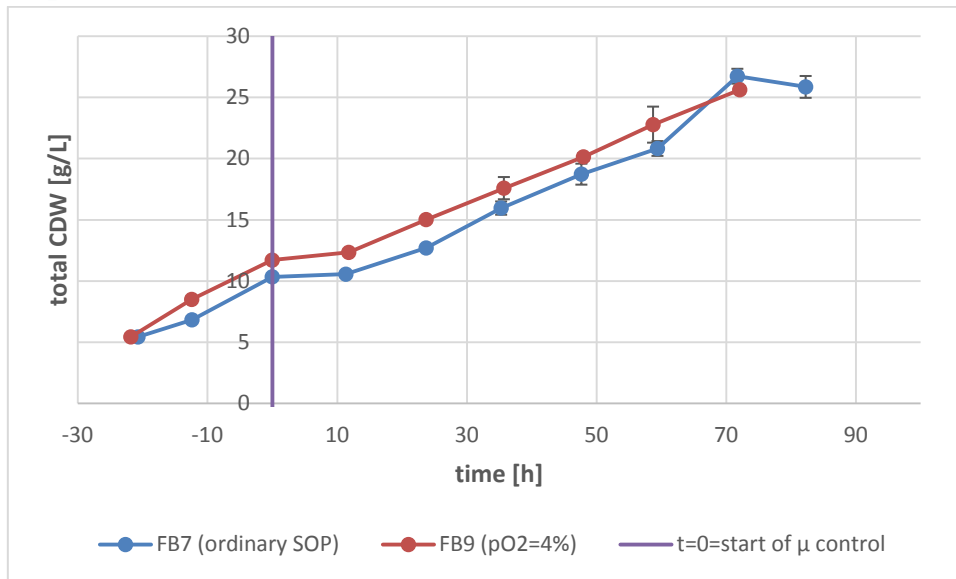


Figure 29: Comparison of the development of the CDW [g/L] of FB7 (ordinary SOP) and FB9 ( $pO_2=4\%$ ) during cultivation.

In Figure 29 the trend of the biomass during the cultivations is illustrated. The two cultivations start with an identical CDW of 5 g/L and exhibit a positive trend during the process, resulting in a final CDW of 25 g/L at the end of the fed-batch. Though FB7 and FB9 start and end with the same cell dry weight, it is not completely identical throughout the process but show differences in the range of maximal 2 g/L. Nevertheless, the trend of the biomass development of the two cultivations shows the same behavior.

#### 3.9.2. Comparison of $\mu_{viable}$

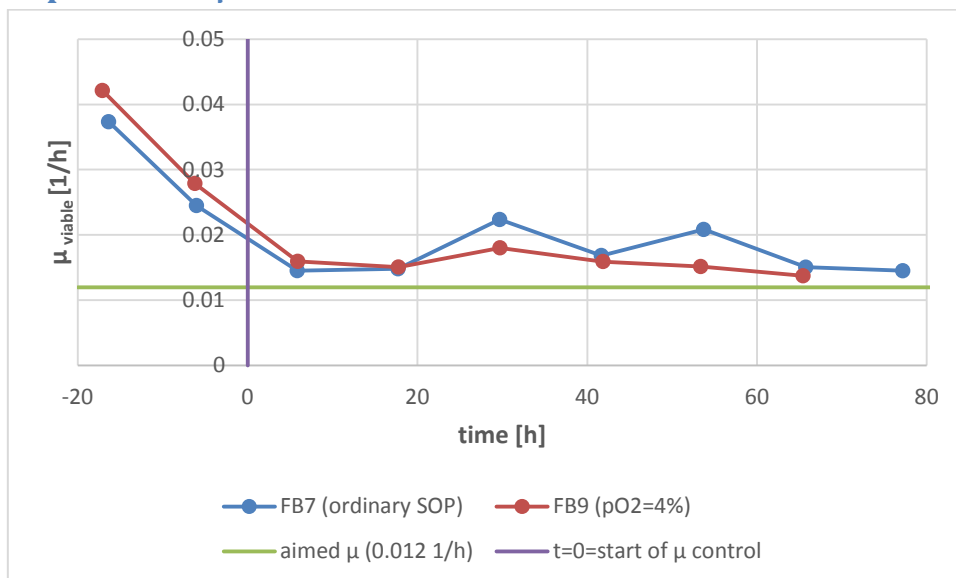


Figure 30: Comparison of  $\mu_{viable}$  of FB7 (ordinary SOP) and FB9 ( $pO_2=4\%$ ) during cultivation.

In Figure 30 the development of  $\mu_{viable}$  for FB7 and FB9 are compared. At the beginning of the fed-batches FB7 and FB9,  $\mu_{viable}$  is at 0.042 1/h and 0.038 1/h, respectively. Throughout the uncontrolled

phase of the fed-batch with a constant feed, both of them exhibit a decreasing  $\mu$  resulting in a viable growth rate of 0.012 1/h of the FB7 as well as FB9 at the beginning of the  $\mu$ -controlled phase. The trend of identical  $\mu_{\text{viable}}$  continues during the remaining cultivation except minor deviations.

### 3.9.3. Comparison of $c_{\text{Pen}}$ [g/L]

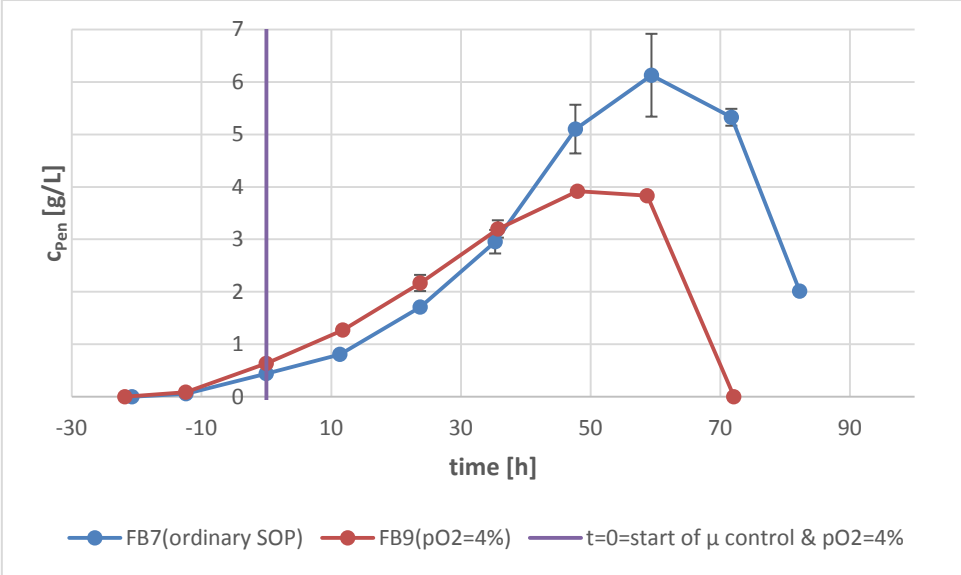


Figure 31: Penicillin concentrations of FB7 (ordinary SOP) and FB9 (pO<sub>2</sub>=4%) during cultivation.

FB7 as well as FB9 start with no detectable penicillin in the supernatant as visible in Figure 31. At the end of the uncontrolled phase of the cultivation, both of them have reached a value of 0.5 g/L. Throughout the  $\mu$  controlled phase which is coupled to the decreased dissolved oxygen of FB9, the penicillin concentration increases during the first 36 hours in FB7 as well as FB9 resulting in 3 g/L. After 48 hours of the  $\mu$  controlled phase, FB9 exhibits lower levels of penicillin than FB7. During the remaining cultivation, the penicillin concentration of FB9 is decreased compared to FB7. Nevertheless, both of them show the same decrease of the penicillin.

### 3.9.4. Comparison of $q_{\text{pen, viable}}$ [mmol/c-mol\*h]

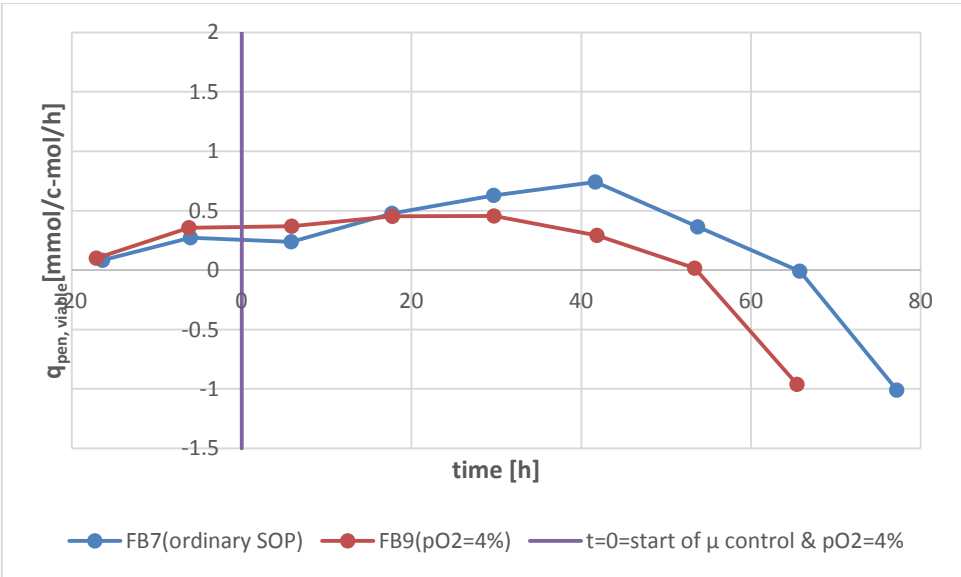


Figure 32: Comparison of  $q_{\text{pen, viable}}$  [mmol/c-mol\*h] of FB7 (ordinary SOP) and FB9 (pO<sub>2</sub>=4%) during cultivation

In Figure 32, the specific penicillin production rates of FB7 and FB9 are illustrated. During the first 24 hours of the fed-batch which are performed with a constant feed and no  $\mu$  control, FB7 as well as FB9 reveal the same trend. At the beginning of the cultivation,  $q_{\text{pen, viable}}$  is 0.10 mmol/c-mol\*h and reaches a value of 0.36 mmol/c-mol\*h at the end of the not controlled phase. During the  $\mu$  controlled phase  $q_{\text{pen, viable}}$  of FB7 slightly increases reaching its maximum of 0.74 mmol/c-mol\*h at 42 hours. Afterwards,  $q_{\text{pen, viable}}$  decreases and takes negative values at the end of the cultivation. Contrary, FB9 stays nearly constant at a level of 0.45 mmol/c-mol\*h during the first 36 hours of the  $\mu$  controlled phase but finally decreases in a similar way to FB7. Nevertheless,  $q_{\text{pen, viable}}$  of FB9 declines earlier compared to FB7.

### 3.9.5. $\mu_{\text{viable}}$ - $q_{\text{pen}}$ relation

#### 3.9.5.1. Single data points

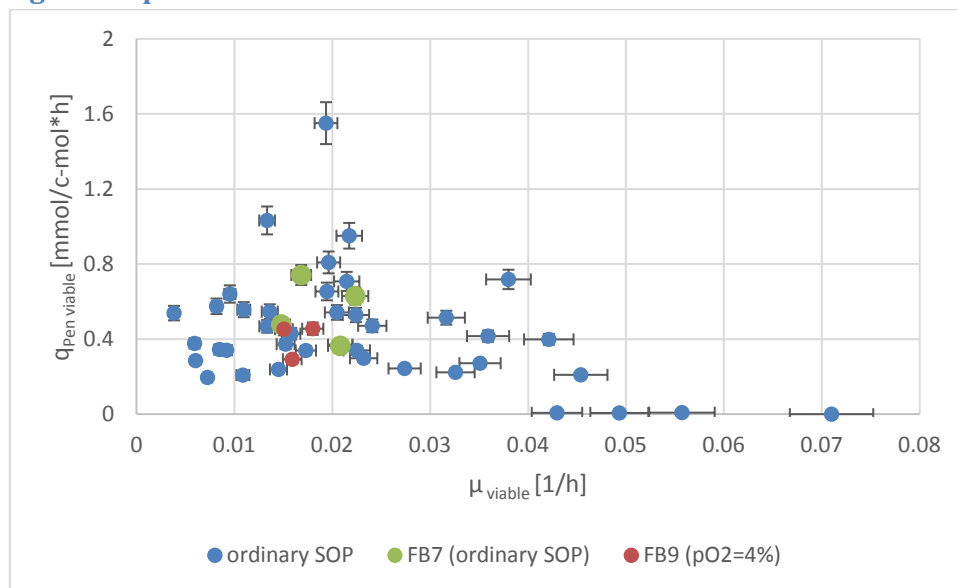


Figure 33: Plot of  $\mu_{\text{viable}}$  and corresponding  $q_{\text{pen, viable}}$  data points of cultivations performed according to standard operation procedure as well as the fermentation run with a decreased oxygen level. Values before  $\mu$  controlled phase are not included, only data pairs recorded during after start of  $\mu$  control are shown.

The graph, figure 33, shows data of the cultivation performed according to the ordinary standard operation procedure, "SOP". Additionally,  $\mu_{\text{viable}}$  and  $q_{\text{pen, viable}}$  data revealed by the fermentation run with a decreased dissolved oxygen level of 4% throughout the  $\mu$  control phase of the fed-batch are plotted. The  $\mu_{\text{viable}}$  -  $q_{\text{pen, viable}}$  data points of the fermentation performed with a decreased dissolved oxygen exhibit a viable growth rate between 0.014 and 0.018 1/h. Corresponding  $q_{\text{pen, viable}}$  varies between a range of 0.29 and 0.47 mmol/c-mol\*h. In relation to data generated by previous runs with ordinary standard operation procedure,  $q_{\text{pen, viable}}$  as well as  $\mu_{\text{viable}}$  are lying in the same ranges.

### 3.9.5.2. Mean values

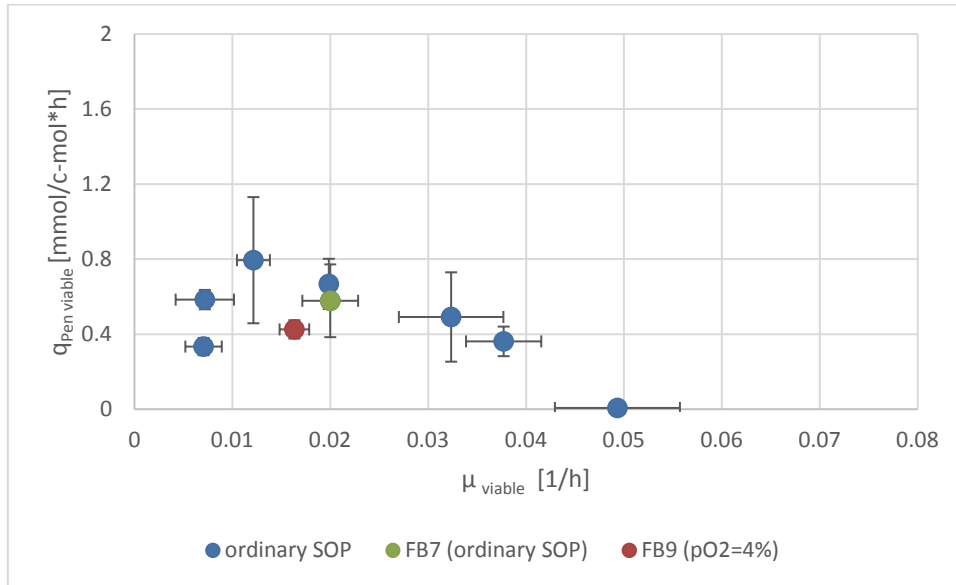


Figure 34: Plot of  $\mu_{viable}$  -  $q_{pen, viable}$  relation. Shown data points are  $\mu_{viable}$  and  $q_{pen, viable}$  mean values of a single fermentation during the  $\mu$  controlled phase as well as over a time period of 24h through which  $\mu$  was considered as constant.

According to Figure 34, the average  $\mu_{viable}$ - $q_{pen, viable}$  viable data of the run with decreased  $pO_2$  exhibits a lower  $q_{pen, viable}$  compared to fermentations with the ordinary dissolved oxygen limits. Nevertheless, there is no directly comparable data point generated from the ordinary SOP as the viable growth rate differs. Moreover the data based on the  $pO_2$  decreased run lies within the standard deviation of data points generated from the ordinary SOP.

### 3.9.5.3. Maximal $q_{pen, viable}$

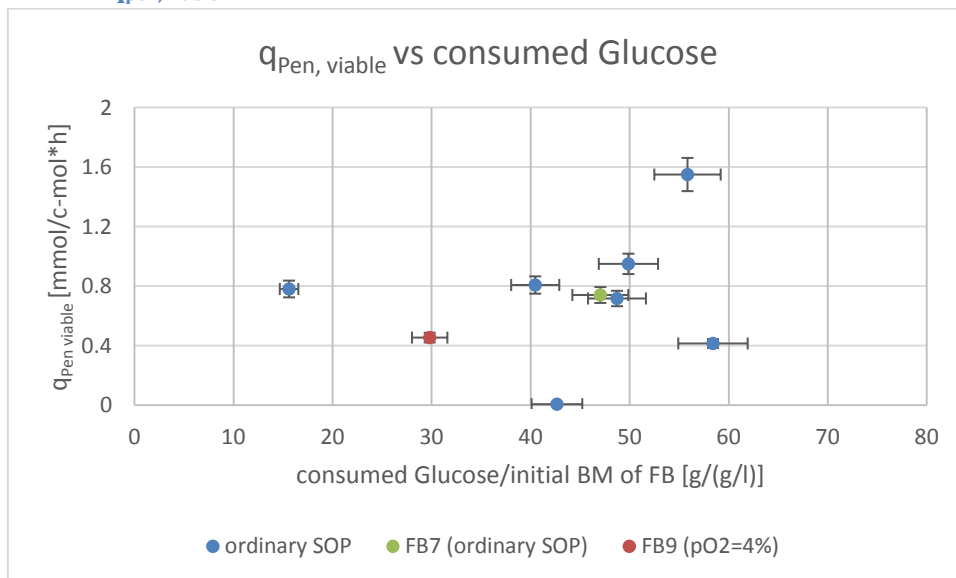


Figure 35: Plot of the maximal  $q_{pen, viable}$  [mmol/c-mol\*h] and corresponding consumed glucose per initial biomass of the fed-batch [g/(g/l)] of runs carried out according to ordinary SOP as well as the cultivation with the altered SOP of a decreased oxygen level of 4%.

As visible in Figure 35, the cultivation performed with a dissolved oxygen level of 4%, FB9, exhibits a significant lower amount of consumed glucose per initial biomass of the fed-batch, 29.8 g/(g/l) before reaching the maximal  $q_{pen, viable}$  of 0.45 mmol/c-mol\*h, excluding the data of FB8. In relation to



FB7, the maximal  $q_{pen, viable}$  is with a value of 0.45 mmol/c-mol\*h compared to 0.74 mmol/c-mol\*h lower as well.

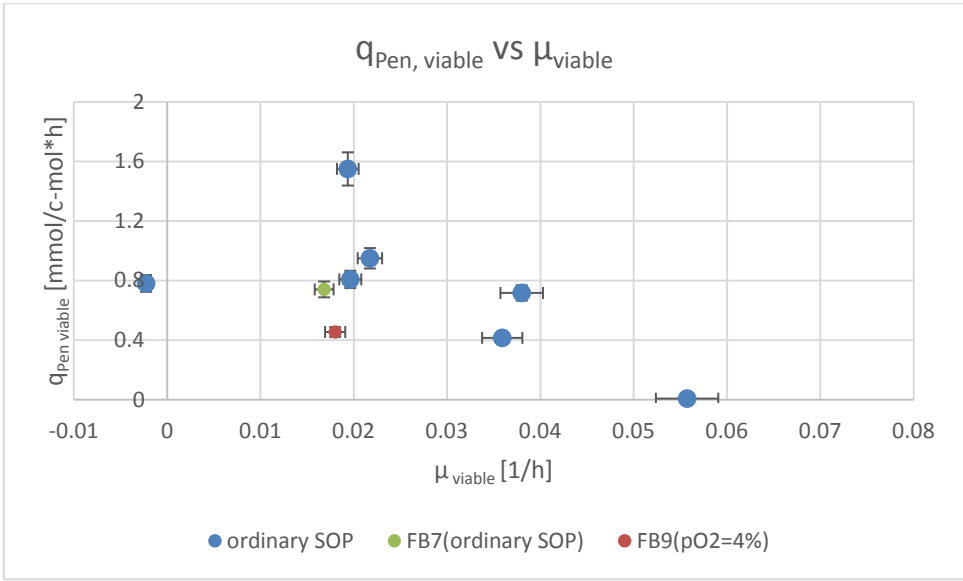


Figure 36: Plot of the maximal  $q_{pen, viable}$  [mmol/c-mol\*h] and corresponding  $\mu_{viable}$  [1/h] of runs performed according to SOP as well as the run with the decreased oxygen level of 4%.

Figure 36 illustrates the results according to the criteria of the maximal specific penicillin production rate. The  $\mu_{viable}$  of the corresponding maximal  $q_{pen, viable}$  of the run with a decreased oxygen level has a value of 0.18 1/h which is nearly identical to the viable growth rate of the cultivation with an ordinary oxygen level, 0.17 1/h. Nevertheless, the maximal  $q_{pen, viable}$  differs. While FB7 has a maximum of 0.74 mmol/c-mol\*h, FB9 exhibit a maximal  $q_{pen, viable}$  of 0.45 mmol/c-mol\*h.

### 3.9.5.4. After ~44 hours since fed-batch start

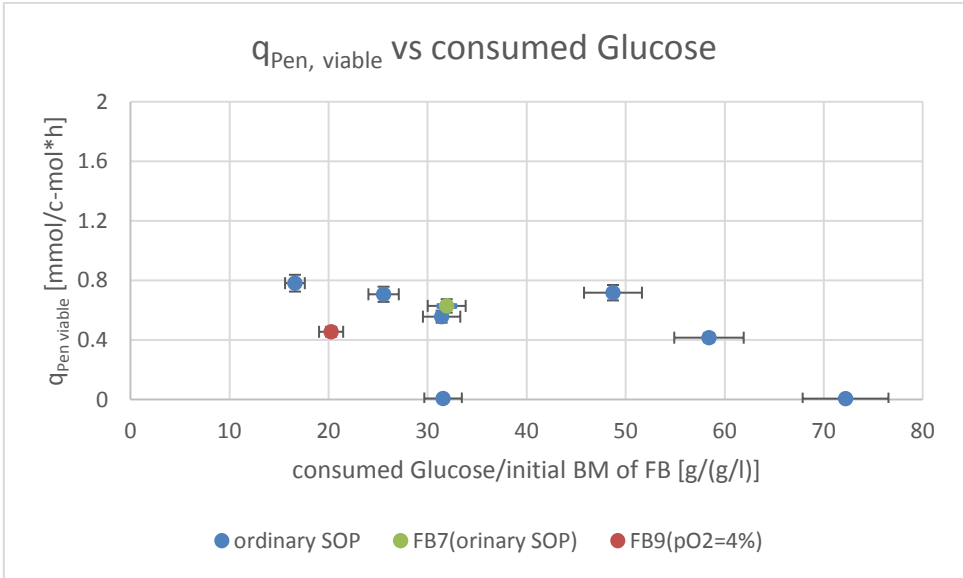


Figure 37:  $q_{pen, viable}$  plotted [mmol/c-mol\*h] against the consumed glucose per initial biomass of the fed-batch [g/(g/l)] of standard runs as well as the run with an oxygen level of 4%.

Comparing FB7 and FB9 in Figure 37, differences in  $q_{pen, viable}$  as well as the consumed glucose per initial biomass of the fed-batch can be seen. The ordinary run of FB7 reaches after 44 hours a  $q_{pen, viable}$

$\mu_{\text{viable}}$  of 0.63 mmol/c-mol\*h while FB9 has a  $q_{\text{pen, viable}}$  of 0.45 mmol/c-mol\*h. Furthermore, during FB9 less glucose per initial biomass of the fed-batch was consumed, 20.3 g/(g/l) compared to 31.9 g/(g/l).

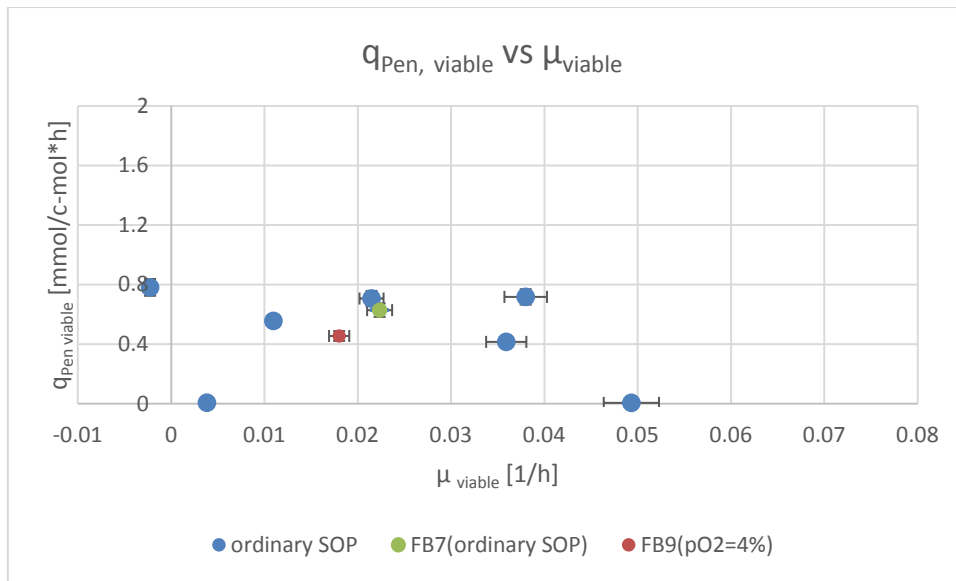


Figure 38:  $\mu_{\text{viable}}$  -  $q_{\text{pen, viable}}$  data points at ~44 hours after start of fed-batch of the standard runs as well as the cultivation performed with a decreased oxygen level.

Figure 38 illustrates the results according to the criteria of passing ~44 h since fed-batch start. In relation to the data of the standard cultivations, especially FB7, the fermentation carried out according to the altered SOP with a dissolved oxygen level of 4% reveals differences in the specific penicillin production rate as well as the growth rate of the viable biomass. Though FB7 and FB9 were performed identically, except the aimed dissolved oxygen level,  $\mu_{\text{viable}}$  of FB7 is 0.022 1/h compared to 0.018 1/h of FB9. While FB7 exhibits a  $q_{\text{pen, viable}}$  of 0.63 mmol/c-mol\*h, FB9 reveals a  $q_{\text{pen, viable}}$  of 0.45 mmol/c-mol\*h.

### 3.9.5.5. After ~45 g/(g/l) consumed Glucose/initial BM of FB

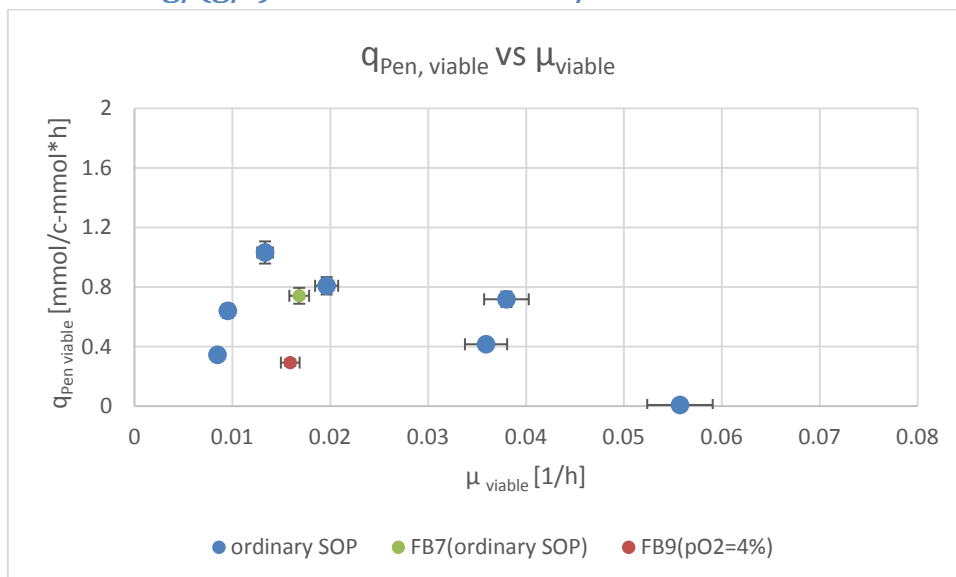


Figure 39:  $q_{\text{pen, viable}}$  [mmol/c-mol\*h] against  $\mu_{\text{viable}}$  [1/h] after the consumption of ~45 g/(g/l) glucose per initial biomass at the start of fed-batch of standard runs as well as the altered run with the decreased oxygen level of 4%.

Though FB7 and FB9 show nearly identical  $\mu_{\text{viable}}$ , 0.017 1/h and 0.016 1/h, they significantly differ in associated  $q_{\text{pen, viable}}$ , as visible in Figure 39. While the standard run reveals a  $q_{\text{pen, viable}}$  of 0.74 mmol/c-mol\*h, the cultivation run with the altered  $pO_2$  level reaches a  $q_{\text{pen, viable}}$  of 0.29 mmol/c-mol\*h.

# 4. Discussion

## 4.1. Batch

Within the first 24 hours after inoculation no significant changes can be detected. The pH, CO<sub>2</sub>, dissolved oxygen level as well as the concentrations of all measured sugars stay constant. This observation leads to the conclusion that there is no traceable metabolic activity of the fungi and can be explained by the fact that fungal spores have to swell and germinate within the first hours of the cultivation (Kalai et al. 2014; Van Long et al., 2017; Lattab et al., 2012). After passing the lag phase, the actual growth starts which is detectable by the increasing CO<sub>2</sub> and the typical pH shifts. As visible in Figure 10, the CO<sub>2</sub> content in the off gas flattens at the same time, the slope of the pH course changes. These phenomena may be linked to the directed consumption of carbon sources in a distinct order and therefore an adaption of concerning transport system as well as metabolic pathways (Jorgensen et al., 2004; Castillo et al., 2006). Therefore, the CO<sub>2</sub> content in the off gas decreases the moment one nutrient is exhausted and the fungi has to adapt its transport systems and metabolic pathways to another nutrient. This adaption includes the synthesis of adequate transporters as well as enzymes. According to the pH shifts, the exhaustion of a distinct media component may explain the differences of the pH course slope due to the individual pK<sub>s</sub> value as well as different concentrations of the contained components. This thesis corresponds to the dissolved oxygen signal and the agitator speed linked to it. The first decrease of the CO<sub>2</sub> content in the off gas is followed by increasing dissolved oxygen levels which may be caused by the earlier mentioned temporarily metabolic inactivity due to a change of the up taken substrate. This effect is visible during second and third decline of the CO<sub>2</sub> content in the off gas but to a lesser extent as well. At the same time, the agitator speed keeps constant until the dissolved oxygen level falls below the threshold of 40%.

Taking a look at the concentrations of different sugars and metabolites, an initial swelling time seems conclusive during which water is absorbed but no detectable metabolism. As visible in Figure 12 the concentrations of all measured substances are constant during the first 12 hours. After 22 hours, only the sucrose concentration has decreased, while all the others have the same concentration as before. Major changes are detectable from the time point 23.6h on. According to the changing concentration of the measured components, *P. chrysogenum* reveals different preferences for distinct carbon sources. Glucose seems to be the preferred carbon source, followed by the disaccharide sucrose which is split into glucose and fructose. Contrary, the sugar acid gluconate is produced from glucose (Mason et al., 1976) during the end of batch while lactose is untouched throughout the whole batch. This suggests that gluconate may act as a carbon hydrate reserve which is only consumed in the absence of more attractive carbon sources as glucose (Nielsen et al., 1994).

However, lactose stays constant throughout the whole batch suggesting that it is a less suitable carbon source in the presence of the sucrose, glucose, fructose and gluconate. This circumstance is supported by prior studies which revealed that lactose as sole carbon source results in slow growth compared to other carbon sources (Pirt et al., 1967). Nevertheless, lactose has been identified as trigger for penicillin production enabling higher penicillin production rates (Saltero et al., 1953).

Throughout the batch, the ergosterol concentration and thus indirectly the biomass was measured at two time points, at 34.1 hours and at the end of the batch at 57.7 hours. Based on these data the

maximal growth rate of  $0.109 \text{ h}^{-1}$  during the batch was calculated. An earlier measurement was not performed due to the germination time of the fungal spore during which isotropic enlargement occurs as consequence of the uptake of water (Kalai et al. 2014). Thus, no actual growth and significant changes in the ergosterol concentration occurs making a biomass calculation based on ergosterol concentration difficult.

## 4.2. Fed-Batch

### 4.2.1. General process evaluation

During the fed-batch cultivation, the total biomass increased constantly, while the viability of culture constantly decreased resulting in a lower content of viable biomass compared to the absolute value. Such a phenomenon may be explained by increased stress levels during ongoing fed-batch cultivation due to higher cell density which causes a limited oxygen transfer (Wang et al., 2005; Posch et al., 2013). Another influence may be the morphology of the fungi which grow either as hyphal elements or agglomerate and build pellets (Grimm, et al, 2005; Nielsen, 1997). As generally known, cultivations with a focus on pellets are easier to aerate as well as mix due to lower viscosity compared to cultivations consisting mostly of hyphae. Nevertheless, studies revealed that pellets lack a sufficient supply of oxygen as well as nutrients (Wang et al., 2005; Posch et al., 2013) and thus have negative effects on the viability of the culture.

The concentration of penicillin increased constantly throughout the cultivations independently from the chosen  $\mu$  set point. Nevertheless, they differed in the slope of the time course and thus in the final penicillin concentration. Moreover, some cultivations revealed a decrease in the absolute penicillin concentrations at the end of the fed batch which can't be explained by dilution effects. Taking a closer look, this trend focuses mainly on fermentations which were cultivated at relatively high growth rate set points. Thus this occurrence may be a result of an early degradation of the product and at the same time complete down regulation of the biosynthetic pathways (Pirt et al., 1967; Douma et al., 2010).

The yield of biomass per substrate reveals significant changes throughout the whole fed-batch phase and reaches its first maxima during the phase with a constant feed and thus no directed  $\mu$  control. As mentioned in Chapter 2.2.1, this phase is planned for the complete depletion of every other carbon source than glucose which is supplied via the feed, namely lactose and gluconate which are residues of the batch phase. This is achieved as a result of the constant feed which does not aim to fill the complete metabolic capacity of the fungi. Thus, the culture is able to utilize every available carbon source, namely lactose and gluconate. The consumption of lactose and gluconate is visible in Figure 16 supporting described thesis. Contrary, the mannitol concentration increases during the cultivation which is visible in Figure 16 as well. The accumulation of mannitol fits previous researches as it is a final metabolite of the glucose catabolism (Boonsaeng et al., 1967).

The second maximum of the biomass per substrate yield is reached during the  $\mu$  controlled phase. This trend is found in all performed cultivations and may be caused by the consumption of another carbon source next to glucose or that the assumed yield for the  $\mu$  control which was constantly adapted was underestimated. Nevertheless, as our results show the  $Y_{x/s}$  is not a constant throughout the cultivation but a dynamic parameter.

As visible in Figure 19, the methods for the atline determination of the biomass differ drastically in the coefficient of determination. The most inaccurate one is the method based on cell culture vials compared to 0.76 compared to 0.91 of the biovolume and 0.99 of the wet weight method respectively. Thus, the first mentioned is dismissed due to inaccurate results. Only the biovolume and wet weight methods deliver sufficient results. Nevertheless, biomass determination based on wet weight is preferred as it is more accurate and part of the CDW measurement.

#### 4.2.2. Control

Nearly 6 h before the  $\mu$  control is started, and thus during the constant feed phase, all fermentations have reached a nearly identical viable growth rate of  $0.022 \text{ h}^{-1}$ . Therefore they exhibit the same  $\mu$  start point before activating the different variations of the control strategy and consequently a comparison is possible. There is no  $\mu$  set point which was chosen identically for all  $\mu$  control variations. Thus, a comparison of the different strategies for one certain growth rate set point is not possible.

During the first two experiments, the atline methods for calculating the absolute biomass of the sampling time point is the one based on the biomass vial method. The resulting course of the viable growth rate is inconsistent, unable to keep a certain  $\mu_{\text{viable}}$  constant for a longer time period, and has a wide variation passing  $\mu_{\text{viable}}$  from  $0.004 \text{ h}^{-1}$  to  $0.045 \text{ h}^{-1}$ . Thus a control strategy based on this atline biomass determination is unable to reach and even less possible to keep a certain  $\mu_{\text{viable}}$  constant at a chosen set point. Keeping the atline biomass determination method per se in mind, the mentioned problems can be related to the biomass vials, the chosen rpm of the centrifuge and the regression used for the calculation of the total biomass. Problem of the biomass vial itself is the thin canal, in which the biomass sediments, as well the low maximal volume. These limitations lead to an inaccuracy of the measured biomass due to the morphology of the fungi and a high dependence on the user. Moreover, a possible clumping of hyphae and/or pellets (Nielsen et al., 1995) occurs which leads in combination with a too low set centrifugation to a blockage of the sedimentation canal, resulting in an inaccurate regression and thus to inaccurate atline biomass estimations.

Contrary, the  $\mu$  control based on the recalibration of the capacitance-biomass regression via the “wet weight” method is able to reach the  $\mu_{\text{viable}}$  set point and keep it constant throughout the fermentation with minor deviations. Thereby, this variation of the  $\mu$  control strategy was chosen to work with during ongoing fermentations until the final one was finished and could be applied for online control.

The final  $\mu$  control strategy which uses a capacitance-biomass regression based on data of previous experiments does not need a continuous recalibration of mentioned regression during the process. Moreover,  $Y_{x/S}$  which was originally adapted manually as well, is now constantly adapted as part of the controller itself. Nevertheless, the method exhibits similar disadvantages like the first one based on cell culture vials but to a drastically lower extent. The chosen  $\mu$  set point is not reached to the extent of the method based on wet weight atline biomass determination, but is significantly closer compared to one based on cell culture vials. During the  $\mu$  controlled phase deviations ranging in between those of the other control strategies based on cell culture vials and wet weight atline biomass determination are detectable.

Comparing the three variations of the same  $\mu_{\text{viable}}$  control strategy, the first one can be dismissed for ongoing cultivations, due to the fact that neither the chosen  $\mu$  set point is reached nor the viable

growth rate can be kept constant. The second as well as the third and final variation have their advantages and disadvantages. While the second one seems to be more suitable for a sufficient  $\mu_{\text{viable}}$  control strategy but needs a regular adjustment, the final strategy allows a sufficient but not optimal control of the viable growth rate but therefore does not need an additional recalibration.

#### 4.2.3. Growth rate and specific penicillin production rate

During the first 24 hours of fed batch cultivation, the phase of a constant feed rate, the viable growth rate is not constant but slowly decreases due to a decreasing amount of available carbon sources left from the batch as well as the fed substrate. This thesis is supported by the data of the ion chromatography which are shown in Figure 16 and reveal a depletion of remaining sugars during the constant feed phase. The behaviour of the viable growth rate changes the moment the  $\mu$  control is activated. First,  $\mu_{\text{viable}}$  approximates the chosen  $\mu$  set point and is kept constant throughout the remaining process. Nevertheless, the success of the  $\mu$  controlled phase depended on the chosen variation of the control strategy.

Contrary, the viable specific penicillin production rate is more dynamic and changes throughout the cultivation. In general, an increase of the specific penicillin production rate is observed during the constant feed, while different trends can be seen during the  $\mu$  controlled phase. These variations of the viable specific penicillin production rate can be seen in dependency of the chosen  $\mu$  set point as well as throughout phases of a constant viable growth rate during a single fermentation. Nevertheless, some commonalities and similar developments are detectable: during fermentation with a  $\mu_{\text{viable}}$  set point of  $0.02 \pm 0.005 \text{ h}^{-1}$  the viable specific penicillin production rate increased constantly within at least the first 24 h of the  $\mu$  controlled phase. Thus indicating, combined with the formerly described observation of an increasing  $q_{\text{pen, viable}}$  during the constant feed phase, that the biosynthetic pathway of *P. chrysogenum* for penicillin synthesis may not be fully developed or at a relatively low content. In order to reach the full potential of productivity, the adequate enzymes, namely isopenicillin N synthase, isopenicillin N acyltransferase and L- $\alpha$ -( $\delta$ -aminoadipyl)-L- $\alpha$ -cysteinyl-D- $\alpha$ -valine synthetase have to be synthesized in sufficient amounts. This circumstance has been described previously in other studies (Douma et al., 2010, Theilgaard et al., 2001) thus our results may support their thesis of an adapting biosynthetic pathway. Another detectable trend throughout our experiments is that the specific penicillin production rate of the viable biomass collapses at some point of the fermentation. Nevertheless, a distinct time point of the  $q_{\text{pen, viable}}$  collapse is not determinable which strongly indicates that time alone may not be causing this phenomenon but in combination with other factors. Such factors may be physiological or process related ones (Vardar et al., 1982; Brakhage, 1998; Posch et al., 2013).

#### 4.2.4. $\mu$ - $q_{\text{Pen}}$ evaluation

In the course of our experiments, the resulting  $\mu_{\text{viable}}-q_{\text{pen, viable}}$  data revealed a more complex connection, possibly influenced by other factors, for example physiological, morphological ones or process parameters (Posch et al., 2014; Smith et al., 1990), than expected. As visible in Figure 22, a relation like it was described by Douma et al. (2010), cannot be directly reproduced. A certain viable growth rate exhibit several possible viable specific penicillin production rates respectively a certain  $q_{\text{pen, viable}}$  can be accomplished with different viable growth rates. Still, some valuable information can be gained from the obtain data: In general, the highest  $q_{\text{pen, viable}}$  is achieved between a viable growth rate from  $0.014 \text{ h}^{-1}$  to  $0.022 \text{ h}^{-1}$  and thus indicates the maximum can be expected in concerning range. The exceeding of a viable growth of  $0.045 \text{ h}^{-1}$  leads to a nearly complete collapse of the viable

specific penicillin production rate and therefore suggests that a  $\mu_{\text{viable}}$  of  $0.045 \text{ h}^{-1}$  corresponds to a  $\mu_{\text{viable, max}}$  for the penicillin synthesis under given conditions. Due to the fact that several  $\mu_{\text{viable}}$  correspond to a  $q_{\text{pen, viable}}$ , a possible interlink to other factors have to be kept in mind and urges to specify the evaluation, as described in “Material & Methods”, in order to gain more information.

The  $\mu_{\text{viable}}-q_{\text{pen, viable}}$  data evaluation based on the mean of (nearly) constant  $\mu_{\text{viable}}$  and corresponding  $q_{\text{pen, viable}}$  seems to allow a better identification of a possible  $\mu_{\text{viable}}-q_{\text{pen, viable}}$  relation but still lacks a clear interlink. Though it can be argued that the mean values of the  $q_{\text{pen, viable}}$  changes depending on the course of  $\mu_{\text{viable}}$ , similar to the curve described by Douma et al. (2010), this effect is rebutted by the large standard deviation of some data points. The only derivable information is the existence of a maximal  $\mu_{\text{viable}}$  whose exceeding causes a collapse of  $q_{\text{pen, viable}}$  as described earlier. Moreover, a maximal  $q_{\text{pen, viable}}$  at a certain viable growth rate cannot be determined due to the large standard deviation which causes an overlapping of the  $q_{\text{pen, viable}}$  ranges of several  $\mu_{\text{viable}}$  data points.

Though one value does not show a similar behaviour like the others, a distinct trend is recognizable: The maximal  $q_{\text{pen, viable}}$  is normally reached within a range of 40.5-48.4 g/(g/L) consumed glucose per initial biomass of the fed-batch. Thus indicating that the fed substrate and thereby the physiological age of the culture are an important factor with a defined optimum to whose sides the productivity may decrease. Moreover, the differing  $q_{\text{pen, viable}}$  within this range lead to the conclusion that other factors may influence the maximal  $q_{\text{pen, viable}}$  during fermentation. This assumption is supported by the plot of the maximal  $q_{\text{pen, viable}}$  against  $\mu_{\text{viable}}$  which reveals that the highest  $q_{\text{pen, viable}}$  are obtained with  $\mu_{\text{viable}}$  close to  $0.02 \text{ h}^{-1}$  and thus urges the idea that  $q_{\text{pen, viable}}$  is not independent from  $\mu_{\text{viable}}$  and its maximum is close to  $0.02 \text{ h}^{-1}$ . Additional information is the fact that at a maximal  $q_{\text{pen, viable}}$  of FB1 is close to 0 at a viable growth rate of  $0.056 \text{ h}^{-1}$ .

After nearly 44 hours since fed-batch start, the  $\mu_{\text{viable}}-q_{\text{pen, viable}}$  data reveal a similar trend as described by Douma et al. (2010), though some deviation occur: the data of two fermentations, FB5 and FB2, diminish the usability of our experiments. Thus a time related data evaluation may not be the most sufficient. Nevertheless, some interesting information can be won: As visible in Figure 26, the  $q_{\text{pen, viable}}$  of most experiments is within a tight range of 0.56-0.78 mmol/(c-mol\*h) till 50 g glucose per initial biomass of the fed-batch are consumed. Fermentations which have been fed with more glucose per initial biomass of the fed-batch reveal a negative trend of  $q_{\text{pen, viable}}$  which corresponds to  $\mu_{\text{viable}}$  values of the right side of the  $\mu_{\text{viable}}-q_{\text{pen, viable}}$  data. Thus, indicating that the pathway for penicillin synthesis is still adapting at the chosen time point as well as an independence of the biosynthetic machinery from a glucose/initial BM of FB-start within a certain range. Only one data point does not fit this thesis: FB2. This aberration can be explained by the very low viable growth rate of the data point visible in Figure 26 despite the amount of 31.6 g/(g/l) consumed glucose per initial BM of FB.

The data selection based on the amount of consumed glucose in relation to the initial biomass of fed-batch reveals a similar correlation as previous criteria. High values of a viable specific penicillin production rate can be found in a certain  $\mu_{\text{viable}}$  area, namely  $0.013$  to  $0.020 \text{ h}^{-1}$ , while a slower or faster growth leads to decreased  $q_{\text{pen, viable}}$ . Again, the data selection shows that a growth rate higher than  $0.05 \text{ h}^{-1}$  causes complete collapse of the viable specific penicillin production rate. Nevertheless, two fed-batches, FB04 and FB07, have strongly differing  $q_{\text{pen, viable}}$  though their viable growth rates are nearly identical.



All of the used variations of data selection for the identification of the assumed  $\mu_{\text{viable}} - q_{\text{pen, viable}}$  correlation exhibit similar results: though the maximal  $q_{\text{pen, viable}}$  slightly differs between single approaches, a certain area of a maximal productivity can be determined in each approach. Nonetheless, some of them seem to be better suitable for a sufficient evaluation than others. While the data evaluation using all data as well as mean values does not allow the identification of a clear  $\mu_{\text{viable}} - q_{\text{pen, viable}}$  correlation, a data selection based on certain criteria enables a clearer picture of mentioned relation. Nevertheless, they still differ in the quality: the selection based on the maximal  $q_{\text{pen, viable}}$  as well as after 44 hours of cultivation may lead to the conclusion of a possible dependency of  $q_{\text{pen, viable}}$  from  $\mu_{\text{viable}}$  but an explicit correlation cannot be detected due to some values outside the expected range. Contrary, the selection based on the consumed glucose per initial biomass of fed-batch leads to the most conclusive picture of a clear  $\mu_{\text{viable}} - q_{\text{pen, viable}}$  correlation. Still, the other criteria for data selection indicate some physiological influences of *P.chrysogenums* metabolism. Nevertheless, the machinery for penicillin synthesis is a complex one, with many interlinks which are not fully known and understood. Thus, every conclusion that goes beyond the above mentioned needs further experiments for verification.

#### 4.2.5. Comparison of differing pO<sub>2</sub> levels

Comparing the development of the CDW as well as the viable growth rate throughout the cultivation of FB7 and FB9, a nearly identical trend of a constantly increasing biomass respectively a constant viable growth rate is visible. Contrary, the development of the penicillin concentration as well as the viable specific penicillin production rate differs between the two fermentations. Though they develop nearly identically throughout the first 48 hours of the cultivation, the cultivation with the dissolved oxygen level of 4% reveals an earlier flattening and final decrease than the ordinary run. This differing development is visible as well in the course of  $q_{\text{pen, viable}}$  during the cultivation.

In relation to the  $\mu_{\text{viable}} - q_{\text{pen, viable}}$  data evaluation, the run with the decreased dissolved oxygen level exhibits in general a significant decreased viable specific penicillin production rate though a nearly identical viable growth rate of the comparison experiment. Again, a clear difference cannot be established using all generated data points as well as mean values due to the fact that a certain viable growth rate has several possible specific penicillin production rates. Contrary, the selection of certain data points reveals a different picture. Independently from the selection criteria, the cultivation with a dissolved oxygen level of 4% shows a decreased viable specific penicillin production rate compared to the cultivation run with pO<sub>2</sub>>40%. The data evaluation based on the maximal  $q_{\text{pen, viable}}$  after 44 hours since fed-batch start as well as the consumed glucose per initial biomass of the fed-batch reveal a significant lower  $q_{\text{pen, viable}}$ . Thus it can be argued that the decreased dissolved oxygen level has significant negative effects on the productivity fitting previous data (Vardar et al., 1982; Henriksen et al., 1997).

# 5. Conclusion

## 5.1. Batch

- The batch phase of the common fermentation process with *P. chrysogenum* is highly reproducible throughout all performed cultivations.
- The nearly identical development of the culture provides the optimal conditions for experiments focusing on the possible optimization of the fed-batch cultivation, such as  $\mu$  control or different  $pO_2$  levels

## 5.2. Fed-Batch

- The control of the growth rate, the first goal, is practicable as we were able to reproduce a single run, FB7, except the fact of decreased oxygen levels, FB9. Nevertheless, there is still room for further fine tuning concerning the accuracy and stability of the control strategy.
- The viable specific penicillin production rate is highly dynamic even if the growth rate was constant for certain amount of time.
- The influence of other factors, including process parameters, the fungal morphology, media composition or spore age, is most probably (Posch et al., 2014, Smith et al., 1990).
- Despite the multiple dependency of  $q_{Pen, viable}$ , a dependency of the growth rate under given conditions with a maximum close to growth rate of  $0.02h^{-1}$  can be established. Thus, the second goal was reached as well.
- The presented correlation is similar to the one described by Douma et al. (2010). Differences may be explainable by the usage of different strain producing PenV, calculating viable growth rate as well as viable penicillin production rate, not the total corresponds, or by the fact that he only used a single fermentation for his calculations while we used data based on 8 cultivations.
- The biosynthetic pathway for penicillin production may not be fully formed, within at least the first 44 hours of fed batch cultivation. Thus, indicating that within this time period a certain amount of fed substrate, namely glucose, may lead to higher growth rates and more biomass but has nearly no effect on the viable specific penicillin production rate.
- The specific penicillin production rate reveals an irreversible decrease and final end during ongoing processes. This demise of penicillin production occurred throughout most of our cultivations and had an earlier onset if the process was run with a relatively high growth rate. Therefore this phenomenon may be linked to physiological parameters, for example a faster aging of the culture caused by the higher amount of fed substrate compared to slower growing cultures.
- Keeping the third goal in mind: The decreased oxygen level of 4% does neither affect the fungal growth nor the viability of the culture but reveal negative effects on the productivity. Compared to the control run, the oxygen limited fed-batch shows a lower maximal  $q_{Pen, viable}$  as well as maximal  $c_{Pen}$ , a slower increase of  $q_{Pen, viable}$  and an earlier decrease of  $q_{Pen, viable}$ .

# 6. Outlook

## 6.1. Batch

Contrary to the fed-batch phase of the cultivation strategy, the media is not a defined one and thus contains complex media components. These complex media components, namely corn steep liquor and cotton seed flour, supply the fungi with essential minerals, vitamins as well as amino acids (Liggett et al., 1948). Moreover, results of earlier performed studies suggest that the addition of corn steep liquor to the media increases penicillin production (Foster et al., 1948). Anyway, due to the complex media components and thus an undefined batch media, the initial media composition slightly differs between different batch cultivation depending on the qualitative differences of the complex media components.

The positive effects of different complex media components on penicillin synthesis have been investigated in the past (Liggett et al., 1948; Foster et al., 1948), their composition and thus a possible identification of distinct components, responsible for the positive effects haven't. Thus, such a research may be useful in future, as mentioned effects may be most probably adaption mechanisms of fungi which could be used for further optimization.

## 6.2. Fed-Batch

Though our results support Douma's thesis of a transferable  $\mu$ - $q_{pen}$  relation from continuous processes to fed-batch cultivation in *P. chrysogenum*, ongoing experiments are needed.

These additional fermentations can be used to identify other factors and maybe determine their range. The investigative process which would be necessary to identify additional parameters for a sufficient prediction of  $q_{pen, viable}$  would include a historical research, meaning literature and previous experiments, as well as an analysis of the own process data. Thereby, the possible factors/parameters could be tested and the range of their influence ought to be determined in form of a design of experiment, "DoE". Such factors could include process parameters as well as physiological ones, as described earlier.

Moreover, these experiments can be used as well as to further enhance and refine the  $\mu$  control strategy. Thereby, it would be possible to obtain more accurate results which could be used to generate an even more accurate model of the control strategy as well as the  $\mu$ - $q_{pen}$  relation. This won information could finally be used to control the process on a whole new level and predict the productivity of single cultivations.

Another essential part which had been excluded from our studies in order to reduce complexity was the presence of lactose within the fed-batch media. For an ordinary process the disaccharide lactose is added to the batch as well as to the fed-batch media due to positive effects on the penicillin production (Pirt et al., 1976). Therefore, it is advisable to perform control cultivations with lactose in the media in order to reproduce the described  $\mu$ - $q_{pen}$  relation or to determine possible differences.

Another interesting aspect for further investigations is lactose as a tuneable factor itself. Though it is generally known that lactose increases the productivity of *P. chrysogenum*, the actual way of action hasn't been much in the centre of scientific interest yet. Nevertheless, a deeper understanding of the

involved regulatory mechanism as well as enzymes may lead to another useful tool for pushing the penicillin production by refining the single levels of regulation. Furthermore, the way the inducer lactose is supplied to the culture may be an interesting screw to adjust, for example as several pulses throughout the cultivation or as an additional feed.

Another factor that may not be neglected is a potential degradation of penicillin, a decay rate, which may lead to inaccurate results. Therefore, experiments determining the decay rate of penicillin under given process conditions which could be included to the calculation would result in more accurate viable specific penicillin production rates. Moreover, the results of these additional experiments may explain the earlier mentioned, observed drop of  $q_{\text{Pen, viable}}$  during certain cultivations.

Last, but not least, it is necessary to evaluate if the final results are transferable to large scale and more important if the control of the fungal growth rate in order to obtain a certain specific production rate would increase the final profits.

Concerning the final experiment performed with low dissolved oxygen levels, additional cultivations aiming different viable growth rates are necessary to replicate the  $\mu$ - $q_{\text{Pen}}$  relation.

In general, the same additional experiments mentioned above can be performed with low dissolved oxygen levels as well in order to gain better understanding under such conditions.

## 7. Literature

- Abraham, Edward P., et al. "Further observations on penicillin." *The Lancet* 238.6155 (1941): 177-189.
- Aminov, Rustam I. "The role of antibiotics and antibiotic resistance in nature." *Environmental microbiology* 11.12 (2009): 2970-2988.
- Aminov, Rustam I. "A brief history of the antibiotic era: lessons learned and challenges for the future." *Frontiers in microbiology* 1 (2010): 134.
- Bajpai, R. K., and M. Reuss. "A mechanistic model for penicillin production." *Journal of Chemical Technology and Biotechnology* 30.1 (1980): 332-344.
- Bassett, Everett J., et al. "Tetracycline-labeled human bone from ancient Sudanese Nubia (AD 350)." AAAS, 1980.
- Bendiner, Elmer. "Alexander Fleming: player with microbes." *Hospital Practice* 24.2 (1989): 283-316.
- Bennett, Joan W., and King-Thom Chung. "Alexander Fleming and the discovery of penicillin." *Advances in applied microbiology* 49 (2001): 163-184.
- Bergh, Katharina Then, and Axel A. Brakhage. "Regulation of the *Aspergillus nidulans* Penicillin Biosynthesis Gene *acvA* (*pcbAB*) by Amino Acids: Implication for Involvement of Transcription Factor PACC." *Applied and environmental microbiology* 64.3 (1998): 843-849.
- Bladt, Tanja, et al. "Anticancer and antifungal compounds from *Aspergillus*, *Penicillium* and other filamentous fungi." *Molecules* 18.9 (2013): 11338-11376.
- Blank, Harvey, et al. "The treatment of dermatomycoses with orally administered griseofulvin." *AMA archives of dermatology* 79.3 (1959): 259-266.
- Boonsaeng, Vichai, Patrick A. Sullivan, and Maxwell G. Shepherd. "Mannitol production in fungi during glucose catabolism." *Canadian journal of microbiology* 22.6 (1976): 808-816.
- Brakhage, Axel A. "Molecular regulation of  $\beta$ -lactam biosynthesis in filamentous fungi." *Microbiology and Molecular Biology Reviews* 62.3 (1998): 547-585
- Gutiérrez, Santiago, et al. "Transcription of the *pcbAB*, *pcbC* and *penDE* genes of *Penicillium chrysogenum* AS-P-78 is repressed by glucose and the repression is not reversed by alkaline pHs." *Microbiology* 145.2 (1999): 317-324.
- Brakhage, Axel A., P. Browne, and G. Turner. "Regulation of *Aspergillus nidulans* penicillin biosynthesis and penicillin biosynthesis genes *acvA* and *ipnA* by glucose." *Journal of bacteriology* 174.11 (1992): 3789-3799.
- Busch, Silke, et al. "Impact of the cross-pathway control on the regulation of lysine and penicillin biosynthesis in *Aspergillus nidulans*." *Current genetics* 42.4 (2003): 209-219.
- Bush, Karen, and Patricia A. Bradford. " $\beta$ -Lactams and  $\beta$ -lactamase inhibitors: an overview." *Cold Spring Harbor perspectives in medicine* 6.8 (2016): a025247.
- Castillo, Nancy Isabel, et al. "Genome-wide analysis of differentially expressed genes from *Penicillium chrysogenum* grown with a repressing or a non-repressing carbon source." *Current genetics* 49.2 (2006): 85-96.

- Cepeda-García, Cristina, et al. "Direct involvement of the CreA transcription factor in penicillin biosynthesis and expression of the pcbAB gene in *Penicillium chrysogenum*." *Applied microbiology and biotechnology* 98.16 (2014): 7113-7124.
- Chain, Ernst, et al. "Penicillin as a chemotherapeutic agent." *The Lancet* 236.6104 (1940): 226-228.
- Clutterbuck, Percival Walter, Reginald Lovell, and Harold Raistrick. "Studies in the biochemistry of micro-organisms: The formation from glucose by members of the *Penicillium chrysogenum* series of a pigment, an alkali-soluble protein and penicillin—the antibacterial substance of Fleming." *Biochemical Journal* 26.6 (1932): 1907.
- Cook, Megan, E. L. Molto, and C. Anderson. "Fluorochrome labelling in Roman period skeletons from Dakhleh Oasis, Egypt." *American journal of physical anthropology* 80.2 (1989): 137-143.
- Cui, Y. Q., R. G. J. M. Van der Lans, and K. C. A. M. Luyben. "Effect of agitation intensities on fungal morphology of submerged fermentation." *Biotechnology and Bioengineering* 55.5 (1997): 715-726.
- Douma, Rutger D., et al. "Dynamic gene expression regulation model for growth and penicillin production in *Penicillium chrysogenum*." *Biotechnology and bioengineering* 106.4 (2010): 608-618.
- Demain, Arnold L. "Inhibition of penicillin formation by lysine." *Archives of biochemistry and biophysics* 67.1 (1957): 244-246.
- Ehgartner, Daniela, Christoph Herwig, and Lukas Neutsch. "At-line determination of spore inoculum quality in *Penicillium chrysogenum* bioprocesses." *Applied microbiology and biotechnology* 100.12 (2016): 5363-5373.
- El-Banna, A. A., J. I. Pitt, and L. Leistner. "Production of mycotoxins by *Penicillium* species." *Systematic and Applied Microbiology* 10.1 (1987): 42-46.
- Engel, C. Roa, et al. "Integration of fermentation and crystallisation to produce fumaric acid." *New Biotechnology* 25 (2009): S173.
- Espeso, Eduardo A., et al. "pH regulation is a major determinant in expression of a fungal penicillin biosynthetic gene." *The EMBO journal* 12.10 (1993): 3947.
- Feng, Bo, Ernst Friedlin, and George A. Marzluf. "A reporter gene analysis of penicillin biosynthesis gene expression in *Penicillium chrysogenum* and its regulation by nitrogen and glucose catabolite repression." *Applied and environmental microbiology* 60.12 (1994): 4432-4439.
- Fierro, Francisco, et al. "The penicillin gene cluster is amplified in tandem repeats linked by conserved hexanucleotide sequences." *Proceedings of the National Academy of Sciences* 92.13 (1995): 6200-6204
- Fleming, Alexander. "On the antibacterial action of cultures of a penicillium, with special reference to their use in the isolation of *B. influenzae*." *British journal of experimental pathology* 10.3 (1929): 226.
- Foster, J. W., et al. "Microbiological Aspects of Penicillin: IX. Cottonseed Meal as a Substitute for Corn Steep Liquor in Penicillin Production." *Journal of bacteriology* 51.6 (1946): 695.
- Grimm, L. H., et al. "Kinetic studies on the aggregation of *Aspergillus niger* conidia." *Biotechnology and bioengineering* 87.2 (2004): 213-218.
- Grimm, L. H., et al. "Morphology and productivity of filamentous fungi." *Applied microbiology and biotechnology* 69.4 (2005): 375.

- Gutiérrez, Santiago, et al. "Transcription of the pcbAB, pcbC and penDE genes of *Penicillium chrysogenum* AS-P-78 is repressed by glucose and the repression is not reversed by alkaline pHs." *Microbiology* 145.2 (1999): 317-324.
- Haas, Hubertus, and George A. Marzluf. "NRE, the major nitrogen regulatory protein of *Penicillium chrysogenum*, binds specifically to elements in the intergenic promoter regions of nitrate assimilation and penicillin biosynthetic gene clusters." *Current genetics* 28.2 (1995): 177-183.
- Henderson, John Warren. "The yellow brick road to penicillin: a story of serendipity." *Mayo Clinic Proceedings*. Vol. 72. No. 7. Elsevier, 1997.
- Henriksen, Claus M., Jens Nielsen, and John Villadsen. "Influence of the Dissolved Oxygen Concentration on the Penicillin Biosynthetic Pathway in Steady-State Cultures of *Penicillium chrysogenum*." *Biotechnology progress* 13.6 (1997): 776-782.
- Houbraken, J., et al. "New penicillin-producing *Penicillium* species and an overview of section *Chrysogena*." *Persoonia-Molecular Phylogeny and Evolution of Fungi* 29.1 (2012): 78-100.
- Jami, Mohammad-Saeid, et al. "Proteome analysis of the penicillin producer *Penicillium chrysogenum*: characterization of protein changes during the industrial strain improvement." *Molecular & Cellular Proteomics* (2010)
- Jarvis, F. G., and M. J. Johnson. "The mineral nutrition of *Penicillium chrysogenum* Q176." *Journal of bacteriology* 59.1 (1950): 51.
- Jónás, Ágota, et al. "Extra-and intracellular lactose catabolism in *Penicillium chrysogenum*: phylogenetic and expression analysis of the putative permease and hydrolase genes." *The Journal of antibiotics* 67.7 (2014): 489-497.
- Jørgensen, Henning, et al. "Growth and enzyme production by three *Penicillium* species on monosaccharides." *Journal of biotechnology* 109.3 (2004): 295-299.
- Kalai, Safaa, Maurice Bensoussan, and Philippe Dantigny. "Lag time for germination of *Penicillium chrysogenum* conidia is induced by temperature shifts." *Food microbiology* 42 (2014): 149-153.
- Kavalier, Lucy. "Mushrooms, molds, and miracles." (1965).
- Keefer, Chester S., et al. "Penicillin in the treatment of infections: a report of 500 cases." *Journal of the American Medical Association* 122.18 (1943): 1217-1224.
- Krull, Rainer, et al. "Morphology of filamentous fungi: linking cellular biology to process engineering using *Aspergillus niger*." *Biosystems Engineering II*. Springer Berlin Heidelberg, 2010. 1-21.
- Lattab, Nadia, et al. "Effect of storage conditions (relative humidity, duration, and temperature) on the germination time of *Aspergillus carbonarius* and *Penicillium chrysogenum*." *International journal of food microbiology* 160.1 (2012): 80-84.
- Liggett, R. Winston, and H. Koffler. "Corn steep liquor in microbiology." *Bacteriological reviews* 12.4 (1948): 297.
- Ligon, B. Lee. "Penicillin: its discovery and early development." *Seminars in pediatric infectious diseases*. Vol. 15. No. 1. WB Saunders, 2004.
- Linares, Juan Francisco, et al. "Antibiotics as intermicrobial signaling agents instead of weapons." *Proceedings of the National Academy of Sciences* 103.51 (2006): 19484-19489.

- Liras, Paloma, and Juan F. Martín. "Gene clusters for  $\beta$ -lactam antibiotics and control of their expression: why have clusters evolved, and from where did they originate?." *International microbiology* 9.1 (2006): 9-19
- Luengo, Jose M., et al. "Lysine regulation of penicillin biosynthesis in low-producing and industrial strains of *Penicillium chrysogenum*." *Microbiology* 115.1 (1979): 207-211.
- Lund, F., O. Filtenborg, and J. C. Frisvad. "Associated mycoflora of cheese." *Food Microbiology* 12 (1995): 173-180.
- Macdonald, K. D., J. M. Hutchinson, and W. A. Gillett. "Heterokaryon studies and the genetic control of penicillin and chrysogenin production in *Penicillium chrysogenum*." *Microbiology* 33.3 (1963): 375-383.
- Makagiansar, H. Y., et al. "The influence of mechanical forces on the morphology and penicillin production of *Penicillium chrysogenum*." *Bioprocess Engineering* 9.2-3 (1993): 83-90.
- Marianski, Stanley, and Adam Mariański. *The art of making fermented sausages*. Bookmagic LLC, 2009.
- Martin, Juan F. "Clusters of genes for the biosynthesis of antibiotics: regulatory genes and overproduction of pharmaceuticals." *Journal of industrial microbiology* 9.2 (1992): 73-90.
- Mason, Hugh RS, and Renton C. Righelato. "Energetics of fungal growth: The effect of growth-limiting substrate on respiration of *Penicillium chrysogenum*." *Journal of Applied Chemistry and Biotechnology* 26.1 (1976): 145-152.
- Moss, Maurice O. "Morphology and physiology of *Penicillium* and *Acremonium*." *Penicillium and Acremonium*. Springer, Boston, MA, 1987. 37-71.
- Nelson, Mark L., et al. "Brief communication: mass spectroscopic characterization of tetracycline in the skeletal remains of an ancient population from Sudanese Nubia 350–550 CE." *American journal of physical anthropology* 143.1 (2010): 151-154.
- Nevalainen, KM Helena, Valentino SJ Te'o, and Peter L. Bergquist. "Heterologous protein expression in filamentous fungi." *Trends in biotechnology* 23.9 (2005): 468-474.
- Nielsen, Jens, Claus L. Johansen, and John Villadsen. "Culture fluorescence measurements during batch and fed-batch cultivations with *Penicillium chrysogenum*." *Journal of biotechnology* 38.1 (1994): 51-62.
- Nielsen, Jens, et al. "Pellet formation and fragmentation in submerged cultures of *Penicillium chrysogenum* and its relation to penicillin production." *Biotechnology Progress* 11.1 (1995): 93-98.
- Nielsen, Jens, and Henrik S. Jørgensen. "Metabolic Control Analysis of the Penicillin Biosynthetic Pathway in a High-Yielding Strain of *Penicillium chrysogenum*." *Biotechnology progress* 11.3 (1995): 299-305.
- Nielsen, Jens. *Physiological engineering aspects of Penicillium chrysogenum*. World Scientific, 1997.
- Ozcengiz, Gulay, and Arnold L. Demain. "Recent advances in the biosynthesis of penicillins, cephalosporins and clavams and its regulation." *Biotechnology advances* 31.2 (2013): 287-311.
- Peñalva, Miguel A., Robert T. Rowlands, and Geoffrey Turner. "The optimization of penicillin biosynthesis in fungi." *Trends in biotechnology* 16.11 (1998): 483-489.



Posch, Andreas E., and Christoph Herwig. "Physiological description of multivariate interdependencies between process parameters, morphology and physiology during fed-batch penicillin production." *Biotechnology progress* 30.3 (2014): 689-699.

Posch, Andreas E., Christoph Herwig, and Oliver Spadiut. "Science-based bioprocess design for filamentous fungi." *Trends in biotechnology* 31.1 (2013): 37-44.

Pirt, S. John, and Biagio Mancini. "Inhibition of penicillin production by carbon dioxide." *Journal of Chemical Technology and Biotechnology* 25.10 (1975): 781-783.

Pirt, S. J., and R. C. Righelato. "Effect of growth rate on the synthesis of penicillin by *Penicillium chrysogenum* in batch and chemostat cultures." *Appl. Environ. Microbiol.* 15.6 (1967): 1284-1290.

Richards, A. N. "Production of penicillin in the United States (1941–1946)." *Nature* 201.4918 (1964): 441-445.

Rolinson, G. N., and R. Sutherland. "Semisynthetic penicillins." *Advances in Pharmacology*. Vol. 11. Academic Press, 1973. 151-220.

Ryu, Dewey DY, and J. Hospodka. "Quantitative physiology of *Penicillium chrysogenum* in penicillin fermentation." *Biotechnology and Bioengineering* 22.2 (1980): 289-298.

Seyer, Bernhard, "Impact of process parameters on morphology, physiology and process performance of the filamentous fungus *Penicillium chrysogenum*", 2015

Shah, Ajit J., et al. "pH regulation of penicillin production in *Aspergillus nidulans*." *FEMS microbiology letters* 77.2-3 (1991): 209-212.

Shen, Y-Q., et al. "Repression of  $\beta$ -lactam production in *Cephalosporium acremonium* by nitrogen sources." *The Journal of antibiotics* 37.5 (1984): 503-511.

Smith, J. J., M. D. Lilly, and R. I. Fox. "The effect of agitation on the morphology and penicillin production of *Penicillium chrysogenum*." *Biotechnology and bioengineering* 35.10 (1990): 1011-1023.

Soltero, Fred V., and Marvin J. Johnson. "The effect of the carbohydrate nutrition on penicillin production by *Penicillium chrysogenum* Q-176." *Applied microbiology* 1.1 (1953): 52.

Stone, R. W., and M. A. Farrell. "Synthetic media for penicillin production." *Science* 104.2706 (1946): 445-446.

Suárez, Teresa, and Miguel Angel Peñalva. "Characterization of a *Penicillium chrysogenum* gene encoding a PacC transcription factor and its binding sites in the divergent pcbAB–pcbC promoter of the penicillin biosynthetic cluster." *Molecular microbiology* 20.3 (1996): 529-540.

Swartz, R. W. "Use of economic-analysis Penicillin-G manufacturing costs in establishing priorities for fermentation process improvement." Band 3, pp 75-110.

Theilgaard, Hanne Aae, et al. "Quantitative analysis of *Penicillium chrysogenum* Wis54-1255 transformants overexpressing the penicillin biosynthetic genes." *Biotechnology and bioengineering* 72.4 (2001): 379-388.

Tilburn, J., et al. "The *Aspergillus* PacC zinc finger transcription factor mediates regulation of both acid-and alkaline-expressed genes by ambient pH." *The EMBO Journal* 14.4 (1995): 779.

Tomasz, Alexander, and Susan Waks. "Mechanism of action of penicillin: triggering of the pneumococcal autolytic enzyme by inhibitors of cell wall synthesis." *Proceedings of the National Academy of Sciences* 72.10 (1975): 4162-4166.

Ustianowski, Andrew P., Tran PM Sieu, and Jeremy N. Day. "Penicillium marneffeii infection in HIV." *Current opinion in infectious diseases* 21.1 (2008): 31-36.

Velasco, Javier, et al. "Exogenous methionine increases levels of mRNAs transcribed from pcbAB, pcbC, and cefEF genes, encoding enzymes of the cephalosporin biosynthetic pathway, in *Acremonium chrysogenum*." *Journal of bacteriology* 176.4 (1994): 985-991.

Van Den Berg, Marco A., et al. "Genome sequencing and analysis of the filamentous fungus *Penicillium chrysogenum*." *Nature biotechnology* 26.10 (2008): 1161-1168.

Van Long, Nicolas Nguyen, et al. "Temperature, water activity and pH during conidia production affect the physiological state and germination time of *Penicillium* species." *International Journal of Food Microbiology* 241 (2017): 151-160.

Vardar, Fazilet, and M. D. Lilly. "Effect of cycling dissolved oxygen concentrations on product formation in penicillin fermentations." *Applied Microbiology and Biotechnology* 14.4 (1982): 203-211.

Wainwright, Milton. "Moulds in ancient and more recent medicine." *Mycologist* 3.1 (1989): 21-23.

Wang, Liping, et al. "Bioprocessing strategies to improve heterologous protein production in filamentous fungal fermentations." *Biotechnology advances* 23.2 (2005): 115-129.

## 8. List of Figures

Figure 1: Illustration of the strain development process of the nowadays used strains of <i>P. chrysogenum</i> in industry. On the left side the genealogical sequence of developed strains is visible while the right side shows the amount of produced Penicillin. Taken from Jami et al., 2010. ....	15
Figure 2: Chemical ground structure of penicillin. “R” represents different residues, characterizing specific penicillin derivates.....	16
Figure 3: Gene cluster encoding for the enzymes necessary for penicillin production (Liras at al., 2006) and biosynthetic pathway of penicillin G (van der Berg et al., 2007) .....	16
Figure 4: Illustration of some penicillion derivates. Taken from Bush et al., 2016.....	17
Figure 5: Morphological development of <i>P. chrysogenum</i> during cultivation conditions. Taken from Posch et al. 2013. ....	19
Figure 6: Illustration of $\mu$ - $q_{pen}$ Model established by Douma et al., 2010. “-“shows $\mu$ - $q_{pen}$ during fed-batch condition simulated by the model, “□” as simulated by the model and “●” during chemostat cultivations. ....	21
Figure 7: Illustration of the fermenter setup (Seyer, 2015) .....	25
Figure 8: Illustration of the cultivation strategy.....	26
Figure 9: $pO_2$ control strategy during the final fed-batch .....	29
Figure 10: $CO_2$ content within the offgas and pH during the batch phase .....	38
Figure 11: Dissolved oxygen [%] as well as stirrer speed [rpm] during the batch phase.....	38
Figure 12: Concentration of the glucose, sucrose, fructose, lactose, lactose, mannitol and gluconate [g/L] within the batch media during the batch phase of the fermentation.....	39
Figure 13: Ergosterol [mg/L] data as well as calculated biomass [g/L] of FB1. ....	40
Figure 14: Development of the total cell dry weight [g/L] (blue) as well as viable cell dry weight [g/L] (red) of the fed-batch phase of the fourth cultivation with a $\mu$ set point of $0.02\ h^{-1}$ . ....	41
Figure 15: Penicillin concentration [g/L] in the supernatant of the fermentation broth during the ongoing cultivation FB4 with a $\mu$ set point of $0.02\ h^{-1}$ . ....	42
Figure 16: Progress of the concentration of different sugars (glucose, gluconate, sucrose, fructose, mannitol, lactose and galactose) within the fermentation broth during the fed-batch phase. Start of fed-batch is $t=0$ .....	42
Figure 17: $Y_{x/s}$ [c-mmol/c-mmol] during the progress of the fermentation FB4. $T=0$ is start of $\mu$ control, before start of $\mu$ control the culture was fed with a constant feed rate.....	43
Figure 18: Growth rate of viable biomass $\mu_{viable}$ [1/h] (blue marks) and specific penicillin production rate of viable biomass $q_{pen, viable}$ [mmol/c-mol*h] (red marks) of FB4. As time point zero, the start of the $\mu$ control was chosen (violet line). The aimed growth rate of the fermentation is $0.02\ [1/h]$ (green line). $T=0$ is start of $\mu$ control, before start of $\mu$ control the culture was fed with a constant feed rate. ....	44
Figure 19: Comparison of the applicable methods for the atline biomass concentration. Cell culture vials and biovolume data fitted with a linear regression, wet weight data with an exponential regression.....	45
Figure 20: Correlation of the delta capacitance signal and the viable biomass concentration. ....	46
Figure 21: Comparison of different variations of the $\mu$ control strategy via the achieved viable growth rate $\mu_{viable}$ . $T=0$ is start of $\mu$ control, before start of $\mu$ control the cultures were fed with a constant feed rate. ....	46

Figure 22: Plot of $\mu_{viable}$ and corresponding $q_{pen, viable}$ data points of all performed cultivations. Values before $\mu$ controlled phase are not included, only data pairs recorded after start of $\mu$ control are shown. ....	48
Figure 23: Illustration of $\mu_{viable}$ - $q_{pen, viable}$ relation. Shown data points are $\mu_{viable}$ and $q_{pen, viable}$ mean values of a single fermentation during the $\mu$ controlled phase as well as over a time period of 24h through which $\mu$ was considered as constant. ....	49
Figure 24: Plot of the maximal $q_{pen, viable}$ [mmol/c-mol*h] of the performed cultivations against the consumed glucose per initial biomass of the fed-batches [g/(g/L)] at the time of the maximal $q_{pen, viable}$ [mmol/c-mol*h]. ....	50
Figure 25: Plot of the maximal $q_{pen, viable}$ [mmol/c-mol*h] of every performed cultivation against their corresponding $\mu$ [1/h]. ....	50
Figure 26: $\mu_{viable}$ - $q_{pen, viable}$ data points at ~44 hours after start of fed-batch from FB1-8. ....	51
Figure 27: $q_{pen, viable}$ [mmol/c-mol] of all performed cultivations after ca. 44h of fed-batch plotted against consumed glucose/initial biomass of FB [g/(g/L)]. ....	51
Figure 28: Illustration of the $q_{pen, viable}$ [mmol/c-mol*h] against $\mu_{viable}$ [1/h] after ca. 45g consumed glucose/initial biomass of FB [g/(g/L)]. ....	52
Figure 29: Comparison of the development of the CDW [g/L] of FB7 (ordinary SOP) and FB9 ( $pO_2=4\%$ ) during cultivation. ....	53
Figure 30: Comparison of $\mu_{viable}$ of FB7 (ordinary SOP) and FB9 ( $pO_2=4\%$ ) during cultivation. ....	53
Figure 31: Penicillin concentrations of FB7 (ordinary SOP) and FB9 ( $pO_2=4\%$ ) during cultivation. ....	54
Figure 32: Comparison of $q_{pen, viable}$ [mmol/c-mol*h] of FB7 (ordinary SOP) and FB9 ( $pO_2=4\%$ ) during cultivation. ....	54
Figure 33: Plot of $\mu_{viable}$ and corresponding $q_{pen, viable}$ data points of cultivations performed according to standard operation procedure as well as the fermentation run with a decreased oxygen level. Values before $\mu$ controlled phase are not included, only data pairs recorded during after start of $\mu$ control are shown. ....	55
Figure 34: Plot of $\mu_{viable}$ - $q_{pen, viable}$ relation. Shown data points are $\mu_{viable}$ and $q_{pen, viable}$ mean values of a single fermentation during the $\mu$ controlled phase as well as over a time period of 24h through which $\mu$ was considered as constant. ....	56
Figure 35: Plot of the maximal $q_{pen, viable}$ [mmol/c-mol*h] and corresponding consumed glucose per initial biomass of the fed-batch [g/(g/l)] of runs carried out according to ordinary SOP as well as the cultivation with the altered SOP of a decreased oxygen level of 4%. ....	56
Figure 36: Plot of the maximal $q_{pen, viable}$ [mmol/c-mol*h] and corresponding $\mu_{viable}$ [1/h] of runs performed according to SOP as well as the run with the decreased oxygen level of 4%. ....	57
Figure 37: $q_{pen, viable}$ plotted [mmol/c-mol*h] against the consumed glucose per initial biomass of the fed-batch [g/(g/l)] of standard runs as well as the run with an oxygen level of 4%. ....	57
Figure 38: $\mu_{viable}$ - $q_{pen, viable}$ data points at ~44 hours after start of fed-batch of the standard runs as well as the cultivation performed with a decreased oxygen level. ....	58
Figure 39: $q_{pen, viable}$ [mmol/c-mol*h] against $\mu_{viable}$ [1/h] after the consumption of ~45 [g/(g/l)] glucose per initial biomass at the start of fed-batch of standard runs as well as the altered run with the decreased oxygen level of 4%. ....	58

## 9. List of Tables

Table 1: Scientific classification of the filamentous fungus <i>Penicillium chrysogenum</i> .....	14
Table 2: Overview of the used instruments which were directly as well as indirectly attached to the fermenter .....	24
Table 3: List of the used feeds and their composition .....	25
Table 4: Initial batch process parameters .....	27
Table 5: Initial fed-batch conditions.....	28
Table 6: Initial rates of POX and nitrogen feed as well as manual regulation criteria during fed-batch. $C_{\text{POX, broth}}$ and $C_{\text{NH}_3, \text{broth}}$ are the concentrations of POX and ammonium, respectively, within the broth	28
Table 7: Composition of the mobile phase used for PEN/POX analytics via HPLC; before usage the buffer was degassed using an ultrasonic bath as described in the ergosterol measurement section .	32
Table 8: TECAN settings which were used for the viability determination.....	33
Table 9: PBS buffer .....	34
Table 10: Excitation and emission wavelength for PI and FDA .....	34
Table 11: Fed-batch number, atline method for estimation of the total biomass, $\mu$ setpoint [1/h], average $\mu$ [1/h], used SOP and fed-batch ID of all performed cultivations. ....	37
Table 12: Result of $\mu_{\text{max}}$ .....	40

# List of Abbreviations

---

°C	Degree celsius
μ	Growth rate
μL	Microliter
(NH <sub>4</sub> ) <sub>2</sub> SO <sub>4</sub>	Ammonium sulfate
ACN	Acetonitrile
ACVS	δ-(L-α-aminoadipyl)-L-cysteinyl-D-valine synthetase
ATCC	American Type Culture Collection
Ca <sup>2+</sup>	Calcium
CaCl <sub>2</sub>	Calcium chloride
CaCl <sub>2</sub> ·2H <sub>2</sub> O	Calcium chloride dihydrate
CaCO <sub>3</sub>	Calcium carbonate
CDW	Cell dry weight
CFU	Colony-forming unit
CO <sub>2</sub>	Carbon dioxide
C <sub>x</sub>	Concentration of biomass
dCapacitance	Delta capacitance
dH <sub>2</sub> O	Deionized water
DNA	Desoxyribonucleic acid
FDA	Fluorescein diacetate
h	hour
H <sub>2</sub> SO <sub>4</sub>	Sulfuric acid
H <sub>3</sub> PO <sub>4</sub>	Phosphoric acid
HPLC	High performance liquid chromatography
IAT	Acyl coenzyme A: isopenicillin N acyltransferase
IC	Ion chromatography
IPNS	Isopenicillin N synthase
KCl	Potassium chloride
kDa	Kilo Dalton
kHz	Kilo Hertz
KH <sub>2</sub> PO <sub>4</sub>	Potassium dihydrogen orthophosphate
KOH	Potassium hydroxide
L	liter
LLD-ACV	δ-(L-α-aminoadipyl)-L-cysteinyl-D-valine
mg	milligram
MQ	Ultrapure type-1 water
Mg <sup>2+</sup>	Magnesium
MgCl <sub>2</sub> ·6H <sub>2</sub> O	Magnesium chloride hexahydrate
min	minute
mL	milliliter
mm	millimeter
ms	milliseconds
NaCl	Sodium chloride
Na <sub>2</sub> HPO <sub>4</sub>	di-sodium hydrogenphosphate
Na <sub>2</sub> HPO <sub>4</sub> ·2H <sub>2</sub> O	Sodium phosphate dibasic dihydrate
NaOH	Sodium hydroxide

NH <sub>3</sub>	ammonia
nm	nanometer
O <sub>2</sub>	oxygen
PBS	Phosphate buffered saline
pH	Pondus hydrogenii
PI	Propidium iodide
PID	proportional-integral-derivative
pO <sub>2</sub>	Dissolved oxygen
POX	Sodium phenoxyacetate
q <sub>pen</sub>	Biomass specific penicillin production rate
rpm	Rounds per minute
RT	Room temperature
sec	seconds
UV	ultraviolet
VIS	visible
vvm	Volume air per volume culture broth per minute
Y	Yield